

DSpace Institution

DSpace Repository

<http://dspace.org>

Hydraulic engineering

Thesis

2020-01

Impact of climate change on Hydrological Response of Mojo River catchment, Awash River Basin, Ethiopia

Getu, Mikhael

<http://hdl.handle.net/123456789/11039>

Downloaded from DSpace Repository, DSpace Institution's institutional repository



BAHIR DAR UNIVERSITY
BAHIR DAR INSTITUTE OF TECHNOLOGY
SCHOOL OF RESEARCH AND POSTGRADUATE STUDIES
FACULTY OF CIVIL AND WATER RESOURCES ENGINEERING

**Impact of climate change on Hydrological Response of Mojo River catchment,
Awash River Basin, Ethiopia**

MASTER THESIS

BY

Mikhael Getu Alemu

Bahir Dar, Ethiopia

January 2020

**Impact of climate change on Hydrological Response of Mojo River
catchment, Awash River Basin, Ethiopia**

Mikhael Getu Alemu

A thesis submitted to the school of Research and Graduate Studies of Bahir Dar Institute
of Technology, Bahir Dar University in partial fulfillment of the requirements for the
degree of Master of Science in Engineering Hydrology in the Faculty of Civil and Water
Resource Engineering

This thesis presented to Faculty of Civil and Water Resources Engineering

Academic Advisors

Advisor Name: **Mamaru Ayalew (Ph.D.)**

Co-Advisor Name: **Dejene Sahlu (Ph.D.)**

Bahir Dar, Ethiopia

DECLARATION

I, the undersigned, declare that the thesis comprises my own work. In compliance with internationally accepted practices, I have acknowledged and refereed all materials used in this work. I understand that non-adherence to the principles of academic honesty and integrity, misrepresentation/ fabrication of any idea/data/fact/source will constitute sufficient ground for disciplinary action by the University and can also evoke penal action from the sources which have not been properly cited or acknowledged.

Name of the student Mikhael Getu Alemu

Signature



Date of submission: March 2, 2020

Place: Bahir Dar

This thesis has been submitted for examination with my approval as a university advisor.

Advisor Name: Mamaru. A. Moges (Ph.D.)

Advisor's Signature: _____



©2020
Mikhael Getu Alemu
ALL RIGHTS RESERVED

BAHIR DAR UNIVERISITY
BAHIR DAR UNIVERISITY INSTITUTE OF TECNOLGY
SCHOOL OF RESEARCH AND POSTGRADUATE STUDIES

Faculty of Civil and Water Resources Engineering

Engineering Hydrology

THESIS APPROVAL SHEET

Student:

Mikhael Getu

Name



Signature

Mar 2, 2020

Date

The following graduate faculty members certify that this student has successfully presented the necessarily written thesis and oral presentation of this thesis for partial fulfillment of the thesis-option requirements for the Degree of Master of Science in Engineering Hydrology.

Approved:

Advisor:

Mamaru A. Moges (Ph.D.)

Name



Signature

Mar 3, 2020

Date

External examiner:

Adugnaw Tadesse (Ph.D.)

Name



Signature

Feb 2, 2020

Date

Internal examiner:

Bitew Genet

Name



Signature

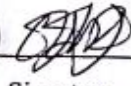
3/03/20

Date

Chair Holder:

Mulugeta Azere (Ph.D.)

Name



Signature

Mar 5, 2020

Date

Faculty Dean: Ebku Nigussie (Ph.D.)
Faculty Dean

Name



Signature

March 05, 2020

Date



“This work is dedicated to my family, friends and who loved me. Special dedication goes to my mother Desta Eshetu, my father Getu Alemu, my Sisters Mehalet, Mhraf, Bethel and to young Brother Alemu Habebe”.

ACKNOWLEDGEMENTS

Above all I thank almighty of GOD with his mother St. Marry for his sympathy, kindness, and grace upon me in all my life.

I would like to express my greatest gratitude to the Bahirdar University Institute of Technology for providing and gaining educational knowledge and especially to ERA (Ethiopian Road Authority) for awarding me the sponsorship. I would like to extend my thanks to My mother Desta Eshetu for her contribution during the process.

I also thank my advisors Dr. Mamaru Ayalew and Dr. Dejene Sahlu who provided me with invaluable ideas and advice over the course of this research. My deepest, maximum respect and special thanks goes to Dr. Dejene Sahlu for his initiation and providing excellent advice and constructive comments. Besides this, Dr. Dejene Sahlu gives his time to provide me a climate data and prepared for me without tiredness.

Also, I would like to thanks Mr. Negash Tessema lecture at Harumaya University, my brother Mr. Alemu Habebe lecture at Semera University and special thanks to Tirusew Assefa (Ph.D., P.E., D.WRE) professor at University of South Florida for his wonderful advice over how to make bias correction of satellite data and for his kindness.

Finally, I would like to say thanks to my family for all the support and encouragement throughout the entire work. I would like to say thanks to my relatives especially for my father Getu Alemu, my mother Desta Eshetu, my brother Alemu Habebe and for my three sisters Mhraf, Bethel and Mahlet for gave me support in order to finish my thesis work.

ABSTRACT

The study focuses on the impact of climate change on the hydrology of Mojo River Catchment. The Soil and Water Assessment tool was used for modeling. As the model reveals that $NSE = 0.74$; $R^2 = 0.73$; $PBIAS = 1.6$ during calibration and $NSE = 0.65$; $R^2 = 0.61$; $PBIAS = 1.6$ during validation. Here the coordinated regional climate downscaling experiment (CORDEX)-Africa data outputs of GCM models (MPI-M-MPI-ESM-LR, MIROC-MIROC5, CCCma-canEM2, and IPSL-IPSL-CM5A-MR) under RCP4.5 and RCP8.5 scenarios with the Regional Model RCA4 was used. Based on their performance two models were highlighted (MPI-M-MPI-ESM-LR and MIROC-MIROC5) after simulated historical data without bias correction and considering the least PBIAS shows good underlying atmospheric dynamic. For bias correction Quantile mapping was used with Gamma and Normal distribution for precipitation and temperature respectively. Then PBIAS become improved from 43.3% to 5.1% under MPI-M-MPI-ESM-LR and 65.7% to 9.6% under MIROC-MIROC5. Future scenarios climate change was analyzed in three-time periods: 2006–2031 near period, 2031–2055 mid-period and 2056-2080 far period. The result MIROC-MIROC5 Model the precipitation increases from +24 to 49% under RCP 4.5 and decreases from 47 to 25 % under 8.5. Similarly, maximum temperature increase from 1.19 to 3.57⁰C under RCP 8.5 and increases from 1 to 1.99 ⁰C under RCP 4.5 this leads to decrease of streamflow from 6.32 m³/s to 5.08 m³/s under near and mid-period in RCP 4.5 but under RCP 8.5 the streamflow become decrease from 6.68, 2.64, and 6.31 m³/s for the period of near, mid and far future period respectively. For MPI-M-MPI-ESM-LR precipitation increase from 31.9 to 34.8% under RCP 8.5 and decreases from 33.8 to 33.1% under RCP 4.5 but the maximum temperature become increase in both scenarios form 0.45 to 1.875⁰C under RCP 4.5 and 0.47 to 1.97⁰C under 8.5 and the streamflow become increase from 4.62, 4.30 and 7.79 m³/s under RCP 4.5 and 6.68, 2.64 and 6.31 m³/s under RCP 8.5 for Near, Mid and Far future Periods respectively. The result of this study indicates that climate will affect the hydrology of the catchment. Due to change streamflow different operations over the catchment should be incorporated with climate change scenarios.

Keywords: GCM, Mojo catchment, RCP 8.5 and RCP 4.5, SWAT

Table of Contents

DECLARATION	i
ACKNOWLEDGEMENTS	v
ABSTRACT	vi
LIST OF FIGURES	x
LIST OF TABLES	xii
LIST OF APPENDIXES	xiii
ABBREVIATIONS AND SYMBOLS	xiv
1. INTRODUCTION	1
1.1. Background	1
1.2. Statement of the problem	3
1.3. Research Questions	3
1.4. General Objective	4
1.5. Scope of the study	4
1.6. Significance of the study	5
1.7. Thesis Organization	6
2. LITERATURE REVIEW	7
2.1. History of Mojo Catchment over the Awash Basin	7
2.2. Climate Change	8
2.3. Global climate change	8
2.4. Climate change in Ethiopia	8
2.5. Climate change scenarios and Global Circulation Models (GCMs)	9
2.5.1. Emissions Scenarios	9
2.5.2. Development of Emission Scenarios	10
2.5.3. General Circulation Models	11
2.6. Climate downscaling Approach's	12
2.6.1. Coordinated Regional Climate Downscaling Experiment (CORDEX)	13
2.7. Uncertainties in Regional Climate Projections	15
2.8. Soil and Water Assessment Tool (SWAT)	16

2.9.	Previous studies on climate change and SWAT application.....	17
2.9.1.	Studies on Climate change over the awash basin.....	17
2.9.2.	Studies using SWAT analysis over the Mojo Catchment	18
3.	MATERIALS AND METHODS	20
3.1.	Description of the study area	20
3.1.1.	Soil Type.....	21
3.1.2.	Land use.....	22
3.1.3.	Climate.....	22
3.1.4.	Hydrology	24
3.2.	Descriptions of the Materials	25
3.2.1.	Data Availability	25
3.2.2.	Streamflow/River Discharge Data	25
3.2.3.	Spatial data.....	25
3.2.4.	Climate Scenario Data	26
3.2.5.	Soil and Land Use Data	26
3.2.6.	Summary of Materials and Data used	27
3.2.7.	Conceptual Framework of Overall Methodology	28
3.3.	Method of Data Quality Analysis	29
3.3.1.	Metrological Data Analysis	29
3.3.2.	Filling of missing data	30
3.3.3.	Data Quality Assessment	30
3.4.	Methodology	36
3.4.1.	Data availability and collection of precipitation and temperature scenarios data..	36
3.4.1.1.	Selection criteria for RCP and GCMs models	37
3.4.1.2.	Uncertainty in climate model selection.....	38
3.4.2.	Evaluation of the GCMs Models	39
3.4.3.	Bias Correction Method.....	40
3.4.4.	Hydrological Modeling Using SWAT	42
3.4.4.1.	SWAT Modelling.....	42
3.4.4.2.	Model Simulation.....	43
3.4.4.3.	Sensitivity Analysis.....	44

3.4.4.4.	Model Calibration	44
3.4.4.5.	Performance Evaluation	45
3.4.4.6.	Model validation	46
3.4.4.7.	The conceptual framework of the SWAT model and Cordex data	47
4.	RESULT AND DISCUSSION	48
4.1.	Hydrological Model Evaluation.....	48
4.1.1.	Catchment Delineation.....	48
4.1.2.	SWAT model HRU Analysis.....	49
4.1.3.	Sensitivity, Calibration, and Validation of the SWAT model.....	50
4.1.4.	Analysis of observed climate data and streamflow	51
4.2.	Analysis of the Performance climate GCM models.....	53
4.2.1.	Selection of GCM Model.....	53
4.2.2.	Validation of GCMs Models.....	54
4.2.3.	Analysis of Bias corrected climate data and observed data	56
4.3.	Analysis of climate change Future scenarios	59
4.3.1.	Change in projected precipitation GCMs scenarios.....	59
4.3.2.	Change in projected Temperature GCMs scenarios.....	63
4.4.	Hydrological Change of Projected Precipitation and Temperature on Streamflow	69
4.4.1.	Change in Projected streamflow	69
4.4.2.	Impact of Future Precipitation and Temperature Change on the streamflow	73
5.	CONCLUSIONS AND RECOMMENDATIONS	75
5.1.	Conclusion	75
5.2.	Recommendation	77
	REFERENCE.....	79

LIST OF FIGURES

Figure 2.1 IPCC AR5 Greenhouse Gas Concentration Pathways (source: http://en.m.wikipedia.org/wiki/Representative_Concentration_Pathway)	11
Figure 3.1 Location map of Mojo Catchment.....	20
Figure 3.2 Soil map of Mojo Catchment	21
Figure 3.3 Landuse map of Mojo Catchment	22
Figure 3.4 Mean monthly rainfall of Mojo catchment (1980 – 2005).....	23
Figure 3.5 Mean monthly temperature maximum and minimum of Mojo catchment (1980 – 2005).....	23
Figure 3.6 Mean Monthly streamflow of Mojo catchment (1981-2005).....	24
Figure 3.7 Annual mean streamflow of Mojo catchment (1981-2005)	25
Figure 3.8 conceptual framework of the climate and SWAT model	28
Figure 3.9 Metrological stations of Mojo catchment.....	29
Figure 3.10 Homogeneity test of four rainfall station (1980-2010).....	31
Figure 3.11. Consistency tests of rainfall data	32
Figure 3.12 Annual Mean streamflow trend analyses 1981-2005	35
Figure 3.13 Annual maximum rainfall trend analysis of four stations (1980-2010)	35
Figure 3.14 CORDEX-Africa 0.440 (50_50 km) grid data coordinates.....	37
Figure 3.15 conceptual frameworks of the SWAT model and Cordex data.....	47
Figure 4.1 HRU Analysis Report of swat model	49
Figure 4.2 Calibration, validation and uncertainty analysis of flow data	52
Figure 4.3 Comparison of observed and historical GCMs Models (variability among the four GCMs) time series of 1981-2005 for Temperature max, min and rainfall before bias correction figure (A) and figure (B) respectively.	54
Figure 4.4 Validation of candidate GCM models simulation output and validated streamflow data of Mojo catchment form 2001-2005	55
Figure 4.5 shows Cumulative Distribution Function before and after bias correction with respect to observed data and Historical data from (1981-2005), fig (A) and (B) Gamma distribution for precipitation of GCMs model MPI-M-MPI-ESM-LR and MIROC-MIROC5 respectively, normal distribution C, D, for temperature min, E and F for temperature max.....	57

Figure 4.6 Validation output Annual mean streamflow of MIROC-MIROC5 and MPI-M-MPI-ESM-LR from (2002-2005).....	58
Figure 4.7 Annual precipitation (1981-2080) at Mojo catchment for model MIROC-MIROC5 and MPI-M-MPI-ESM-LR under RCP 4.5 and RCP 8.5 climate scenario	60
Figure 4.8 Annual Monthly mean of Precipitation (2006-2080) for the Model MPI-M-MPI-ESM-LR under RCP 4.5 and 8.5	61
Figure 4.9 Annual Monthly mean of Precipitation (2006-2080) for the Model MIROC-MIROC5 under RCP 4.5 and 8.5	62
Figure 4.10 Annual monthly mean of temperature maximum and minimum (1981-2080) at Mojo catchment for model MPI-M-MPI-ESM-LR (A) and MIROC-MIROC5 (B) under RCP4.5 and RCP8.5 climate scenario	64
Figure 4.11 Annual Monthly mean of temperature maximum and minimum (2006-2080) for the Model MIROC-MIROC5 under RCP 4.5 and 8.5.....	66
Figure 4.12 Annual Monthly mean of Temperature maximum and minimum change (2006-2080) for the Model MPI-M-MPI-ESM-LR under RCP 4.5 and 8.5.....	67
Figure 4.13 The annual mean of simulated streamflow (1981-2080) at Mojo catchment for model MPI-M-MPI-ESM-LR (A) and MIROC-MIROC5 (B) under RCP4.5 and RCP8.5 climate scenarios	70
Figure 4.14 The annual mean of simulated streamflow change (%) (1981-2080) at Mojo catchment for model MPI-M-MPI-ESM-LR and MIROC-MIROC5 under RCP4.5 and RCP8.5 climate scenarios	72

LIST OF TABLES

Table 3.1 Area coverage of soil type of Mojo catchment (source: Ministry of Water and Energy office)	21
Table 3.2 Data's and their source used for this study	27
Table 3.3 Material and their purpose used in this study	27
Table 3.4 List of meteorological stations used in the study	29
Table 3.5 Candidate GCM Models	36
Table 3.6 GCM Model selection criteria and their variables	38
Table 3.7 Performance evaluation criteria (PEC), Statistical threshold value and corresponding assigned weight	46
Table 4.1 Detailed Landuse/Soil/Slope distribution SWAT model class	48
Table 4.2 List of top 17 sensitive parameters at Mojo catchment at the locations of Awash basin	50
Table 4.3. SWAT hydrological model performance under validation and calibration periods of observed streamflow in Mojo catchment	52
Table 4.4. SWAT hydrological model performance under validation and calibration periods of GCM models and observed data.	55
Table 4.5 Selected GCM Models used for analysis	56
Table 4.6. Performance evaluation streamflow validation output of model MIROC-MIROC5 and MPI-M-MPI-ESM-LR	58
Table 4.7 Annual Monthly mean variation of Precipitation change (2006-2080) for the Model MPI-M-MPI-ESM-LR under RCP 4.5 and 8.5	62
Table 4.8 Annual Monthly mean variation of Precipitation change (2006-2080) for the Model MIROC-MIROC5 under RCP 4.5 and 8.5	63
Table 4.9 Mean Monthly variation of temperature maximum and minimum change (2006-2080) for the Model MIROC-MIROC5 (A) and MPI-M-MPI-ESM-LR under RCP 4.5 and 8.5	68
Table 4.10 Mean Monthly variation of Streamflow change (%) (2006-2080) for the Model MIROC-MIROC5 and MPI-M-MPI-ESM-LR under RCP 4.5 and 8.5	72

LIST OF APPENDIXES

Appendix 1 Test of Homogeneity of rainfall	92
Appendix 2 Test of outlier of rainfall of four stations	92
Appendix 3 Test of outlier of Streamflow at Mojo gauge stations (1980-2010).....	94
Appendix 4 Table 4.2 trend analysis of streamflow (1981-2011)	95
Appendix 5 Trend analysis of rainfall of four stations	95
Appendix 6 GCM model and their institutions (source: https://is-enes-data.github.io/CORDEX_RCMs_info.html)	96
Appendix 7 Selected sensitivity parameters and their ranges fitted maximum and minimum value	97
Appendix 8 Sensitive parameters fitted value descriptions	98
Appendix 9 Global sensitive parameters of SWAT-CUP.....	98
Appendix 10 The change of Bias correction of Historical data with respect to observed rainfall from (1981-2005) for the two GCM models	99
Appendix 11 The change of Bias correction of Historical data with respect to observed maximum and minimum temperature from (1981-2005) for the two GCM models.....	99
Appendix 12 CORDEX-Africa (AFR-44) regional and global circulation models (Source: http://is-enes-data.github.io/CORDEX_status.html)	100

ABBREVIATIONS AND SYMBOLS

AR5	IPCC report - Assessment Report Five
°C	Degree calicules
ANN	Artificial Neural Network
CCCM,	The Canadian Climate Change Model
CDF	Cumulative Distribution Function
CMIP5	the fifth Coupled Model Intercomparison Project
CORDEX	Coordinated Regional Climate Downscaling Experiment
CREAMS	Chemicals, Runoff, and Erosion from Agricultural Management Systems
DEM	Digital Elevation Model
DQM	Detrended Quantile Mapping
EPIC	Environmental Impact Policy Climate
ET	Evapotranspiration
FMWRE	Federal Ministry of Water Resources of Ethiopia
GCM	Global Circulation Model
GCM	Global Climate Model
GF01	Geophysical Fluid Dynamics Transient
GFD3	Geophysical Fluid Dynamics model
GHG	Greenhouse Gases
GIS	Geographic Information System
HRU	Hydrological Response Units
HSPF	Hydrologic Simulation Program Factor
IPCC	Intergovernmental Panel for Climate Change
ITAM	Innovative Trend Analysis Method
LAM	limited Area Model
LARS-WG	Long Ashton Research Station Weather Generator
LS	linear Scaling
LULC	Land Use land Cover
MUSLE	Modified Universal Soil Loss Equation
NMSA	National Metrology Service Agency
NOAA	National Oceanic and Atmospheric Administration

NSE	Nash-Sutcliffe efficiency coefficient
NSRP	Neyman-Scott Rectangular Pulses
PD	<i>Peak and Decline</i>
PET	Potential Evapotranspiration
PT	Power Transpiration
QDM	Quantile Delta Mapping
QM	Quantile Mapping
QUAL2E	The enhanced stream water quality of the stream model
RCM	Regional Climate Models
RCP	Representative Concentration Pathways
ROTO	Routing Output To Outlet
RSR	Root mean square error observation standard deviation ratio
RUSLE	Revised Universal Soil Loss Equation
SCS	Soil Conservation Service
SDSM	Statistical Down-Scaling Method
SMHI	Switzerland Metrological and Hydrological Institute
SRES	The Special Report on Emissions Scenarios
SUFI-2	Sequential Uncertainty Fitting
SWAT	Soil Water Assessment Tools
SWMM	Stormwater Management Model
SWRRB	Simulator for Water Resources in Rural Basins
TAR	Third Assessment Report
USDA	United State Department of Agriculture
USEPA	United States Environmental Protection Agency
USLE	Universal soil loss equation
W/m ²	Watt per square meter
WatBal	Integrated water balance model
WCRP	World Climate Research Program
WG	Weather Generator

1. INTRODUCTION

1.1. Background

Water is a mobile resource it falls from the clouds, seeps into the soil, flows through aquifers, runs along with stream courses, and eventually returns to the clouds. This natural cycle is the basis of all life forms and of the economy of nature (Rahmato, 1999). Water may be "managed" in different ways: it may be harvested, extracted from the ground, diverted, transported, and stored. This makes it different from all other natural resources (Rahmato, 1999). However, each form of management that interferes with the natural cycle exacts a price, not just in economic terms but in terms of environmental damage and greater health hazards. Moreover, water does not occur alone, it is rather part of a complex ecosystem consisting of the land, plants, aquatic and other life forms (Pirozynski and Malloch, 1975). At the global scale, projections suggest wetter regions will become wetter and drier regions will get drier according to Loucks and Van Beek, (2017). Since water resource issues are transboundary due to that we face different challenges, some of the issues could be based on human activity, deforestation or greenhouse effects, that leads to climate change Impacts and that changes also lead to the failer of water structure not only that the movement of the water, sediment but also sudden high floods which is the main cause due to climate change.

Climate change impact studies associated with global warming as a result of an increase in greenhouse gases (GHG) has been given ample attention worldwide in recent decades (Dodman, 2009) and (Papadimitriou, 2004). Climate Change on future projections, precipitation and temperature will increase over eastern Africa in the coming century (Jaramillo *et al.*, 2011) and also in sub-Saharan Africa, there are many vulnerable river basins. These basins are vulnerable both in terms of the climate system that is highly variable and the potential future changes in climate, but also in terms of management as weak governance and high levels of poverty in the population restrict actions to adapt to climate change (Cooper *et al.*, 2008). The advancements in climate models have increased confidence in the outputs required as inputs for hydrological applications (Wood *et al.*, 2004). However, hydrological impact studies ought to receive more attention as there are still grey areas (area of activity not readily conforming to climate

change) related to the interfacing of climate and hydrological models. Vulnerable hydrological resources are too important to defer climate change investigations (Taye *et al.*, 2011).

Africa's river systems have been the target of development planners since the 1960s, and many of the major rivers of the continent have been dammed for irrigation, for power generation and flood control (Richter *et al.*, 2010). Indeed, river basin development planning has been widely adopted in Africa, and often enough water resource development has come to be synonymous with river basin development (Rahmato, 1999). Water has always played a central role in Ethiopian society it is an input, to a greater or lesser extent, to almost all production (Haile and Kasa, 2015) and it is also a force for destruction.

In Ethiopia, as in all societies, there has always been a struggle to reduce the destructive impacts of water and increase its productive impacts (Grey and Sadoff, 2007). Res and Hailemariam, (1999) develop a better understanding of the impact of climate change on the water resources of the Awash River Basin in Ethiopia, a temperature increases of 2.4 and 3.0°C, respectively, is projected by models for a doubling of CO₂. Therefore, the Awash River Basin would be significantly affected by the changing climate since then; for instance, Taye, (2018) and Daba, (2015) indicate that the projections for the future period show an increase in water deficiency in all seasons and for parts of the basin, due to a projected increase in temperature and decrease in precipitation. This decrease in water availability will increase water stress in the basin. In Ethiopia, most studies on the impact of climate change on water resources focus on catchment s of the Nile basin, for instance (Conway, (1997): Alemseged and Tom, (2015): Worku *et al.*, (2018)) Since the vulnerability climate change on the study area in the Mojo catchment was analyzed as subbasin of Awash basin.

1.2. Statement of the problem

There is strong scientific evidence that indicates the average temperature of the Earth's surface is increasing due to greenhouse gas emissions. The IPCC (Intergovernmental Panel on Climate Change) scenarios project temperature rises of 1.4⁰C -5.8⁰C, and sea level rises of 9-99 cm by 2100 (IPCC, 2014).

Most research on climate impacts discusses one of the most important consequences of climate change will be alterations in major climate variables, such as temperature, precipitation, and evapotranspiration. This, in turn, will lead to changes in the hydrological cycle, influencing the components of the water balance of drainage basins in several ways such as the availability and distribution of water resources in space and time, streamflow, frequency of extreme events, etc. (Wale and Texas, 2015).

One of the most important potential concerns of climate change is hydrological components alteration and subsequent changes in river Hydrology (Girma, 2013). The water balance components, water yield (flow) from un-gauged and gauged catchment s, precipitation and temperature pattern variability change and their impact over Mojo Catchment are not yet researched. Most of the researches over the Mojo catchment focus on the sediment accumulation for instance (Gonfa and Kumar, (2016): Gonfa *et al.*, (2015)) and also Mojo catchment contribute water for irrigation for the society nearby the river and Rapid growth of agriculture, industries, and urbanization within catchment of Mojo become increase recently so analyzing of the impact of climate change is more important task. Therefore, this study examines the pattern of hydrological change and determines the pattern of climate change with its impact on the Mojo catchment.

1.3. Research Questions

In particular, I shall address the following questions:

- What are the better-performed GCM models for Mojo catchment?
- What will be the expected outputs of Streamflow based on different climate scenarios?
- What will be the response of Mojo catchment on future precipitation and temperature?

1.4. General Objective

The aim of this study was to investigate the possible impact of climate change on the hydrology of the Mojo River catchment using SWAT and GCMs Models.

Specific Objectives:

- To establish hydrologic modeling using the Soil and Water Assessment Tool (SWAT) over the Mojo Catchment.
- To select and evaluate the performance of CORDEX-Africa GCMs models over the Mojo catchment.
- To quantify the possible impact of climate change on the streamflow with different periods using GCMs CORDEX-Africa Models with RCP 4.5 and 8.5 scenarios.

1.5. Scope of the study

There are several methods of analysis of climate impact in this study the climate change is analyzed using CORDEX-Africa output data by different GCMs models with two representative scenarios (4.5 and 8.5) and using one Regional model RCA4. The analysis of CORDEX data was done with one ensemble value (r1i1p1). Selecting of GCMs model based on their performance after calibration and validation of observed data form (1981-2005) analysis with the GCMs historical data (1981-2005) using the SWAT (Soil and Water Assessment Tool) software and calibration and validation by SWAT CUP (SUFI-2 algorithm) software was analyzed. With the better perform GCM models correction of the bias appropriate after that for future climate change scenario the GCMs data are classified into three base period Near (2006-2030), (2031-2055) and (2056-2080). Then with two better-performed GCM models, the seasonal variation over temperature and precipitation change with respect to base period data were analyzed. And finally, the streamflow change at the future period under two scenarios as well as three periods with the seasonal variation and effect of climate change Temperature and precipitation on the streamflow was analyzed over the Mojo catchment.

1.6. Significance of the study

According to the IPCC, (2014), report continued emission of greenhouse gases will cause further warming and long-lasting changes in all components of the climate system, increasing the likelihood of severe, pervasive and irreversible impacts for people and ecosystems. Limiting climate change would require substantial and sustained reductions in greenhouse gas emissions which, together with adaptation, can limit climate change risks (Woodward and Scheraga, 2014).

Application of hydrological model in the catchment at spatial scale would be essential to know water hydrology and to study the impact of climate change on the catchment which helps to set different management scenarios that will lead to sound environmental sustainability. Therefore, it is necessary to study the hydrologic responses to climate change at this catchment level in order to take the effect into account by the policy and decision-makers when planning water resources management. The contribution of this study is that it can be a tool for the local and regional community/policymakers and concerned bodies what types of problems are happening and will happen due to climate impact. It can also inform stakeholders of the extent of the impacts that affect the hydrology of Mojo catchment.

In order to design efficient conservation strategies for sustainable development, it is essential to know the patterns of climate change of the area over time and space and to quantify the extent to which these changes influence the hydrological processes of the catchment. In the past, the lack of decision support tools and limitations of data were the main factors that significantly hindered research and development in the study area. Recently desertification has started at lower Awash River Basin identifying the impact over the catchment is more advantageous. In the high land part deforestation and sedimentation have increased in the past three decades Socolofsky *et al.*, (2001) so analyzing the variation of climate impact for future gives as additional input how much or might change the climate and mitigate over the catchment. Considering the hydrological behavior of the catchment and applicability of the existing models for the solutions of the aforementioned problems, this study was undertaken using the Soil Water Assessment Tool (SWAT) model.

1.7. Thesis Organization

The research report has been formulated in five chapters, with a brief layout of each of them. Chapter one: in this chapter represents the introduction, statement of the problem, general objective, research questions and significance of the study are briefly discussed. Chapter two: In this chapter, the historical background of Awash basin with related to Mojo catchment is discussed and the climate change starts from global to local which is Ethiopian climate condition and different methods to downscaled the climate data with their brief description of the history of emission scenarios and use of the hydrological models to assess climate changes on stream flows is discussed and finally previous studies which are focused on the climate change as well as the hydrological models in Awash basin and Mojo catchment. Chapter three: presents the study of the area, materials used for analysis, bias correction methods and methods in order to build and simulate models for climate change scenarios discussed. Chapter four: In this chapter result and discussion of the selected model, bias-corrected scenario data, model sensitivity, calibration, and validation of the model are discussed. Chapter five: In this chapter discuss the conclusion and recommendation of the thesis.

2. LITERATURE REVIEW

2.1. History of Mojo Catchment over the Awash Basin

The Awash River Basin is the most important river basin in Ethiopia, and covers a total land area of 110,000 km² and serves as home to 10.5 million inhabitants (Sonder, 2015). The river rises on the High plateau near Ginchi town west of Addis Ababa in Ethiopia and flows along the rift valley into the Afar triangle, and terminates in salty Lake Abbe on the border with Djibouti, being an endorheic basin (Sonder, 2015).

The Awash and Mojo, the major rivers of the northern, show a distinctive pattern as well on entering the Rift, the Awash runs approximately southward (Abebe *et al.*, 2005). At Ombole it turns sharply eastward and maintains this direction as far as Koka reservoir. Before the dam construction, the Awash river flowed to the north-east following the Wonji Fault Belt (Sagri *et al.*, 2008). Beyond the Koka dam, the Awash cuts across the Wonji Fault Belt and proceeds to the east, toward the Afar depression. This latter river reach is characterized by alternating deep gorges and swampy areas associated with fairly active horst and graben structures (Abebe *et al.*, 2005). The Mojo river system follows the southward-trending regional slope developing a trellis, sub-parallel pattern, under the influence of volcanic and tectonic structures (Abbate and Sagri, 1980) and then turns east at right angle near Koka reservoir, which masks the former confluence with the Awash. Moreover, the upper reaches of the Mojo were captured by the Kesem river, which flows to the Afar depression suggesting the past catchment of the Mojo was larger than the modern one (Abebe *et al.*, 2005).

Awash Basin is divided into Upland (all lands above 1500m), Upper Valley, Middle (area between 1500m and 1000m), Lower Valley (area between 1000m and 500m) and Eastern Catchment (closed sub-basin are between 2500m and 1000m), and the Upper, Middle, and Lower Valley are part of the Great Rift Valleys systems (Sonder, 2015). The Lower Awash Valley comprises the deltaic alluvial plains in the Tendaho, Assaita, Dit Behri area, and the terminal lakes area. The 1.2 km long Awash River rises at an altitude of approximately 2.500 m in the high plateau some 150 km of Ethiopia's capital and major urban center Addis Ababa (Wehner, 2001).

2.2. Climate Change

Climate change is the average deviation climate variable weather over a long period of time. According to Solomon *et al.*, (2007) defines climate change as “a change in the state of the climate that can be identified by changes in the average and/or the variability of its properties, and persist for an extended period of time, normally a decade or longer”.

2.3. Global climate change

Human activities such as the usage of fossil fuels, changes in land use (e.g. deforestation), agriculture and industrial activities contribute to the emissions of greenhouse gasses thereby increasing the concentration of greenhouse gases in the atmosphere. There is evidence that most of the warming observed over the last 50 years is attributable to human activities (IPCC III, 2001).

The largest known contribution comes from the burning of fossil fuels, which releases carbon dioxide gas into the atmosphere (Solomon, 2007). In the same report it is also indicated that the global mean surface temperature has increased by about 0.74°C (0.56°C to 0.92°C) over the past hundred years (between 1906 and 2005) and without further action to reduce greenhouse gas emission the global average surface temperature is projected to be likely increased further by 1.8- 4.0°C this century (Bernstein *et al.*, 2008).

2.4. Climate change in Ethiopia

According to Gissila *et al.*, (2004) based on the 42 meteorological stations, the country has experienced both dry and wet years over the last 50 years. Trend analysis of the annual rainfall showed there was a declining trend in the northern half of the country and southern Ethiopia while there is an increasing trend in the central part of the country (Cheung *et al.*, 2008). Associated with rainfall and temperature change and variability, there were recurrent drought and flood events in the country. There was also an observation of water level rise and dry up of lakes in some parts of the region depending on the general trend of the temperature and rainfall pattern of the regions (Abraham *et al.*, 2007). However, the general trend showed there was an increase in temperature over the last 50 years. The average annual minimum temperature over the country has been increasing by about 0.25 °C every ten years while the average annual maximum

temperature has been increasing by about 0.1 °c. The study also noted that the minimum temperature is increasing at a higher rate than the maximum temperature.

Different studies using many GCMs in the Nile Basin and northwest of the Upper Awash River Basin indicated that the streamflow in the basin will be potentially reduced in the upcoming years due to the changing climate (Getahun 2018). On the other hand, there have been studies that indicated the increase in streamflow for the coming decades, for instance, Abraham *et al.*, (2007) study on Ziway Catchment, which is are Awash River Basin indicates that the increasing trend of both climatic variables, such as the increase in precipitation seems to be suppressed by increases in temperature that results in insufficient streamflow in the future.

2.5. Climate change scenarios and Global Circulation Models (GCMs)

Climate scenario refers to a possible future climate that has been constructed for explicit use in investigating the potential consequence of anthropogenic climate change (Kattsov *et al.*, 2013). A scenario is not a forecast; rather, each scenario is one alternative image of how the future can unfold. The range of possible scenarios is determined by assumptions in the future's energy demand, emission of greenhouse gases, and land-use change and climate behavior in long time periods (Riahi *et al.*, 2011). Impact assessment studies can be done using various types of climate scenarios. The most common method is to use scenarios that are based on different climate model outputs (Riahi *et al.*, 2011).

2.5.1. Emissions Scenarios

Climate models are used for a variety of purposes from the study of dynamics of the weather and climate system to projections of future climate (Feser *et al.*, 2011). According to Ming *et al.*, (2005) over NOAA's Geophysical Fluid Dynamics Laboratory has created several ocean-atmosphere coupled models to predict how greenhouse gas emissions following different population, economic, and energy-use projections may affect the planet.

"Representative Concentration Pathways (RCPs) are not new, fully integrated scenarios (i.e., they are not a complete package of socioeconomic, emissions and climate projections) (Van Vuuren *et al.*, 2011). They are consistent sets of projections of only the

components of radiative forcing that are meant to serve as input for climate modeling, pattern scaling, and atmospheric chemistry modeling.

2.5.2. Development of Emission Scenarios

According to Wayne, (2013), there are many climate modeling teams around the world. If they all used different metrics, made different assumptions about baselines and starting points, then it would be very difficult to compare one study to another. In the same way, models could not be validated against other different, independent models, and communication between climate modelling groups would be made more complex and time-consuming (Knutti, 2008). Another problem is the cost of running models (Knutti, 2008). The powerful computers required are in short supply and great demand. Simulation programming that had to start from scratch for each experiment would be wholly impractical. Scenarios provide a framework by which the process of experiments can be streamlined (Van Vuuren *et al.*, 2014). In order to address these issues, in 1992 the Intergovernmental Panel on Climate Change (IPCC) published the first set of climate change scenarios, called IS92 (Leggett *et al.*, 1992). In the year 2000, the IPCC released a second generation of projections, collectively referred to as the Special Report on Emissions Scenarios (SRES) (CHANGE-IPCC, 2000). These were used in two subsequent reports; the Third Assessment Report (TAR) and Assessment Report Four (AR4) and have provided common reference points for a great deal of climate science research in the last decade. In 2007, the IPCC responded to calls for improvements to SRES by catalyzing the process that produced the Representative Concentration Pathways (RCPs). The RCPs are the latest iteration of the scenario process, and are used in the next IPCC report - Assessment Report Five (AR5) in preference to SRES.

According to Pachauri *et al.*, (2014) over the Intergovernmental Panel on Climate Change (IPCC), Fifth Assessment Report (AR5) is due for publication in 2013-14. Its findings were based on a new set of scenarios that replace the Special Report on Emissions Scenarios (SRES) standards employed in two previous reports. The new scenarios are called Representative Concentration Pathways (RCPs). There are four pathways: RCP8.5, RCP6, RCP4.5, and RCP2.6 - the last is also referred to as RCP3-PD. (The numbers refer to forcing for each RCP; PD stands for *Peak and Decline*) (Wayne, 2013). One high pathway for which radiative forcing reaches $> 8.5 \text{ W/m}^2$ by 2100 and continues to rise for

some amount of time; two intermediate “stabilization pathways” in which radiative forcing is stabilized at approximately 6 W/m² and 4.5 W/m² after 2100; and one pathway where radiative forcing peaks at approximately 3 W/m² before 2100 and then declines. These scenarios include time paths for emissions and concentrations of the full suite of GHGs and aerosols and chemically active gases, as well as land use/land cover (Wayne, 2013).

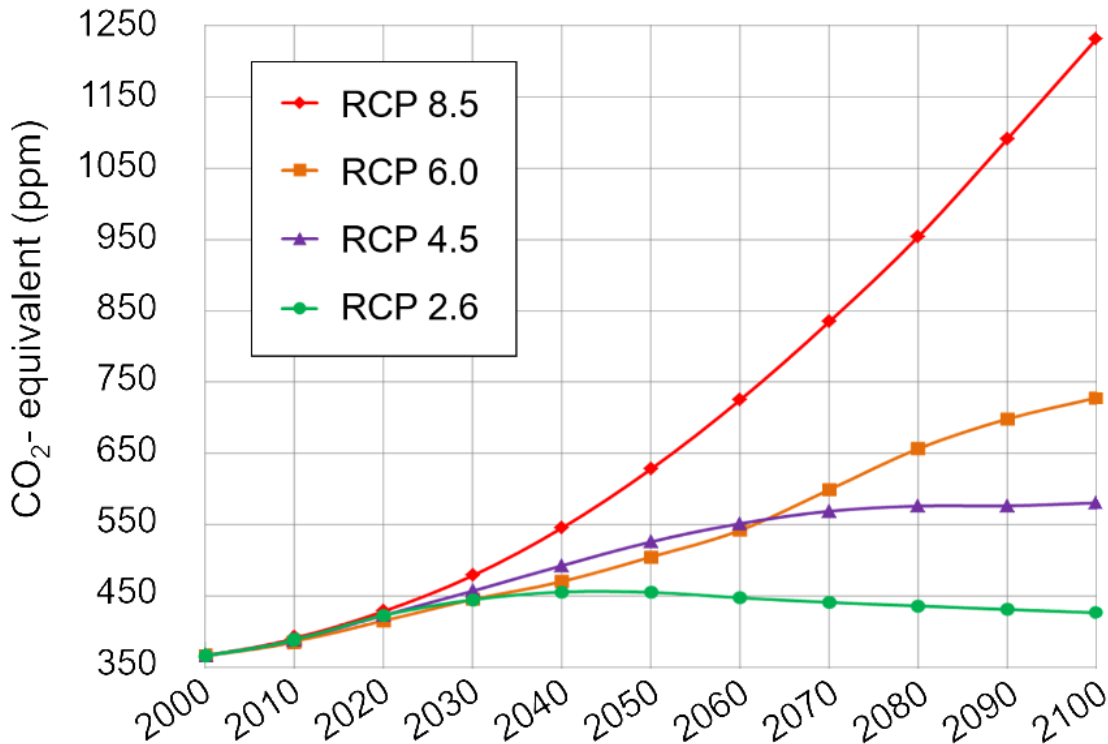


Figure 2.1 IPCC AR5 Greenhouse Gas Concentration Pathways (source: http://en.m.wikipedia.org/wiki/Representative_Concentration_Pathway)

2.5.3. General Circulation Models

According to IPCC, (2014) (www.ipccdata.org/guidelines/pages/gcm_guide.html) General Circulation Models or GCMs, representing physical processes in the atmosphere, ocean, cryosphere and land surface. And also the most advanced tools currently available for simulating the response of the global climate system to increasing greenhouse gas concentrations (Rahman, 2019). While simpler models have also been used to provide globally- or regionally-averaged estimates of the climate response, only GCMs, possibly in conjunction with nested regional models, have the potential to provide geographically

and physically consistent estimates of regional climate change which are required in impact analysis.

2.6. Climate downscaling Approach's

General Circulation Models (GCMs) are used to study the change of climate due to increases in greenhouse gases in the atmosphere. As GCMs operate on large spatial scales, and, furthermore, as the GCM-simulated temporal resolution corresponds to monthly averages at best, the usefulness of GCM data in impact studies and other applications is limited (Rummukainen, 1997). The present-day free troposphere is modeled relatively well by the course GCMs, whereas local or even regional characteristics in surface or near-surface climate variables, their variability and the likelihood of extreme events cannot be obtained directly from GCMs. The same is likely true in the case of climate change experiments with GCMs. The results from GCMs can be superimposed on climatological local scale time series or interpreted in some other way in order to address the needs of impact studies. This is known as "downscaling" of GCM simulations (Rummukainen, 1997).

GCMs used for climate studies and climate projections are typically run at spatial resolutions of the order of 150 to 200 km and are limited in their ability to resolve important sub-grid scale features such as convection clouds and topography (Flato *et al.*, 2014). As a result, GCM based projections may not be robust for local impact studies.

To overcome this problem, downscaling methods are developed to obtain local scale weather and climate scale, particularly at the surface level, from regional-scale atmospheric variables that are provided by GCMs.

Principally any data can be refined by downscaling techniques (Christensen *et al.*, 2010). Coarse GCM output might be satisfactory, for example when the variation within a single grid cell is low or in case of a global assessment. The main advantage of information directly obtained from GCM is the certainty that physical consistency remains unattached (Mearns *et al.*, 2003). GCMs are valuable predictive tools, but they cannot account for fine-scale heterogeneity and reflect on features like mountains, water bodies, infrastructure, land-cover characteristics, convective clouds, and coastal breezes. Bridging this gap between the resolution of climate models and regional and local scale processes represents a considerable challenge. Moreover, the uncertainties that

characterize the GCMs/RCMs are generally aggravated when these models are downscaled, which is the crucial step for identifying the city-specific impacts and, consequently, to identify vulnerabilities. Hence, the climate community put significant emphasis on the development of techniques for downscaling (Fowler *et al.*, 2007).

There are many approaches to the downscaling technique some of them conventional downscaling methods, Stochastic method, composite method, dynamical method and statistical methods (Rummukainen, 1997). But two of them are recently used technique. One form is dynamical downscaling, where the output from the GCM is used to drive a regional, numerical model in higher spatial resolution, which therefore is able to simulate local conditions in greater detail (Wilby *et al.*, 2004). The other form is statistical downscaling, where a statistical relationship is established from observations between large scale variables, like atmospheric surface pressure, and a local variable, like the wind speed at a particular site (Wilby *et al.*, 2004). The relationship is then subsequently used on the GCM data to obtain the local variables from the GCM output.

2.6.1. Coordinated Regional Climate Downscaling Experiment (CORDEX)

An important aspect of regional modeling is that it lends itself easily to fragmentation, as different groups or individuals are often interested in different problems or regional settings. However, the use of common modeling protocols offers invaluable opportunities to better understand models, processes, and uncertainties (e.g., the Climate Model Intercomparison Project Klimont *et al.*, (2013) for GCM research). Within the RCM community, a number of regional Intercomparison projects have occurred some of them are for instance (Mearns *et al.*, (2013): Curry and Lynch, (2002): Fu *et al.*, (2005):(Paeth *et al.*, (2011)) which have led to considerable improvements in the understanding of RCMs. However, differences in model setups and simulation protocols have made it difficult to transfer knowledge from one regional program to another. It has been recognized that global coordination of such efforts can further advance RCM development, analysis, and application (Takle *et al.*, 2007) but it was not until the inception of CORDEX that a truly globally coordinated downscaling framework was established. CORDEX represents a major evolution in downscaling research and has now become the main international reference framework for downscaling activities.

CORDEX represents the first attempt at full worldwide coordination of regional downscaling work using a common experimental framework. The CORDEX vision is to advance and coordinate the science and application of regional climate downscaling through global partnerships. Its main goals (Giorgi *et al.*, (2009): Jones *et al.*, (2011)) are as follows: To improve understanding of relevant regional/local climate phenomena, their variability, and changes, through downscaling, To evaluate and improve regional climate downscaling models and techniques (including both dynamical and statistical downscaling), To produce coordinated sets of downscaled climate projections for regions worldwide and To foster communication and knowledge exchange with the users of regional climate information.

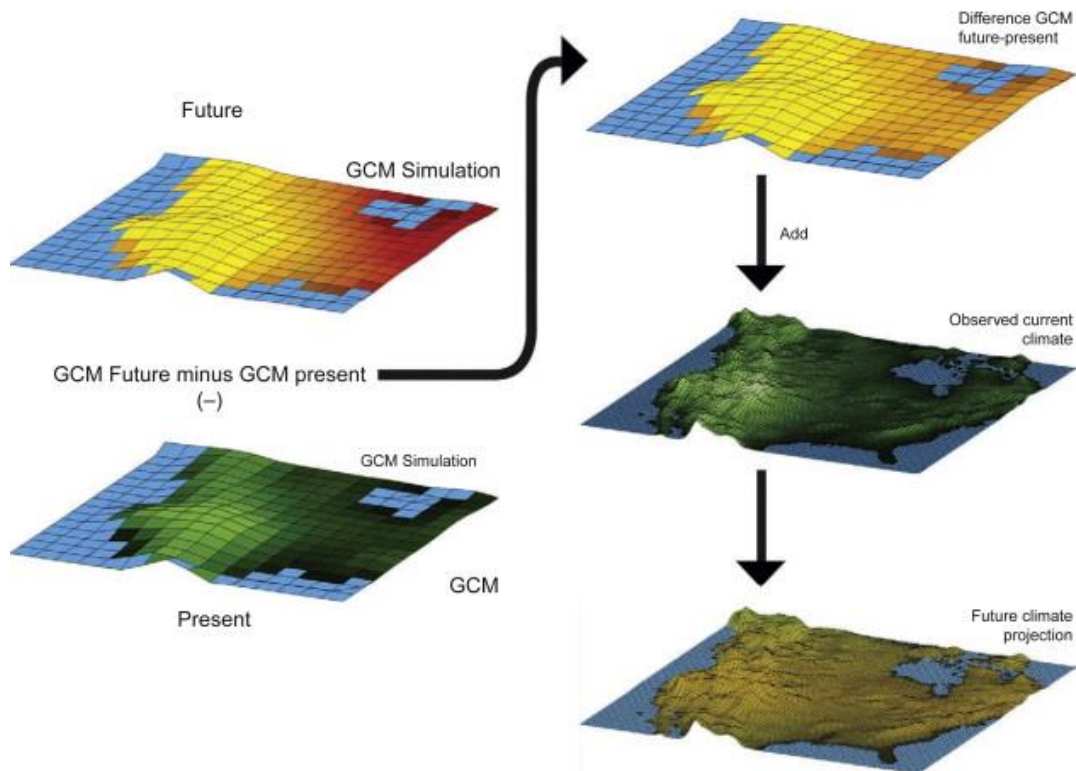


Figure 2.2. An over view of General Circulation Model (source: <https://www.sciencedirect.com/topics/earth-and-planetary-sciences/general-circulation-model>)

2.7. Uncertainties in Regional Climate Projections

The process of producing downscaled climate change projections for assessments is affected by different sources of uncertainty (Giorgi, 2005). The first step in a regional projection consists of running GCMs for a historical period (say 1850–2014) using observed or reconstructed natural and anthropogenic forcing (GHG concentration, solar activity, volcanic eruptions). This is followed by a transient future climate simulation for the twenty-first century (2015–2100) using scenarios of time-evolving GHG concentrations. A range of time-dependent twenty-first century GHG concentration scenarios have been proposed (called the representative concentration pathways (RCPs)), going from the low-end RCP 2.6 and RCP 4.5 to the high-end RCP 8.5 (Moss *et al.*, 2010).

Another uncertainty source is associated with the GCM response to a given GHG scenario forcing, often referred to as the GCM structural uncertainty. This is because GCMs have different representations of dynamical and physical processes and thus respond differently to the same GHG forcing. The structural uncertainty provides a substantial contribution to the full uncertainty range both in near-term and late twenty-first century projections (Hawkins and Sutton, 2009) and (Hawkins and Sutton, 2011). In fact, different RCMs can produce substantially different projections even when driven by the same GCM, especially for variables related to convection and for tropical domains (Paeth *et al.*, 2011). Finally, in the assessment of a projection, it is important to evaluate to what extent systematic model errors (by both GCMs and RCMs) affect the projection itself, which we can call systematic error uncertainty. A full characterization of these uncertainty sources is critical for the provision of climate information for work and, in principle, would require the completion of a multidimensional matrix of simulations sampling the different dimensions of the uncertainty space, i.e., ensembles of multiple scenarios, multiple GCMs, multiple realizations for each GCM, multiple RCMs, and multiple downscaling techniques (Giorgi *et al.*, 2008). Given that the size of this matrix can rapidly lead to extremely large ensembles, it is important to design optimal GCM-RCM experiment matrices to best explore the uncertainty space while limiting the ensemble size, and the selection of this optimal matrix is still an active area of research (McSweeney *et al.*, 2015). Statistical principles of experiment design should govern the

development of appropriate matrices, which can allow the extraction of different sources of uncertainty (Mearns *et al.*, 2013).

2.8. Soil and Water Assessment Tool (SWAT)

The Soil and Water Assessment Tool (SWAT) model has proven to be an effective tool for assessing water resource and non-point source pollution problems for a wide range of scale and environmental conditions across the globe (Arnold and Fohrer, 2005). The development of SWAT is a continuation of the United States Department of Agriculture (USDA) Agricultural Research Service (ARS) modeling experience that spans a period of roughly 30 years (Arnold *et al.*, 2012). Early Origins of SWAT can be traced to previously developed USDA ARS models including Chemicals, Runoff, and Erosion from Agricultural Management Systems (CREAMS) model Agricultural Management Systems (GLEAMS) model (Leonard and Knisel, 1995) and The current SWAT model is a direct descendant of the Simulator for Water Resources in Rural Basins (SWRRB) model Gassman *et al.*, (2013), which was designed to simulate management impacts on water and sediment movement for ungaged rural basins across the U.S. SWRRB begin to develop 1980s additional modification of the daily rainfall, expansion of surface runoff and other computation for up to ten subbasin. Then 1995 Arnold developed the routing output to outlet (ROTO) to support the assessment of downstream impact of water management and ROTO merge into single SWAT in this case the model retained all the feature that made SWRRB such valuable simulation model allowing simulation of very extensive areas (Gassman *et al.*, 2007). Finally, SWAT created with an enhancement of different versions of model (SWAT 94.2, 96.2, 98.1, 99.2 and 2000).

Soil and Water Assessment Tool is also a non-point source pollution model with the capability of simulating hydrology, missing weather elements, sediment and pollutant transport (Borah and Bera, 2003). It is capable to simulate long-term processes based on daily time steps. SCS curve numbers can also be varied throughout the year to take into account variations in the management conditions. SWAT divides the catchment into Hydrologic Response Units (HRU) that has uniform properties (Winchell *et al.*, 2010). Edge-of filter strips may be defined in an HRU (Kalin and Hantush, 2003). The filter strip trapping efficiency for sediment is calculated empirically as a function of the width of the

filter strip. When calculating sediment movement through a water body, SWAT assumes the system is completely mixed. Settling occurs only when the sediment concentration in the water body exceeds the equilibrium sediment concentration specified by the user (Kalin and Hantush, 2003). The sediment concentration at the end of a day is determined based on an exponential decay function (Kalin and Hantush, 2003). SWAT also simulates the buildup and wash off mechanisms similar to the SWMM model. SWAT has its own GIS interface and currently integrated into USEPA's BASINS and USDA's AGWA modeling systems (Gupta, 2009). SWAT is also linked to the water quality model QUAL2E (Kalin and Hantush, 2003).

2.9. Previous studies on climate change and SWAT application

2.9.1. Studies on Climate change over the awash basin

Previous studies which examine the climate change in the Awash basin, as well as Mojo catchment, includes Jilo *et al.*, (2019) focus investigate the impacts of climate change on sediment yield from the Logiya catchment in the lower Awash Basin, Ethiopia using CORDEX-Africa using Hadley Global Environment Model 2-Earth System (HadGEM2-ES) under representative concentration pathway (RCP) scenarios (RCP4.5 and RCP8.5) and finally conclude that climate variable increments were expected to result in intensifications in the mean annual sediment yield of 4.42% and 8.08% for RCP4.5 and 7.19% and 10.79% for RCP8.5 by the 2030s and the 2060s, respectively.

Another study Getahun, (2018) which is based on the comparison of old SRES and new RCP scenarios, GCMs that include CMIP3 and CMIP5 in correspondence with SRES A2, RCP4.5, and RCP8.5 scenarios using HVB hydrological model and finally conclude that The projected streamflow increase using RCP was 12% for intermediate and 29% for far future, whereas using SRES it was a decrease in 2% for intermediate and an increase in 4% for far future. Also Taye, (2018) also by quantifying the potential impact of climate change on water availability of the Awash basin in different seasons used three climate models from Coupled Models Inter-comparison Project phase 5 (CMIP5) and for three future periods (2006–2030, 2031–2055, and 2056–2080) and The projections for the future three periods show an increase in water deficiency in all seasons and for parts of the basin, due to a projected increase in temperature and decrease in precipitation. Res and Hailemariam, (1999) in the other hand, the impact of climate change on the water

resource of Awash river basin with an attempt is made to investigate the sensitivity of water resources to climate change in the Awash River Basin in Ethiopia by dividing the basin into 3 sub-catchments for better resolution in calibration and simulation station based meteorological data were processed to obtain areal averages necessary for the simulation. Different sets of temperature and rainfall scenarios were developed using GCM (both transient and CO₂ doubling) and incremental scenarios. Integrated water balance model (WatBal) was used to estimate runoff under a changing climate and finally conclude that the impact assessment over the basin showed a projected decrease in a runoff, which ranged from -10 to -34%, with doubling of CO₂ and transient scenarios of CO₂ increase (GFD3, CCCM, GF01). Sensitivity analysis based on incremental scenarios showed that a drier and warmer climate change scenario results in a reduced runoff, respectively.

2.9.2. Studies using SWAT analysis over the Mojo Catchment

SWAT has been widely used for the determination of the performance of catchment s for land-use/landcover changes and climate variability. This is done in the form of sensitivity analysis where baseline conditions of climate and streamflow are established and then used to compare the effect on streamflow due to changes in precipitation, temperature and other climate variables. These analyses provide information on the direction and change of magnitude of streamflow and insight into which variables are most significant in predicting these changes. This would be very important for decision-makers who require such information to evaluate management alternatives or the effects of different climate scenarios, as well as to support policies about water allocations between various sectors such as agriculture, hydropower generation, ecosystems, domestic and industry. According to that Gonfa and Kumar, (2016) and Gonfa *et al.*, (2015) which is focused on sediment and runoff estimation by SWAT model classifying the soil erosion hazard area namely none to slightly, moderate and highly-serve and very-serve then finally suggested that Areas with higher runoff condition and higher erodibility characteristics due to poor soil physical properties contributed for a higher sediment yield than others, and also in 2015 in order to generate basic technical information on optimal land use planning for stakeholders and decision maker a multi-objective linear programme optimization model was developed for Mojo catchment on solving the problem using a Goal computer

program net income from the catchment is increased by 29.91 % and soil erosion decreased by 16.14 % with the reduction of dry land farming by 18.45 % and increasing the current rangeland 946.36 ha to 15419.74 ha and 45.96 ha under irrigated agriculture to 25526.69 ha.

3. MATERIALS AND METHODS

3.1. Description of the study area

Mojo (also transliterated as Modjo) is a town in central Ethiopia, named after the nearby Modjo River. It is located in the Eastern Shewa Zone of the Oromia region, geographically lies between 38°54'22" to 39°17'18"E and 08°24'15" to 09°07'49"N with an elevation between 1607 and 3091 meters above sea level. Modjo River, the present study area is a perennial river that flows through Modjo, a town located some 43 km southeast of Addis Ababa. It is a tributary of Awash River receiving effluents. In addition, extensive agricultural practices and human settlements have been altering the catchment and riparian zone of the Modjo River. The catchment covers a surface area of 1601.84km² (Figure 3.1).

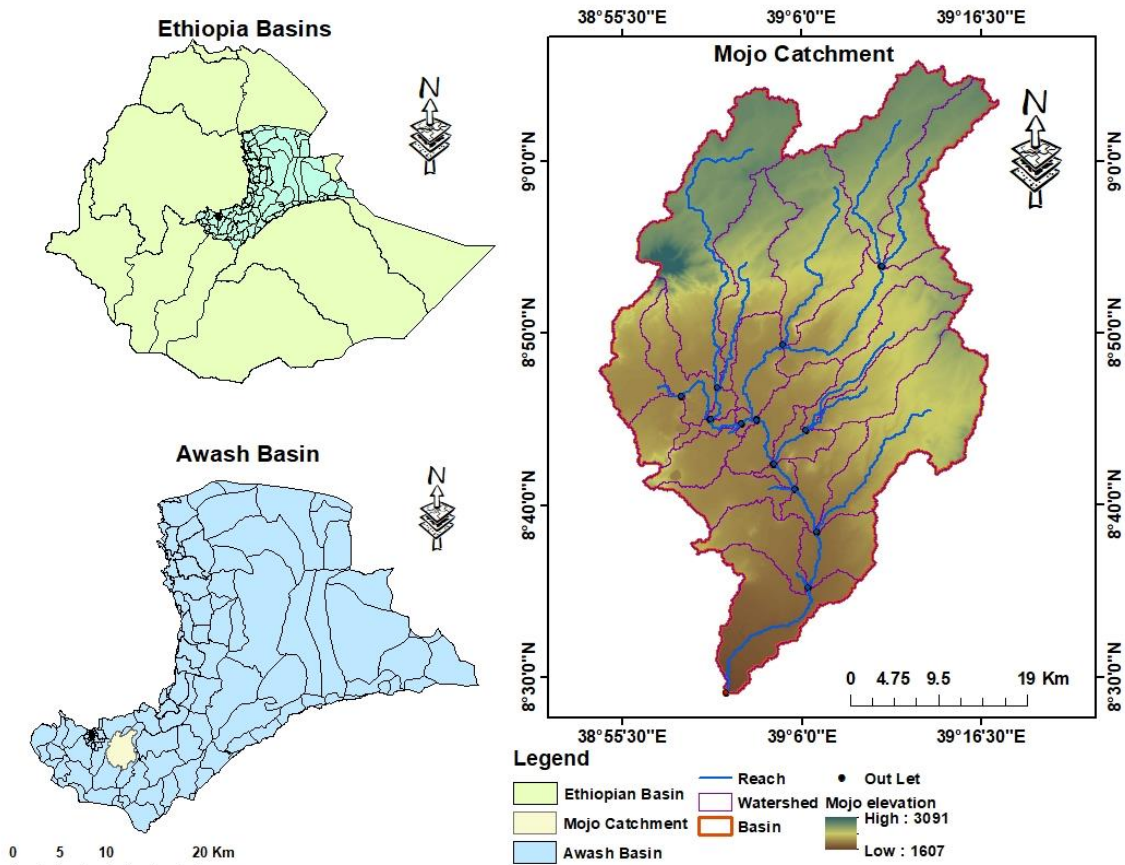


Figure 3.1 Location map of Mojo Catchment

3.1.1. Soil Type

According to the Ministry of Water and Energy's dominant soil types identified in the Mojo, the catchment includes Eutric Vertisols, Vertic cambisols, Haplic Luvisols, Luvic Phaeozems, and Lithic Leptosols covers, Chromic lavisols Mollic Andosols Figure (3.2) and Table (3.1) shows soil types and the area coverage of Mojo Catchment respectively which is extracted from awash basin soil map.

Table 3.1 Area coverage of soil type of Mojo catchment (source: Ministry of Water and Energy office)

Object id	Soil Type	Shape Area (Km)	Area (%)
1	Chromic lavisols	19.87	0.12
2	Eutric Vertisols	7150.92	44.64
3	Haplic Luvisols	867.52	5.42
4	Lithic Leptosols	157.67	0.98
5	Ludovic Phaeozems	696.62	4.35
6	Mollic Andosols	0.76	0.05
7	Vertic cambisols	7125.03	44.48

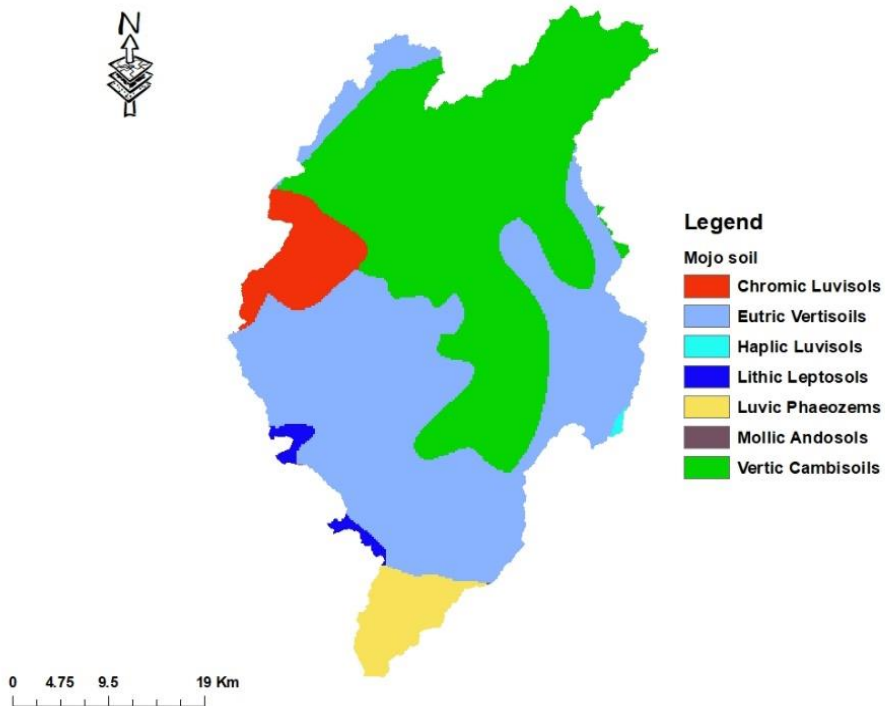


Figure 3.2 Soil map of Mojo Catchment

3.1.2. Land use

The dominant land use type in Mojo catchment is rainfed agricultural land. According to the Oromiya water and design office Land cover classification, the major land use found in the catchment areas are Agriculture, settlement, waterbody, sugarcane plantation, and others are available in the catchment (Figure 3.3).

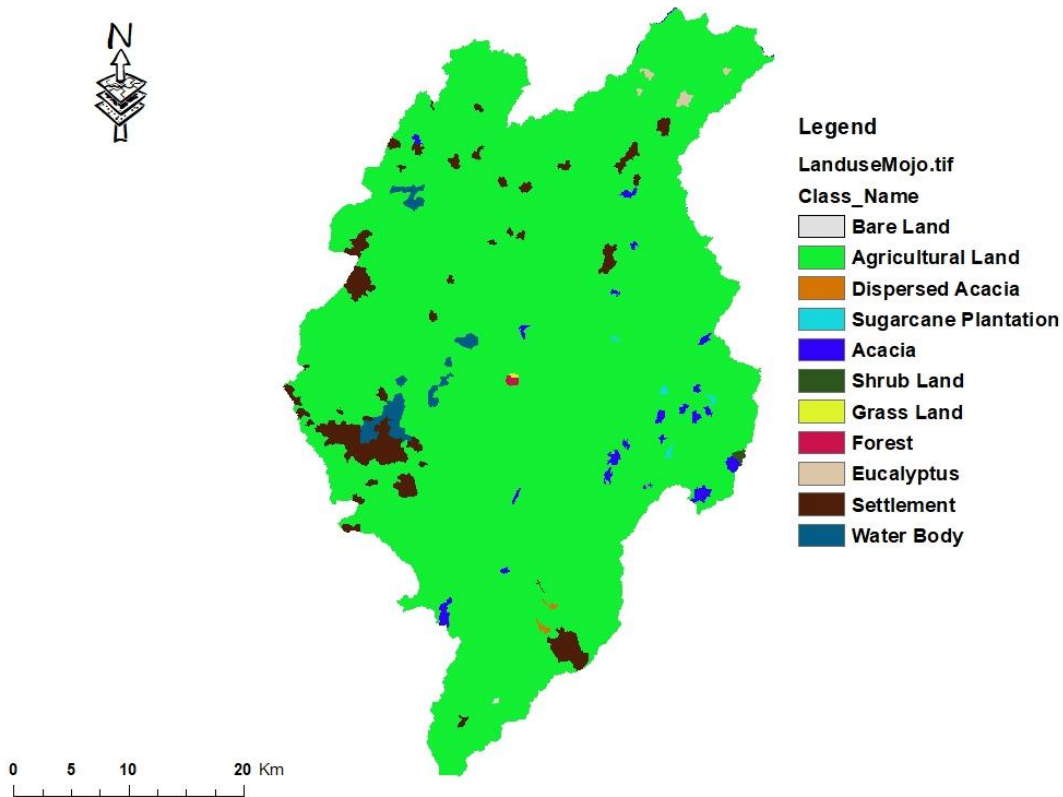


Figure 3.3 Landuse map of Mojo Catchment

3.1.3. Climate

The study area was reported to exhibit most rainfall occurs between June and October thirty years from (1980-2010) rainfall records for 4 stations within and adjacent to the study area show an average annual rainfall between 980.8 mm/day and 913 mm/day with a mean annual value of 947.3 mm air temperature that averaged 20.40 °C varying between a minimum of 11.6 °C in August and a maximum of 29.20 °C in May, with average annual temperature decreasing with an increase in altitude.

The climate data for 4 stations found within and nearby the Mojo River from 1980 to 2010 is collected from the Ethiopian National Meteorological Service Agency. However, there are missing for both precipitation and temperature. The three steps namely visual inspection, comparison to the nearest station with in the same zone, and regression relations between neighboring stations were taken to detect outliers and fill in the missing gaps in the data series.

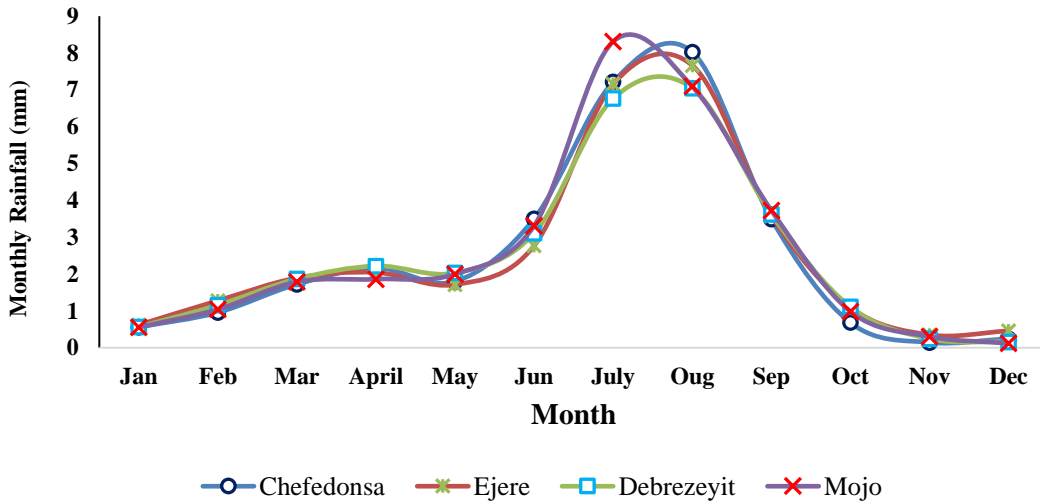


Figure 3.4 Mean monthly rainfall of Mojo catchment (1980 – 2005)

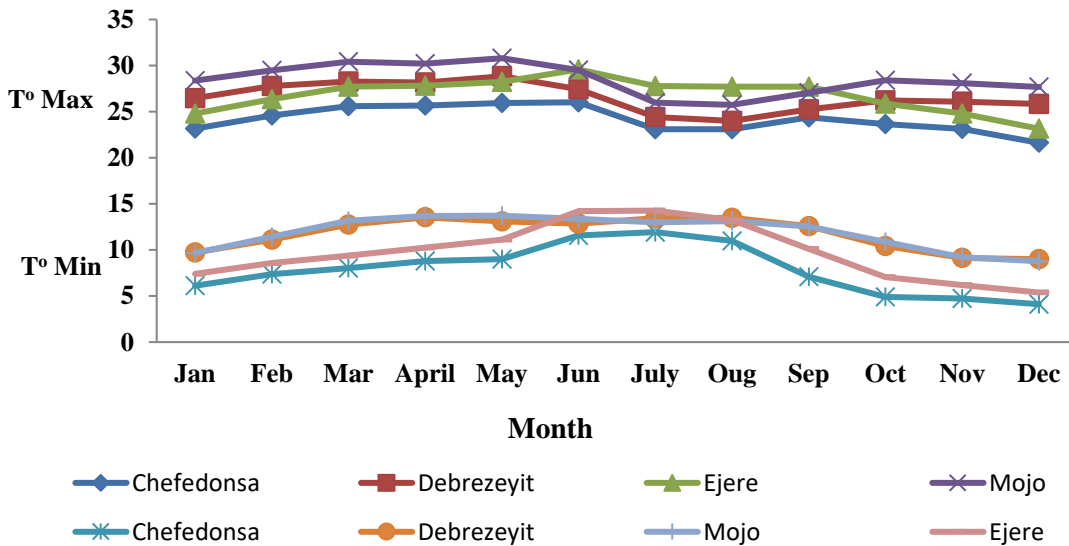


Figure 3.5 Mean monthly temperature maximum and minimum of Mojo catchment (1980 – 2005)

3.1.4. Hydrology

The Mojo catchment and its tributaries are a perennial source of water in the study area. The total annual mean flow of catchment 214.55 m³/s. Mojo river, which joins lake Koka from the north, the storage is mainly fed during the wet season from June to September. After being released through the dam the Awash descends into the Rift Valley northwest towards Awash Station from where the river follows the valley northwards into Gedebassa Swamp near Hertale. However, this river is highly polluted due to the discharge of chemicals from the various industrial plants located along the catchment (Gudeta, 2010). The Mojo River drains the area flowing southward and finally entering into the Koka reservoir. Other major surface water in the catchment includes Koka reservoir, Bishoftu, Hora, Kuriftu lakes. The catchment drains to Mojo river and to Koka hydroelectric power dam and finally into Awash River. The majority of the catchment particularly the central and lower part of the catchment has a monomodal rainfall pattern whereas the upper part of the catchment characterized as bimodal (Gonfa and Kumar, 2016).

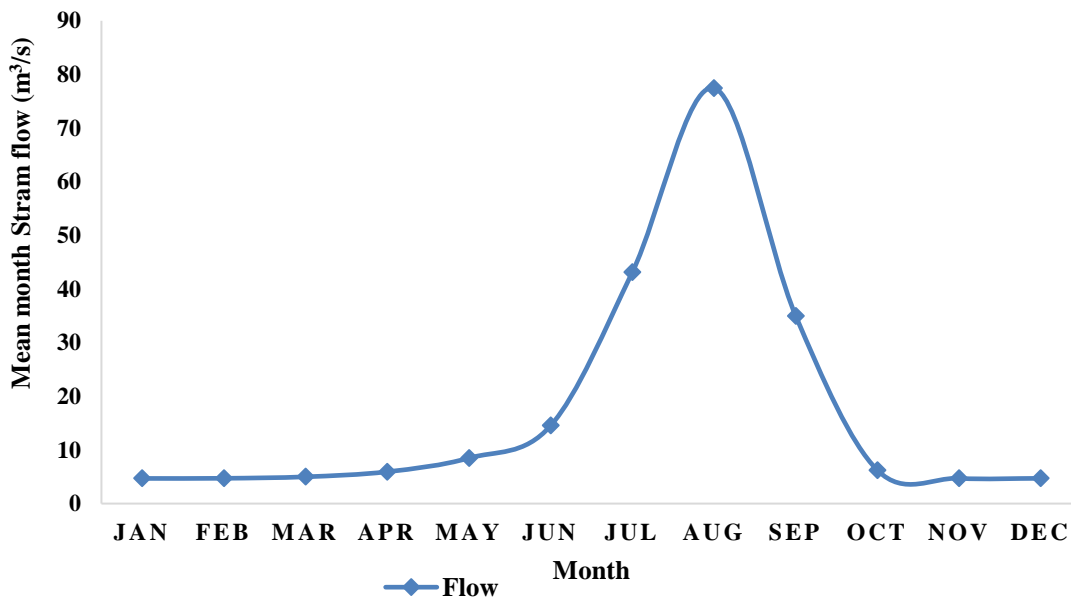


Figure 3.6 Mean Monthly streamflow of Mojo catchment (1981-2005)

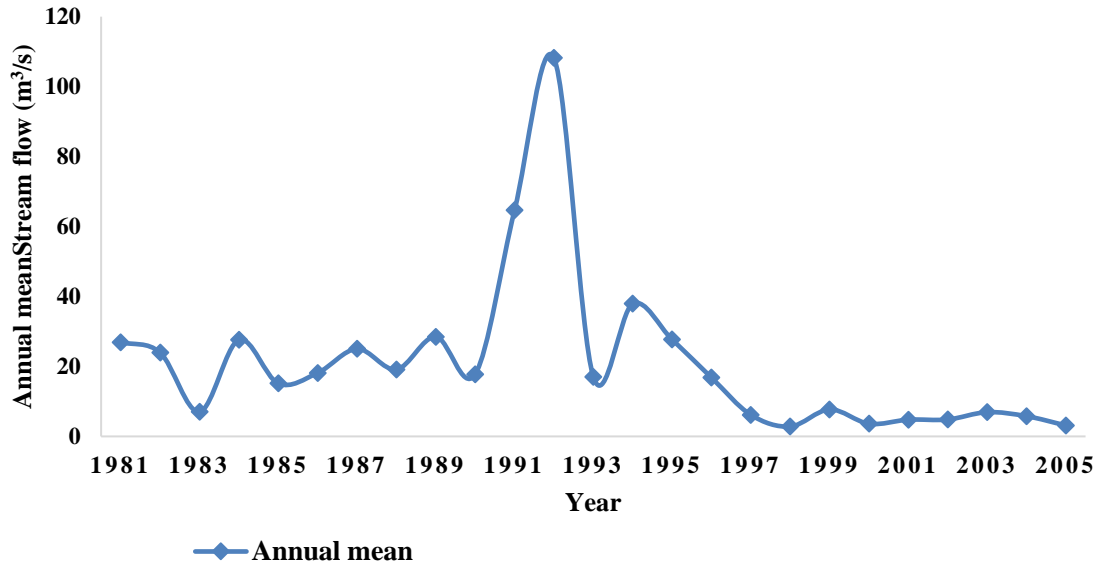


Figure 3.7 Annual mean streamflow of Mojo catchment (1981-2005)

3.2. Descriptions of the Materials

3.2.1. Data Availability

The Federal Ministry of Water Resources of Ethiopia (FMWRE) and the National Metrology Service Agency (NMSA) are the major sources of data required for this research.

3.2.2. Streamflow/River Discharge Data

Mojo River Basin has streamflow gauging stations found in the outlet Mojo River. The data which is from 1980-2010 is collected from the Ethiopian Ministry of Water, Irrigation, and Electricity and the outlet point is collected primarily using field Surveys.

3.2.3. Spatial data

Digital elevation model (DEM), 30*30 resolution is downloaded from (<https://urs.earthdata.nasa.gov>) and describes the elevation of any point in a given area at a specific spatial resolution as a digital file. DEM of the essential inputs required by SWAT: (1) to delineate the catchment into a number of sub-catchments or sub-basins and (2) to analyze the drainage pattern of the catchment, slope, stream length, a width of a channel within the catchment.

3.2.4. Climate Scenario Data

Climate change scenarios data from the newly available in the website (<https://esgf-node.llnl.gov/projects/esgf-llnl/>) CMIP5 RCM ensemble output of CORDEX-Africa for African domain projections under Representative Concentration Pathways (RCP4.5 and RCP8.5) is used as input to the hydrological model. RCP scenarios have a better resolution that helps in performing regional and local comparative studies compared to previous climate scenarios, and RCP scenarios also represent an attractive potential approach for further research and assessment, including emissions mitigation and impact analysis. RCP4.5 mid-range and RCP8.5 high-level climate scenarios with assumed stabilization of radiative forcing to 4.5 and 8.5 W/m² by 2100 respectively were expected to capture a reasonable range in climatic and hydrological projections for Mojo catchment. Precipitation and temperature data from these scenarios are available from an ensemble of CORDEX-Africa regional climate model for the domain of Ethiopia at 0.44° resolution from 1951 to 2005 for historical to calibrate and validate with observed data and 2006 to 2100 for future periods. The values of relative humidity, solar radiation, and wind speed in the historical period were used in a future scenario period without making any change, as the change in these values may not have a significant impact when modeling climate change scenarios. Some of the regional as well as global models which are available based on the domain AFR-44 in Appendix 12.

3.2.5. Soil and Land Use Data

Soil and land use/land cover data are used as input into the SWAT hydrological model to delineate sub-catchment s further into hydrologic response units (HRUs). The soil data used includes the information to describe the physical and chemical properties of the soil like soil texture, hydraulic conductivity, bulk density, water content, organic carbon content, and percentage of sand, silt, and clay content for each soil horizon. Land use/land cover influences the hydrological properties of the catchment and used as an input for the SWAT model. Mojo catchment land use/land cover changes in time to time due to several factors mainly changing agricultural practice, urbanization, new hydropower, and irrigation development. Soil 90*90 and land use/land cover 2010 data of Mojo catchment is obtained from the Ethiopian Ministry of Water, Irrigation, and Energy as a shapefile format.

3.2.6. Summary of Materials and Data used

Table 3.2 Data's and their source used for this study

Id	Data	Source of Data	Description
1	SRTM DEM 30*30	https://urs.earthdata.nasa.gov Ministry of water and energy office	Slope map, use for modeling For HRU analysis in SWAT modeling
2	Soil 90*90	Oromiya water and design office Ministry of water and energy office	For HRU analysis in SWAT modeling
3	LULC 2010	Oromiya water and design office Ministry of water and energy office	For HRU analysis in SWAT modeling
4	Streamflow	Eastern and middle Oromiya Metrological Agency	For performance checking with simulated data
5	Weather data Cordex-Africa RCP	https://esgfnod.llnl.gov/projects/e sgf-llnl/	For WGEN preparation For analysis of future climate scenario
6	4.5 and 8.5		

Table 3.3 Material and their purpose used in this study

Id	Name of software's	Purpose
1	Arc GIS 10.1	Uses for map preparation and uses SWAT models extension
2	Arc SWAT 2012	Act as a GIS interface for SWAT modeling
3	WGEN (Weather Generator)	For the preparation of weather data for the SWAT model
4	SWAT-Cup	SWAT calibration, validation, and sensitivity analysis
5	Xlstat	For data Quality analysis

3.2.7. Conceptual Framework of Overall Methodology

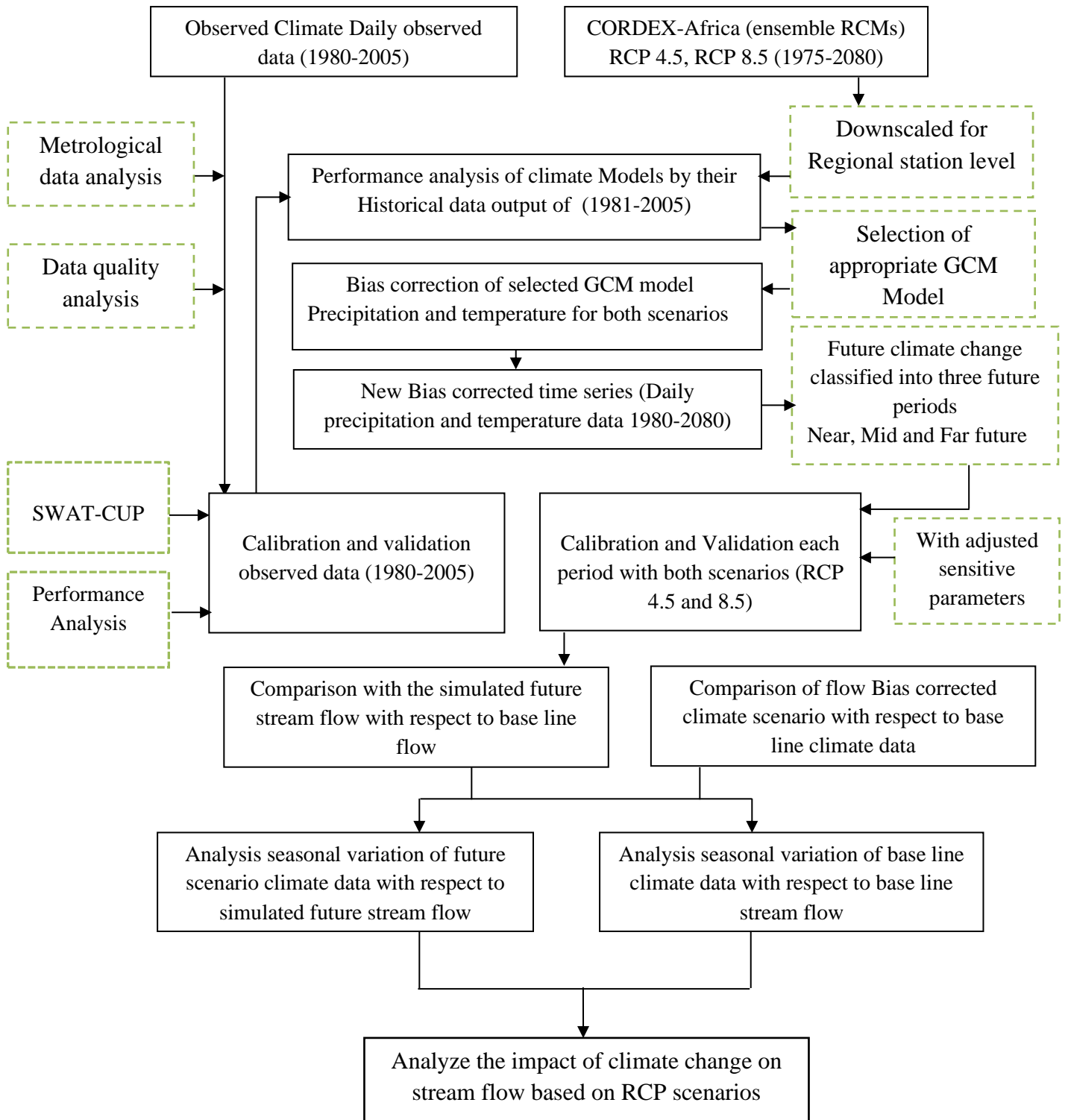


Figure 3.8 conceptual framework of the climate and SWAT model

3.3. Method of Data Quality Analysis

3.3.1. Metrological Data Analysis

Metrological data is the main input for hydrological modeling the station which is representing the catchment is selected based on the data availability including the existence of enough length of record and distance from the area of interest and also the location of the station available in the catchment area. Accordingly, four-station is available in the study area Table 3.4 and Figure 3.9

Table 3.4 List of meteorological stations used in the study

ID	Name	Latitude	Longitude	Elevation
1	Debrezeyit	8.73	38.95	1900
2	Modjo	8.61	39.11	1763
3	Chefedonsa	8.97	39.12	2392
4	Ejere	8.77	39.26	2254

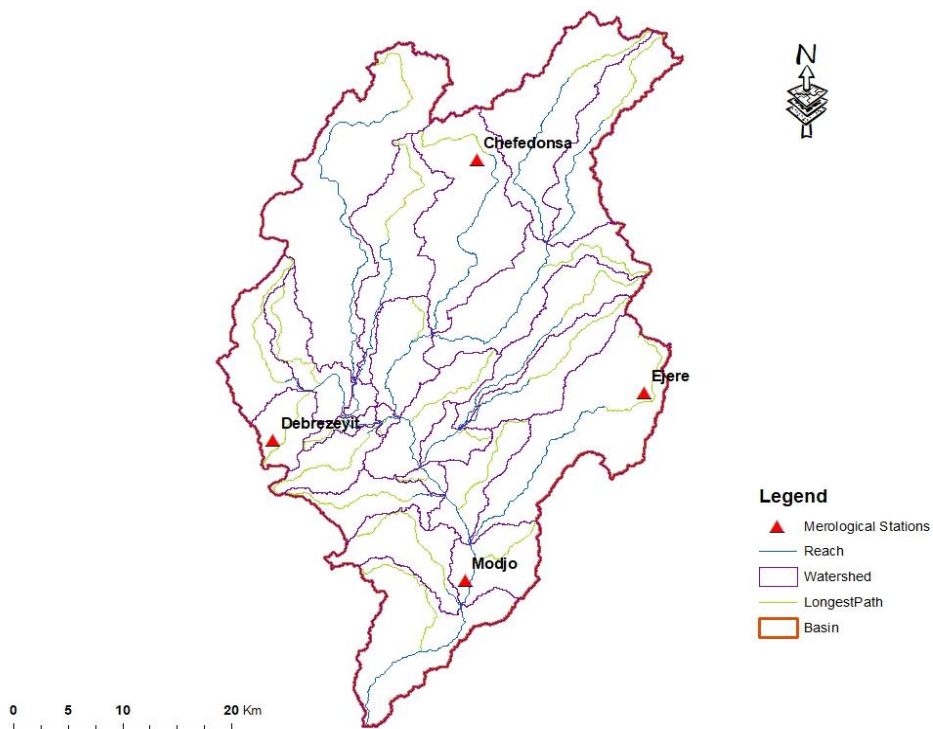


Figure 3.9 Metrological stations of Mojo catchment

3.3.2. Filling of missing data

In the modeling of climate, the complete record of hydrological data is very important in the case this climate data like temperature, rainfall, humidity, solar radiation and wind speed of four stations should be filled. Data for the period of those missing data could be filled using different estimation techniques (Ismail *et al.*, 2017). The arithmetic mean Normal ratio, Regression, and distance power method are the most commonly used methods for estimation of missing climate data sets. Estimation of missing data using Normal Ratio used if any the neighboring station has a normal annual and streamflow data which exceeds more than 10% (De Silva *et al.*, 2007). In this case, the Normal ratio method was used to fill the climate data because of the missing data which is greater than ten percent and also regression also used for streamflow data because far most hydrological data regression analysis gives us better approximation for missing data.

$$P_x = \frac{1}{N} * \left(\frac{N_x}{N_A} P_A + \frac{N_x}{N_B} P_B + \dots + \frac{N_x}{N_N} P_N \right) \quad (3.1)$$

Where P_x is the precipitation for a station with missing records $P_A, P_B \dots P_N$ is the corresponding precipitation at the index station and N_A, N_B, \dots, N_N and the long term mean monthly precipitation at the index and the station x under consideration respectively.

3.3.3. Data Quality Assessment

In engineering, water resource development and management studies hydrological as well as metrological data are more dependent so assessing the quality of those data should be properly managed. According to this thesis, the quality of the data passed through four methods.

I. Homogeneity test

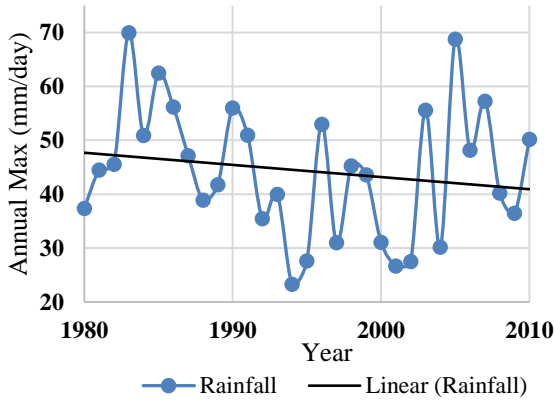
Homogeneity is an important issue to detect the variability of the data. In general, when the data is homogeneous, it means that all collection of data belongs to the same statical population having the time-invariant mean, therefore test of homogeneity of data series are based on evaluating the significance of change of mean value, However, it is a hard task when dealing with rainfall data because it is always caused by changes in measurement techniques and observational procedures, environment characteristics and

structures, and location of stations. There are a lot of methods used for analyzing the homogeneity for instance,, Haktanir and Citakoglu, (2014) and Yozgatligil and Yazici, (2016). In this study, the homogeneity analysis was used by the Pettitt test using XLSTAT software and calculated as:

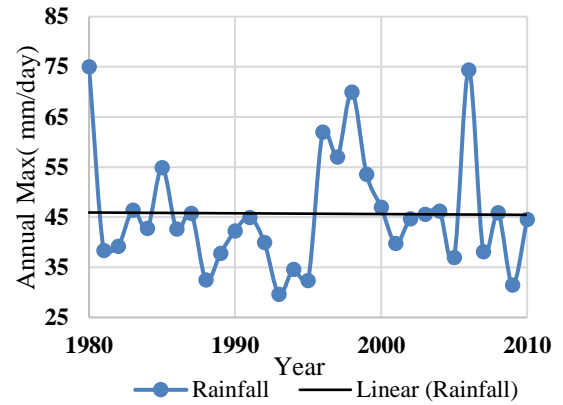
$$Z_k = 2 \sum_{i=1}^k R_i - k(n + 1), \quad k = 1, \dots, n \quad (3.2)$$

If a break occurs in year K , then the statistic is maximal or minimal near the year $k = K$. So, if the break occurs, then $Z_K = \max Z_k$. The figure (3.10) below and Appendix (1) shows that the homogeneity of rainfall and in all four metrological stations the data is homogeneous.

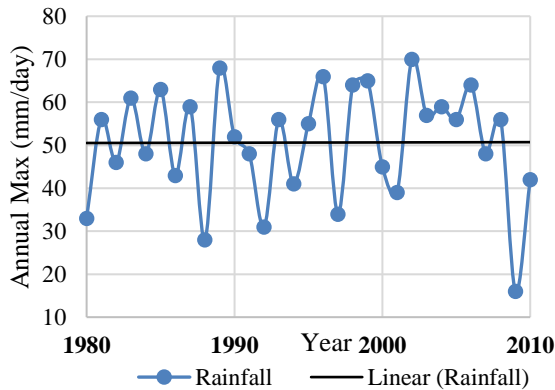
Chefedonsa (1980-2010)



Debrezeyit (1980-2010)



Ejere (1980-2010)



Mojo (1980-2010)

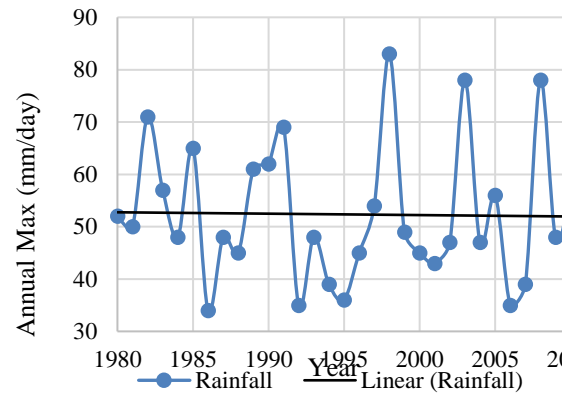


Figure 3.10 Homogeneity test of four rainfall station (1980-2010)

II. Consistency test

A consistency record is the one where the characteristics of the record have not to change with time. Inconsistency of rainfall data happens in different ways some of them caused by due to replacement of old instruments by a new one or shifting of the rain gauge station some of them by a change of ecosystem or observational error. Therefore, adjustment of the inconsistency of rainfall data used by the double mass curve method which is a widely used method. Analysis of inconsistency of hydrological data done by a different methods (Renard *et al.*, 2008) but The double mass curve is a graphical method for identifying and adjusting inconsistency more preferable in a station record by comparing its time trend with those of adjacent stations.

$$P_m = P_x \frac{M_c}{M_a} \quad (3.3)$$

Where P_m is the corrected precipitation of any time period t_1 at station x , P_x is the original precipitation of time period t_1 at station x M_c corrected slope of a double mass curve and M_a original slope of the mass curve. The graphical sketch below shows there is no slope variation between the time series data of all rainfall stations and all the selected stations are consistent.

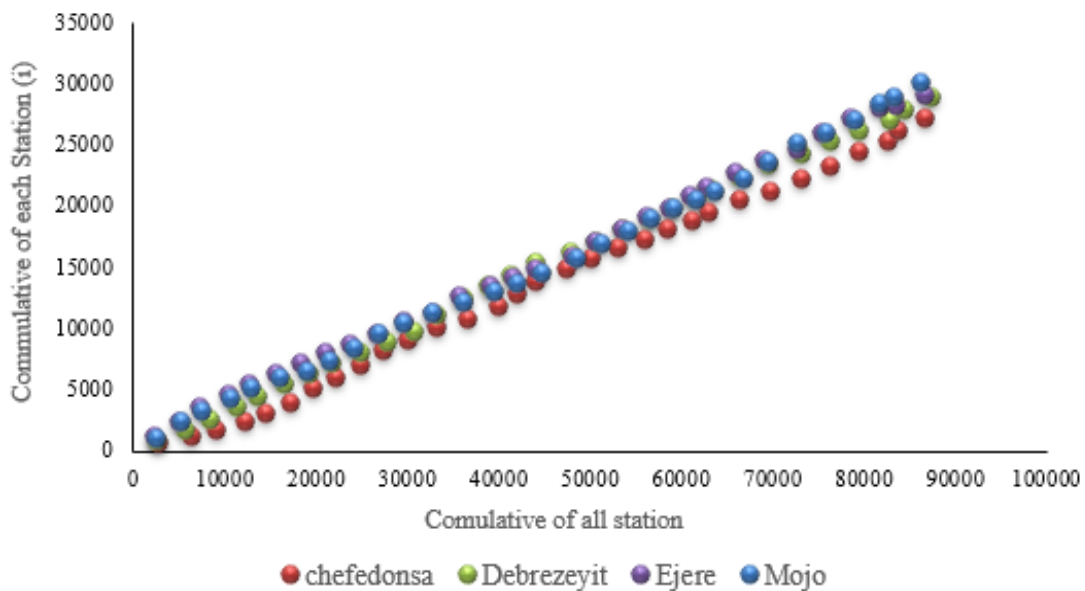


Figure 3.11. Consistency tests of rainfall data

III. Test of outlier

An outlier in maximum daily rainfall can play a considerable role in the unreal analysis leading to false prediction therefore accurate statistical determination of data to find the outlier is very important. The different methods of a testing outlier Garcia, (2012) conclude that The Grubbs and Beck method of a testing outlier is a more easy and better method. Outlier causes may be due to errors in data collection, or recording, or due to natural causes. In the present work data related to maximum daily rainfall obtained from the four stations and streamflow at Mojo station using Grubbs and Beck, (1972) test (G-B) used to detect outliers.

$$X_H = \exp(\bar{x} + K_N S) \quad (3.4)$$

$$X_L = \exp(\bar{x} - K_N S) \quad (3.5)$$

where \bar{x} and s is the mean and standard deviation of the natural logarithms of the sample, respectively, and k_N is the G-B statistic tabulated for various sample sizes and significance levels by Grubbs and Beck (1972) At the 10% significance level, where N is the sample size.

$$k_N = -3.62201 + 6.28446N^{\frac{1}{4}} - 2.49835N^{\frac{1}{2}} + 0.491436N^{\frac{3}{4}} - 0.037911N \quad (3.6)$$

Sample values greater than X_H are considered to be high outliers, while those less than X_L are considered to be low outliers. Analysis of the outlier in Appendix (2 and 3) shows that the rainfall from (1980-2010), as well as the stream flow from (1980-2010), shows that there is no outlier detected.

IV. Trend test Analysis

Information about the trend is important to highlight the spatial and temporal change of hydroclimatic variables and to gain knowledge of the status of development and suitability management of water resources in the future as well as to plan for the stability of the environmental condition. Trend analyses of precipitation and discharge are essential to study the impacts of climate change. There are different methods of detecting the trend mostly method which mostly familiar with is Mann-Kendall and Innovative Trend Analysis Method (ITAM).

According to Gedefaw *et al.*, (2018) trend analysis using the Mann-Kendall method is

better and easily detect than ITAM also due to analysis of Long-term trends in the observed data Mann-Kendall method gives a better result over the Awash basin. In this study, streamflow and the rainfall data of four stations are analyzed using the Mann-Kendall test using XLSTAT software and calculated as:

$$S = \sum_{i=1}^{n-1} \sum_{k=i+1}^n \text{sgn}(X_k - X_i) \quad (3.7)$$

In this calculation, the time series x_i is from $i = 1, 2, \dots, n - 1$, and X_k from $k = i + 1, \dots, n$.

$$\text{sgn}(X_k - X_i) = \begin{cases} -1, & \text{if}(X_k - X_i) > 0 \\ 0, & \text{if}(X_k - X_i) = 0 \\ -1 & \text{if}(X_k - X_i) < 0 \end{cases} \quad (3.8)$$

The normalized test statistic is calculated by the equation given below:

$$Z_c = \begin{cases} \frac{s-1}{\sqrt{\text{Var}(s)}} & S > 0 \\ \frac{s+1}{\sqrt{\text{Var}(s)}} & S < 0 \end{cases}, \quad \begin{matrix} S=0 \\ S < 0 \end{matrix} \quad (3.9)$$

The test statistic is Z_c and when $|Z_c| > Z_{1-\alpha/2}$, in which $Z_{1-\alpha/2}$ are the standard normal variables and α is the significance level for the test, H_0 will be rejected. The extent of the trend is given as follow:

$$\beta = \text{Median} \frac{X_i - X_j}{i - j}, \forall_j < i, \text{ where } 1 < j < i < n$$

A positive value of β displays an increasing trend, while a negative value of β displays a decreasing trend. The result of change point analysis indicated that the change point for mean annual streamflow and annual maximum rainfall was 1981-2005 and 1980-2010 respectively. As a result of trend analysis, a decreasing trend was found for mean annual flow (1997-2011) figure (3.12) and Appendix 4 and trend for rainfall show that from four metrological stations Debrezeyit and Mojo stations show that a decreasing trend figure (3.13) and Appendix 5.

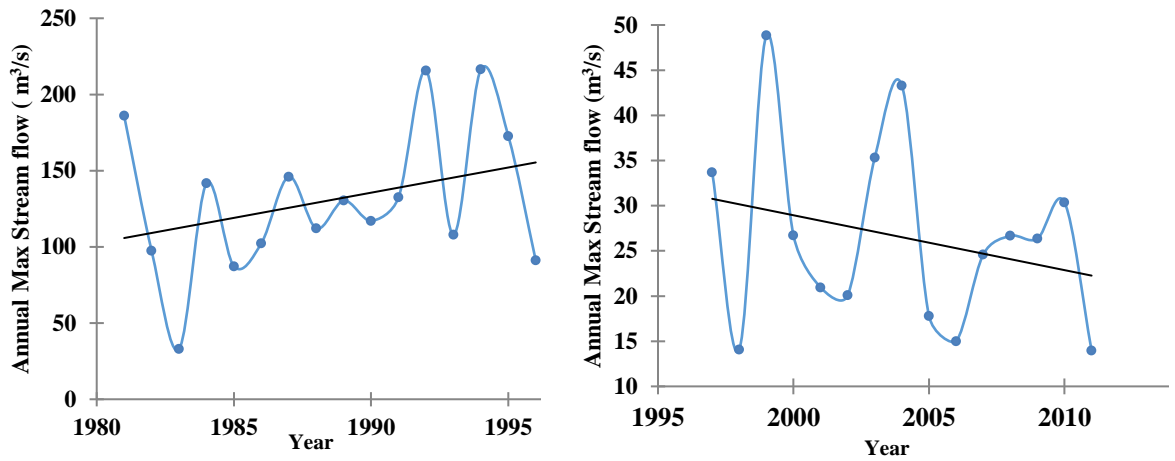
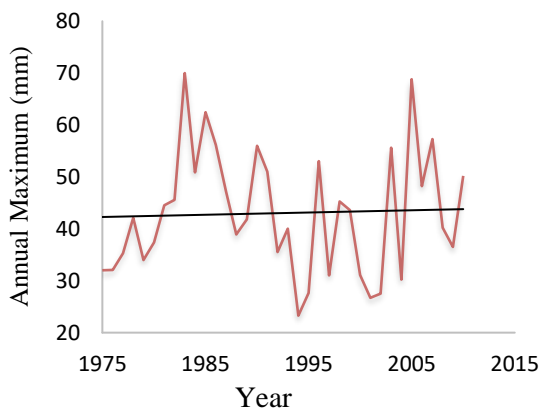
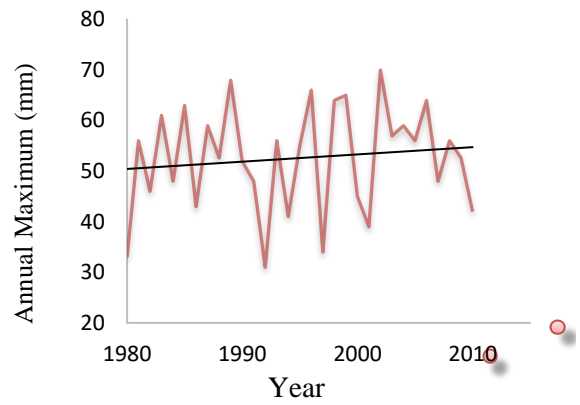


Figure 3.12 Annual Mean streamflow trend analyses 1981-2005

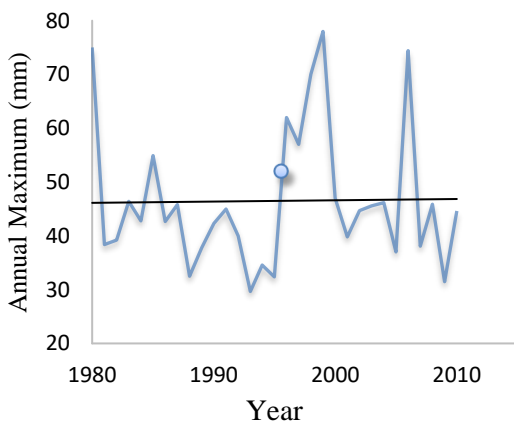
Chefedonsa (1980-2010)



Ejere (1980-2010)



Debrezeyit (1980-2010)



Mojo (1980-2010)

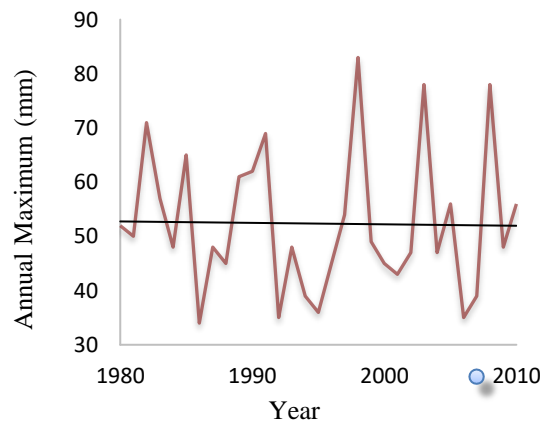


Figure 3.13 Annual maximum rainfall trend analysis of four stations (1980-2010)

3.4. Methodology

3.4.1. Data availability and collection of precipitation and temperature scenarios data

The data which needed for climate change analysis available on the website of (<https://esgf-node.llnl.gov/projects/esgf-llnl/>) portal those data are based on the project CORDEX-Africa (AFR-44) as experimental data which is historical, RCP 4.5 and RCP 8.5 of daily data scenarios, the time-frequency is daily data, Regional Climate Model (RCM) is RCA4, four different GCMs and The institute which is data available is SMHI. The table shows the candidate models download in order to analyze the impact of climate change.

Table 3.5 Candidate GCM Models

Global Climate Models (GCM)	Regional Climate Models
CCCma-CanESM2	RCA4
IPSL-IPSL-CM5A-MR	RCA4
MIROC-MIROC5	RCA4
MPI-M-MPI-ESM-LR	RCA4

The data which is downloaded from with the format of NetCDF and should be extracted using different extracting mechanisms of programming languages those are different programming language like R programming (<https://agrimetsoft.com/netcdf-extractor>), MatLab, and Netcdf extractor, etc. in this case, MatLab is used in order to extract the data.

The daily precipitation, temperature maximum and minimum from 1980 to 2100 was extracted from grid cells covering Mojo catchment. the period from 1980 to 2005 defended as the historical period, based on good quality of observational climatic data and hydrological data was used for model calibration and validation. In this study, the period 1981–2005 is used as the historical reference period and three-time slices are used for the future: Near future (2006–2030), mid future (2031–2055) and far future (2056–2080).

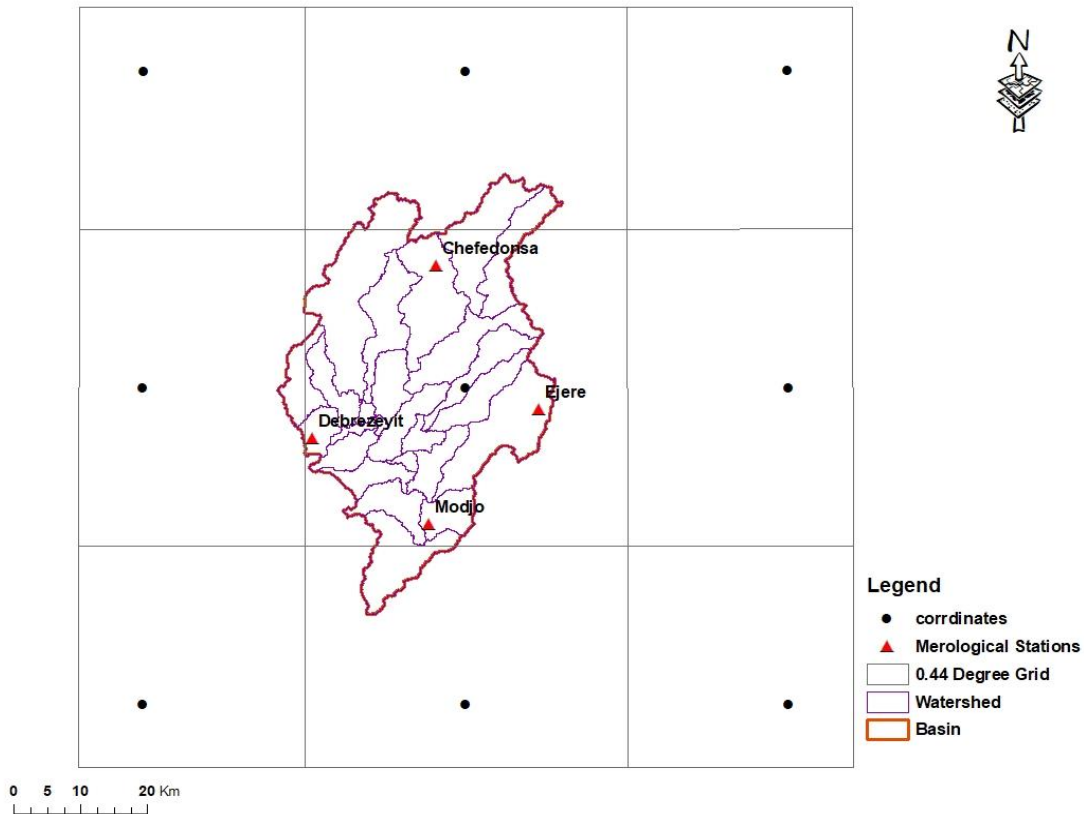


Figure 3.14 CORDEX-Africa 0.440 (50_50 km) grid data coordinates

3.4.1.1. Selection criteria for RCP and GCMs models

According to IPCC, (2014) report, four Emission scenarios available from those emission scenarios RCP 4.5 and RCP 8.5 are used. The emission scenarios RCP4.5 mid-range and RCP 8.5 high-level climate scenarios with assumed stabilization of radiative forcing to 4.5 and 8.5 W/m^2 by 2100 respectively were expected to capture a reasonable range in climatic, hydrological projections and The two Representative Concentration Pathways (RCPs), high concentrations scenario (RCP8.5: Moss *et al.*, (2010)) and moderate concentrations scenario (RCP4.5: Thomson *et al.*, (2011)) were chosen for this study because they are the most widely simulated global emission scenarios in all models. For Mojo catchment from these scenarios, precipitation and temperature are available in the Cordex-Africa regional climate model for the domain of 0.44⁰ (AFR-44) as historical scenarios and for calibration and validation of future data which is climate change scenario data.

Selection of GCMs models depends based on different criteria's some of them on the availability of data, according to (<https://esgf-node.llnl.gov/projects/esgf-llnl/>) portal CORDEX data for AFR-44⁰ with CMIP5 (fifth Coupled Model Intercomparison Project), based on experimental family historical and RCP, time-frequency and data provider institutes the availability of GCM model limited for those institutes which provide CORDEX-Africa data (CLMcom, DMI, GERICS, ICTP, KNMI, MPI-CSC, SMHI, UQAM) model description is discussed in (Appendix 6) and in recent year the mostly widely used institute is SMHI for instance (Pasten-Zapata *et al.*, (2019): Chokkavarapu and Mandla, (2019): Larsson, (2019)) because of the availability of more options over the requirement. In the other criteria, the GCM model also had a big factor in the selection of the models. The criteria for selecting the GCM models for analysis indicated in the Table (3.6).

Table 3.6 GCM Model selection criteria and their variables

Model selection criteria	Variables
Project	CORDEX
Institute	SMHI
Experiment	Historical, RCP 4.5, and 8.5
Ensemble	r1i1p1
Variable	pr, tmax, tmin
Time-frequency	Daily
Regional climate model (RCM)	RCA4
Domain	AFR-44

Where r1i1p1, which represents realization #1, initialization I #1, and physics p #1; SMHI: Swedish Meteorological and Hydrological Institute; RCA4: Rossby Centre; pr: precipitation; tmax: maximum temperature; tmin: minimum temperature.

3.4.1.2. Uncertainty in climate model selection

The selection of climate model was an order of magnitude more influential on uncertainty in the Streamflow, direct runoff, and evapotranspiration projections than that of parameter selection, but it was not always the case for groundwater and potential evapotranspiration (Her et al., 2019).

The Intergovernmental Panel on Climate Change IPCC, (2014), launched the Coupled Model Intercomparison Project Phase 5 (CMIP5) in the fifth Assessment Report (AR5), whereby a multi-GCM ensemble analysis was facilitated through the provision of climate model outputs that comply with community standards. Multi-GCM ensembles have served as a framework for accommodating probabilistic approaches in interpreting climate predictions and developing climate adaptation plans, and many studies have attempted to quantify uncertainty with the information of ensemble spread and to identify its sources (Her *et al.*, 2016). Ensemble averaging can improve the accuracy of a climate projection by allowing GCM errors to cancel each other out and GCMs that poorly performed to be down-weighted. However, the approach often does not employ all models available and thus may underestimate uncertainty and/or produce a bias in an ensemble prediction. According to Her *et al.*, (2019) selection of GCMs can be guided by various information including the amount of uncertainty in projections, the accuracy of reproducing historical data (or observations), perceived accuracy of climate models (based on an understanding of the simulation mechanisms), and the overall performance of the model.

3.4.2. Evaluation of the GCMs Models

Evaluating the GCM models is important in order to choose which model more appropriate to the area based on evaluation of observed data with each GCMs model after passing through sensitive parameters. Evaluation of the model includes trend Analysis and choosing a better perform model without bias correction of the GCMs Models and make bias correction and also indicating the density function of historical, observed and corrected results. After selecting the model mostly Hydrological models used to assess climate change in this case the SWAT model is used in order to analyze the climate change scenarios which is temperature and precipitation of different GCMs after bias correction on the Hydrology of Mojo catchment by the year 2080. For this purpose, average monthly changes in precipitation and temperature predicted by different GCMs have been taken and these estimates were used to adjust the daily time series of precipitation and temperature.

3.4.3. Bias Correction Method

Precipitation and temperature are anticipated as direct during RCM (Regional Climate Models) are providing a new opportunity for climate change since they are highly spatial resolution than Global climate models. Numerous studies for instance (Cannon *et al.*, (2015); Luo *et al.*, (2018); Haerter *et al.*, (2010)) have shown that RCM output improves the representation of climate change information at the mesoscale by providing spatially and physical coherent output with observation. However original RCM has an error that is inherited from the forcing of GCMs or produced by systematic error.

Many bias correction methods, ranging from simple scaling techniques to the rather more sophisticated distribution mapping techniques, have been developed to correct biased RCM outputs (Luo *et al.*, 2018). The scaling approach mainly includes linear or nonlinear approaches that adjust the climatic factors based on the differences between observed and RCM means in a linear or nonlinear formula, such as the linear scaling method (LS) and the power transpiration method (PT) (Luo *et al.*, 2018). Distribution mapping, involving distribution-based and distribution-free quantile mapping methods, matches the statistical distribution of RCM-simulated climatic factors to the distribution of observations. Distribution-based quantile mapping is based on the assumption that climatic factors obey a certain distribution, such as Gamma and Gaussian distributions, while the distribution-free quantile mapping technique employs the empirical distribution (Luo *et al.*, 2018). Selecting a suitable bias correction method is important for providing reliable inputs for impact analysis of a region.

Bias correction methods that have the ability to better transfer the observed precipitation and temperature statistics to the raw ensemble GCM/RCM CORDEX-Africa RCP 4.5 and RCP 8.5 climate scenarios were used. Precipitation is more difficult to correct its bias due to its physical characteristics but it has more significant influence than the temperature on streamflow simulation of Mojo catchment. Therefore, in this research, the precipitation and the temperature bias are corrected by Quantile mapping method. Because of the different characteristics of meteorological variables, bias correction methods provide different performances depending upon the variables of interest (Heo *et al.*, 2019). In a bias correction of precipitation data, the quantile mapping (QM), the detrended quantile mapping (DQM), and the quantile delta mapping (QDM) methods

have been widely employed because they can correct biases considering high order moment (Seo and Kim, 2018). Additionally, these methods were designed to preserve long-term changes in quantiles projected by climate models (Seo and Kim, 2018). Thus, the QM-based bias correction method is employed for precipitation correction in this study.

$$Q_m(t) = \begin{cases} F_o^{-1}[F_s[Q_s(t)]], & Q_s \geq Q_{th} \\ 0, & Q_s \leq Q_{th} \end{cases} \quad (3.6)$$

Where $Q_m(t)$ and $Q_s(t)$ are t^{th} bias-corrected data and simulated data from the RCM during the reference period (also known as the historical period), F_s and F_o^{-1} are the cumulative distribution function (CDF) of the raw data from the RCM and the inverse CDF of the observed data, respectively. To categories between the wet and the dry day threshold value $Q(\text{observed})$ is used (day with precipitation greater than 1 mm is assumed to be a wet day).

In QM, the probability distribution of the observed data for a future period is assumed to be the same. Because of the assumption of the same distribution of the observed data for the present and future periods, the long-term trend simulated by a climate model can be biased in QM. According to Seo and Kim, (2018) proposed the QM method is designed to correct the bias in climate projections, and the ability to correct seasonally. The temperature is corrected using Normal Distribution Quantile mapping.

$$Q_m(t) = Q_s F_o^{-1}[F_s[Q_s(t)]] - F_{mh}^{-1}(F_s(Q_s(t))) \quad (3.8)$$

Where (O=observed, h=historical, and S=simulated). F_s And F_o^{-1} are a CDF of the simulation data during a predefined future period and an inverse CDF of the simulated data during the reference period, respectively.

According to Heo *et al.*, (2019) discuss using eight probability distribution models are tested for the candidate distributions and form those candidates Gamma method is more corrected to the observed data and Gamma method is most common method in order to correct the bias so in this case, the gamma distribution method used for precipitation correction the equation as follows:

$$F(x, \alpha, \beta) = \frac{\gamma(k, \frac{x}{\alpha})}{\Gamma(\beta)} \quad (3.9)$$

Where Γ and Υ are a gamma function and a lower incomplete gamma function, respectively.

3.4.4. Hydrological Modeling Using SWAT

3.4.4.1. SWAT Modelling

SWAT is widely used to simulate hydrological processes under the scenario of changes in land use, land management, as well as climate change. The SWAT model is a physically-based, continuous-time catchment model that simulates hydrological processes in the catchment. This model is coupled with ArcSWAT in ArcGIS Geographical Information System interface to process the datasets and construct the required input for the initial modeling setup.

In SWAT, catchments are divided into sub-catchments, which are further delineated into hydrological response units (HRUs) that consist of homogeneous soil, land use, and climate. HRUs are defined separately for each sub-catchment, based on land cover, soil, and slope in a specific sub-catchment. Thresholds for HRU definition are sequentially applied to land covers, soils in each land cover, and slopes in a combination of land cover and slope. According to Winchell *et al.*, (2010) if a land cover percentage in the sub-catchment is below the land cover threshold, no HRU for that specific land cover will be defined, regardless of the distribution of soils, and the land cover areas will be reapportioned into the other qualified land covers mean that the threshold value which added in the HRU definition will depend on the value of land use, soil and slope of the each subbasin catchment if the value percent of land use is smaller than the threshold value of land cover no HRU is created in the subbasin and addition of land use and soil is smaller than the threshold still no HRU is created for a particular subbasin and also for slope, In this case, the threshold value which is given in the modelling Mojo catchment is 5% for land use and soil and 6% for slope. The model predicts the hydrology ultimately stream low at each HRU using a water balance equation, contains precipitation, surface runoff, evapotranspiration, infiltration, and subsurface inflow. The water balance equation of the hydrologic cycle is:

$$SW_t = SW_0 + \sum_{i=1}^t (R_{day} - Q_{surf} - E_a - W_{seep} - Q_{gw}) \quad (3.10)$$

In which SW_t is the final soil water content (mm), SW_o is the initial soil water content on a day i (mm), t is the time in days, R_{day} is the amount of precipitation on a day i (mm), Q_{surf} is the amount of surface runoff on a day i (mm), E_a is the amount of evapotranspiration on a day i (mm), W_{seep} is the amount of water entering to vadose zone from the soil profile on a day I (mm), and Q_{gw} is the amount of return flow on a day I (mm).

Surface runoff was estimated using the Soil Conservation Service Curve Number (SCS-Curve number) method

$$Q_{surf} = \frac{(R_{day} - I_a)^2}{(P_{day} - I_a - S)} \quad (3.11)$$

Where I_a is the initial abstraction which includes surface storage, interception, and infiltration prior to runoff and S is the retention parameter (mm).

Retention parameter defined by:

$$s = 25.4 \left(\frac{1000}{CN} \right) - 10 \quad (3.12)$$

CN is the curve number for the day which varies from 0 to 100 depending on soil permeability, land use, and the antecedent soil water condition. Initial parameter approximated as 0.2 S; the equation becomes: -

$$R_{sur} = \frac{(P_{day} - 0.25)^2}{(P_{day} + 0.85)} \quad (3.13)$$

3.4.4.2. Model Simulation

Before proceeding to the model calibration and validation of the model keeping in view the available period of observation flow series at the gauging station is important, in order to run the simulation, the data is classified into 80% for calibration and 20% for validation, following period were selected as warm-up, calibration, and validation Warm-up period for Calibration 1980-1981, Warm-up period for Validation 1999-2000 Calibration 1981-2000 and Validation 2001-2005

The model simulation is performed for the period of 25 years from January first, 1980 up to December last 2005 finally after adjusting the warm-up, calibration and validation the next step become simulation of the model.

3.4.4.3. Sensitivity Analysis

Sensitivity analysis is the process of identifying the model parameters that exert the highest influence on model calibration or on model predictions. Even though 25 parameters were used for the sensitivity analysis, all of them have a meaningful effect on the daily flow of the Mojo catchment. seventeen hydrological model parameters of the SWAT model underwent sensitivity and uncertainty analyses using the Global sensitivity analysis method in SWAT-CUP SUFI2 (Molla and Abdisa, 2018). The parameter sensitivity compares based on the *t-stat* of a parameter with the values in the *Student's t-distribution* table to determine the *p-value*, which is the number that you really need to be looking at. The *Student's t-distribution* describes how the mean of a sample with a certain number of observations is expected to behave. The *p-value* for each term tests the null hypothesis that the coefficient is equal to zero (no effect). A low *p-value* (< 0.05) indicates that you can reject the null hypothesis. In other words, a predictor that has a low *p-value* is likely to be a meaningful addition to your model because changes in the predictor's value are related to changes in the response variable. Conversely, a larger *p-value* suggests that changes in the predictor are not associated with changes in the response. So that parameter is not very sensitive. A *p-value* of < 0.05 is the generally accepted point at which to reject the null hypothesis (i.e., the coefficient of that parameter is different from 0). With a *p-value* of 0.05, there is only a 5% chance that results you are seeing would have come up in a random distribution, so you can say with a 95% probability of being correct that the variable is having some effect (Abbaspour, 2007).

3.4.4.4. Model Calibration

Model calibration is the process that comes after the sensitive parameters identified. This involved optimizing the values of the important parameters in the input files (e.g. *.hru files, *.gw files, *.sol files, etc.) and evaluating the model quality. However, when the number of parameters used in the manual calibration is large, especially for complex hydrologic models, manual calibration can become labor-intensive and automated calibration methods are preferred. Both manual algorithms and automated methods have been developed for calibration of SWAT simulations due to that in this case automated as well as manual method was used.

3.4.4.5. Performance Evaluation

The following statistical performance indices i.e. Nash and Sutcliffe efficiency (NSE) the coefficient of determination (R^2) and percent of bias (PBIAS) was used to assessing the closeness of simulated results with corresponding observations for instance (Setegn *et al.*, 2011), (Jilo *et al.*, 2019) and (Choi *et al.*, 2008).

The most widely used statistics reported for calibration and validation are R^2 , NSE, and PBIAS. The R^2 statistic can range from 0 to 1, where 0 indicates no correlation and 1 represents perfect correlation, and it provides an estimate of how well the variance of observed values are replicated by the model predictions Arnold *et al.*, (2012) and the statics calculated as:

$$R^2 = \frac{\sum_{i=1}^n (x_i - \bar{x})(y_i - \bar{y})}{(n-1)s_x s_y} \quad (3.14)$$

NSE values can range between $-\infty$ to 1 and a perfect fit between the simulated and observed flow is indicated by an NSE value of 1. NSE values ≤ 0 indicate that the observed data mean is a more accurate predictor than the simulated output. Both NSE and R^2 are biased toward high flows. The sum is taken over the whole period of the data used for calibration. A value closer to unity means the model explains the variance better. A negative modeling efficiency means that the model prediction is worse than simply using the mean of the observed flows (Nash and Sutcliffe, 1970).

$$NSE = 1 - \left\{ \frac{\sum_{i=1}^n (Z_{Obs} - Z_{simu})^2}{\sum_{i=1}^n (Z_{Obs} - Z_{mean})^2} \right\} \quad (3.15)$$

Percent bias measures the average tendency of the simulated data to be larger or smaller than the observations. The optimum value is zero, where low magnitude values indicate better simulations. Positive values indicate model underestimation and negative values indicate model overestimation (Gupta *et al.*, 1999).

$$PBIAS = 100 * \frac{\sum_{i=1}^n (Q_m - Q_s)_i}{\sum_{i=1}^n Q_{m,i}} \quad (3.16)$$

Table 3.7 Performance evaluation criteria (PEC), Statistical threshold value and corresponding assigned weight (Moriassi *et al.*, 2015)

PEC	NSE	R ²	PBIAS
Very good	$1 \geq NSE \geq 0.75$	$0.75 \leq R^2 \leq 0.85$	PBIAS <10
Good	$0.75 \geq NSE \geq 0.65$	$0.60 \leq R^2 \leq 0.75$	15 >PBIAS>10
Satisfactory	$0.65 \geq NSE \geq 0.5$	$R^2 \leq 0.60$	25 >PBIAS>15
Unsatisfactory	$NSE \leq 0.5$	$0 \leq R^2 \leq 0.5$	25 >PBIAS

3.4.4.6. Model validation

The calibrated model needs to be validated prior to its application for climate change scenarios. The model, calibrated in the previous step, was simulated for an independent period of 2001-2005 and evaluated using annual water yield, graphical comparison, and goodness of fit statistics.

3.4.4.7. The conceptual framework of the SWAT model and Cordex data

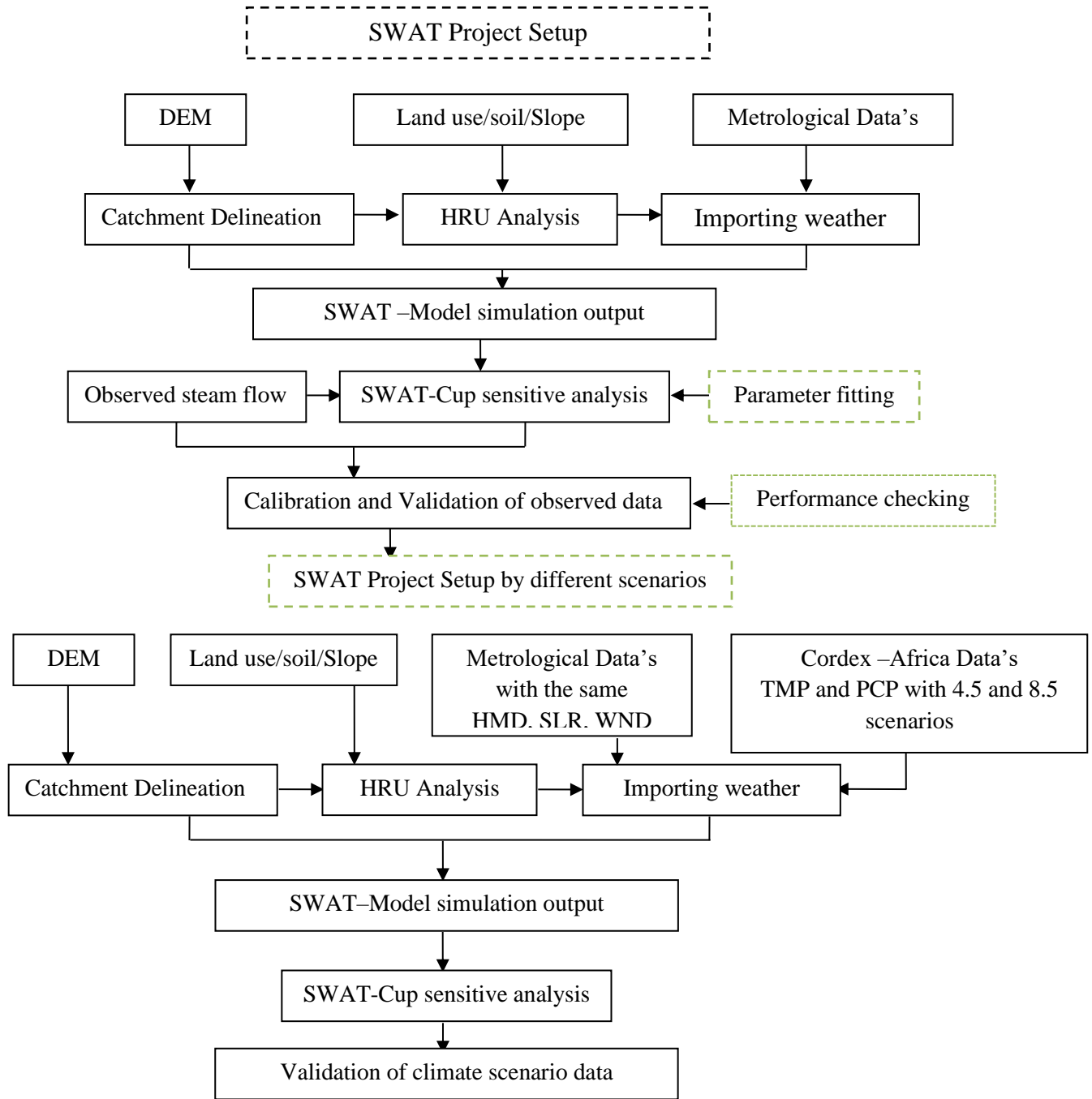


Figure 3.15 conceptual frameworks of the SWAT model and Cordex data

4. RESULT AND DISCUSSION

4.1. Hydrological Model Evaluation

4.1.1. Catchment Delineation

Catchment delineation based on the digital elevation model (DEM) is the prerequisite to set up the SWAT model. After delineation of Mojo catchment topographic report statics show that the elevation minimum, maximum and mean of the catchment is 1765, 3060 and 2160 respectively and also 25 sub-basins are formed and the land use, soil and slope distribution of the catchment are shown in the (table 4.1).

Table 4.1 Detailed Landuse/Soil/Slope distribution SWAT model class

		Area [ha]	Area[acres]	% Wat.Area
Landuse:				
Bare Land	--> BARR	27.56	68.11	0.02
Agricultural Land	--> AGRL	150712.58	372418.32	94.09
Dispersed Acacia	--> BSVG	90.16	222.80	0.06
Sugarcane Plantation	--> SUGC	141.87	350.56	0.09
Acacia	--> FOEN	1308.86	3234.25	0.82
Shrub Land	--> RNGB	91.15	225.25	0.06
Grass Land	--> RNGE	22.70	56.09	0.01
Forest	--> FRST	78.00	192.75	0.05
Eucalyptus	--> EUCA	237.97	588.05	0.15
Settlement	--> URBN	5842.25	14436.50	3.65
Water Body	--> WATR	1631.05	4030.41	1.02
Soil:				
Mollic Andosols	--> ANm	7.57	18.70	0.00
Vertic Cambisoils	--> CMv	71250.43	176063.37	44.48
Lithic Leptosols	--> LPq	1576.74	3896.19	0.98
Chromic Luvisols	--> LVh	198.70	491.00	0.12
Haplic Luvisols	--> LVx	8675.24	21436.96	5.42
Luvic Phaeozems	--> PHI	6966.19	17213.80	4.35

Eutric Vertisols	-->VRe	71509.30	176703.05	44.64
Slope:				
	0-10	126202.43	311852.51	78.79
	10-20	23174.99	57266.57	14.47
	20-30	5655.71	13975.54	3.53
	30-40	2369.38	5854.86	1.48
	40	2781.65	6873.59	1.74

4.1.2. SWAT model HRU Analysis

The result of HRU threshold analysis is classified based on the Landuse, Soil and slope of the Mojo catchment result which based on Winchell *et al.*, (2010) classification over the analysis of SWAT. In the study area, 25 subbasin created and the HRU threshold is for Landuse 5 %, for soil 6%, and for slope 5% and finally,129 HRU was created.

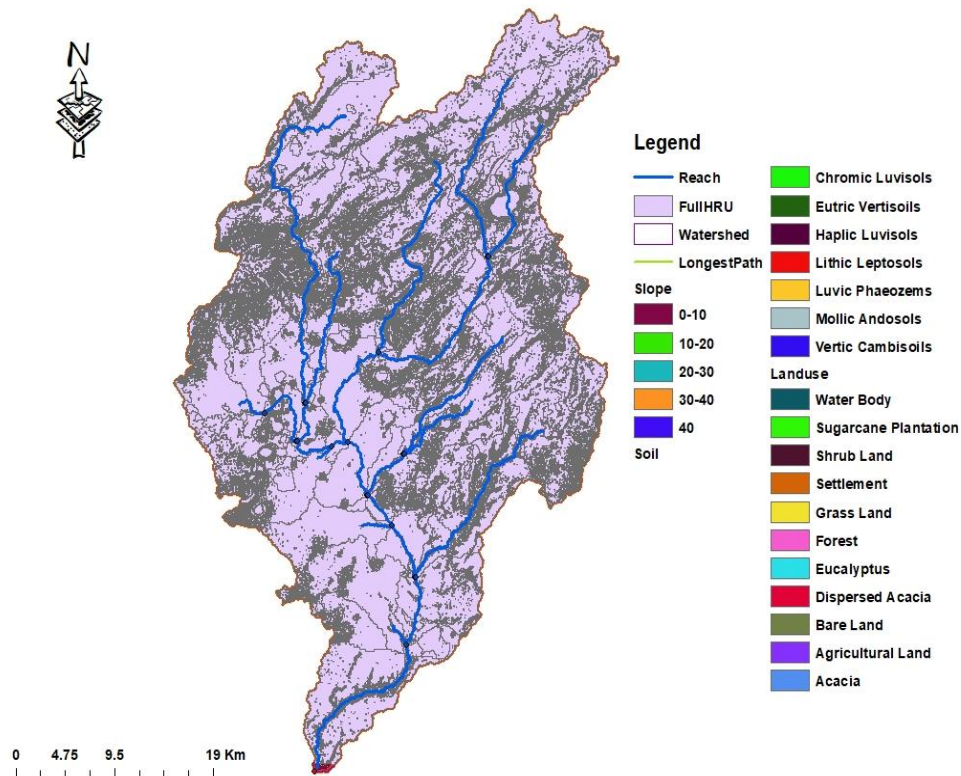


Figure 4.1 HRU Analysis Report of swat model

4.1.3. Sensitivity, Calibration, and Validation of the SWAT model

The SWAT model is a unique function of soil, land use, and topography parameters at HRU level and initial estimates of parameter values from the soil, land use, surface and subsurface process parameters were adjusted during calibration based on the recommended upper and lower boundary numbers. Parameter sensitivity and ranking in SWAT CUP was measured using the t-stat and p-values. Where t-stat is the coefficient of a parameter divided by its standard error. The p-value is used to determine the significance of the sensitivity. Parameters are significant for a larger absolute t-stat and lower p-values (Abbaspour *et al.*, 2007). Appendix (7) shows 23 influential parameters were selected for calibration which is the partially same as (Gonfa and Kumar, 2016). These parameters are related to surface runoff (SURLAG, and CH_K2), evapotranspiration (ESCO), soil water (SOL_AWC and SOL_K, USLE_K), groundwater (GW_DELAY, GWQMN, ALPHA_BF, GWHT, and GW_REVAP), management (CN2 and USLE_P) form those 17 of them shows reasonable influence on the catchment Table (4.2).

Table 4.2 List of top 17 sensitive parameters at Mojo catchment at the locations of Awash basin

Parameter Name	t-Stat	P-Value	Rank	Min value	Max value
R_SOL_AWC(..).sol	-8.69	0.00	1	0.2	0.4
R_CH_N2.rte	-2.72	0.03	2	0.4	0.9
V_GW_DELAY.gw	2.47	0.04	3	0.3	0.7
R_SOL_K(..).sol	-1.90	0.10	4	54.4	101.0
R_CANMX.hru	1.70	0.13	5	0.1	0.4
R_ESCO.hru	-1.66	0.14	6	38.8	71.6
V_ALPHA_BF.gw	-1.38	0.21	7	0.4	0.7
R_CH_K2.rte	-1.29	0.24	8	221.4	395.3
R_SLSUBBSN.hru	1.18	0.28	9	-0.1	0.1
R_EPCO.hru	1.12	0.30	10	-99.6	242.8
R_CN2.mgt	1.09	0.31	11	0.0	0.1
R_SOL_ALB(..).sol	1.08	0.32	12	206.3	1091.8
R_SURLAG.bsn	-1.03	0.34	13	5.6	14.9

R_SLSOIL.hru	1.02	0.34	14	1.0	1.5
R_USLE_K(..).sol	0.95	0.37	15	-24.7	116.4
V_GWQMN.gw	0.88	0.41	16	-0.2	0.2
R_USLE_P.mgt	-0.16	0.88	17	80.0	98.0

Where: CN2: Initial SCS runoff curve number; ESCO: Soil evaporation compensation factor; SOL_AWC: Available water capacity of soil layer (mm H₂O); ALPHA_BF: Baseflow alpha-factor (days); CH_K2: Effective hydraulic conductivity in main channel alluvium (mm/hr); canmx: Maximum canopy storage (mm H₂O); SURLAG: Surface runoff lag coefficient; SOL_K: Saturated hydraulic conductivity of soil (mm/hr); SOL_ALB: Moist soil albedo; GWQMN: Threshold depth of water in the shallow aquifer for return flow to occur (mm H₂O); GW_REVAP: Groundwater revap coefficient; EPCO: Plant uptake compensation factor; GW_DELAY: Groundwater delay time (delays); SLSOIL: Slope length for lateral subsurface flow; CANMX: Maximum canopy storage; SLSUBBSN: Average slope length; USLE_P: USLE equation support; USLE_K: USLE equation soil erodibility (k) factor; CH_N2: Manning's "n" value for the main channel. V_ means the existing parameter value is to be replaced by the given value and R_ means the existing parameter value is multiplied by (1+a given value).

Global sensitive parameters in Appendix (9) and Table (4.5) indicates that (SOL_AWC, CH_N2, and GW_DELAY) those sensitive parameters are more influential over the Mojo catchment as well as Awash basin because an increasing of SOL_AWC causes a decreasing of water yield (Adeba *et al.*, 2015). On the other hand, the response of the model towards parameter over the management (USLE_P), soil water (SOL_ALB and USLE_K), groundwater (GWQMN) which is line with (Gonfa and Kumar, 2016), surface runoff (SURLAG and SLSOIL) and soil water (SOL_K) are very low influential. parameters involving surface runoff (CN2), evaporation (EPCO and ESCO), surface runoff (CANMX and SLSUBBSN), groundwater (ALPHA_BF) and groundwater process (CH_K2) found moderately sensitive parameter in flow simulation.

4.1.4. Analysis of observed climate data and streamflow

Calibration of models at a catchment scale is a challenging task because of the possible uncertainties that may exist in the form of process simplification, processes not accounted for by the model, and processes in the catchment that are unknown to the modeler. Because of its simplicity SWAT CUP (SUFI-2 algorithm) was used for calibration, validation and uncertainty analysis of the SWAT model in Mojo catchment.

The SWAT simulation period was divided into two (calibration and validation). the monthly flow data is available from 1980-2010. After a five-year warm-up period from

(1985-2001) used for calibration and from (2001-2010) with the same warm-up (1995-2000) period used for the validation period.

calibration and validation results showed that the SWAT model was able to simulate the monthly streamflow well with a coefficient of determination (R^2) and Nash-Sutcliffe efficiency (NES) greater than 0.70. Also, percent bias (PBIAS) is positive with reasonable underestimates which is less than 10% (Table 3.7).

Table 4.3. SWAT hydrological model performance under validation and calibration periods of observed streamflow in Mojo catchment

Parameter	Calibration	Validation
Nash-Sutcliffe efficiency (E_{NS})	0.73	0.61
Coefficient of determination (R^2)	0.74	0.65
Percent bias (PBIAS)	1.6	0.7

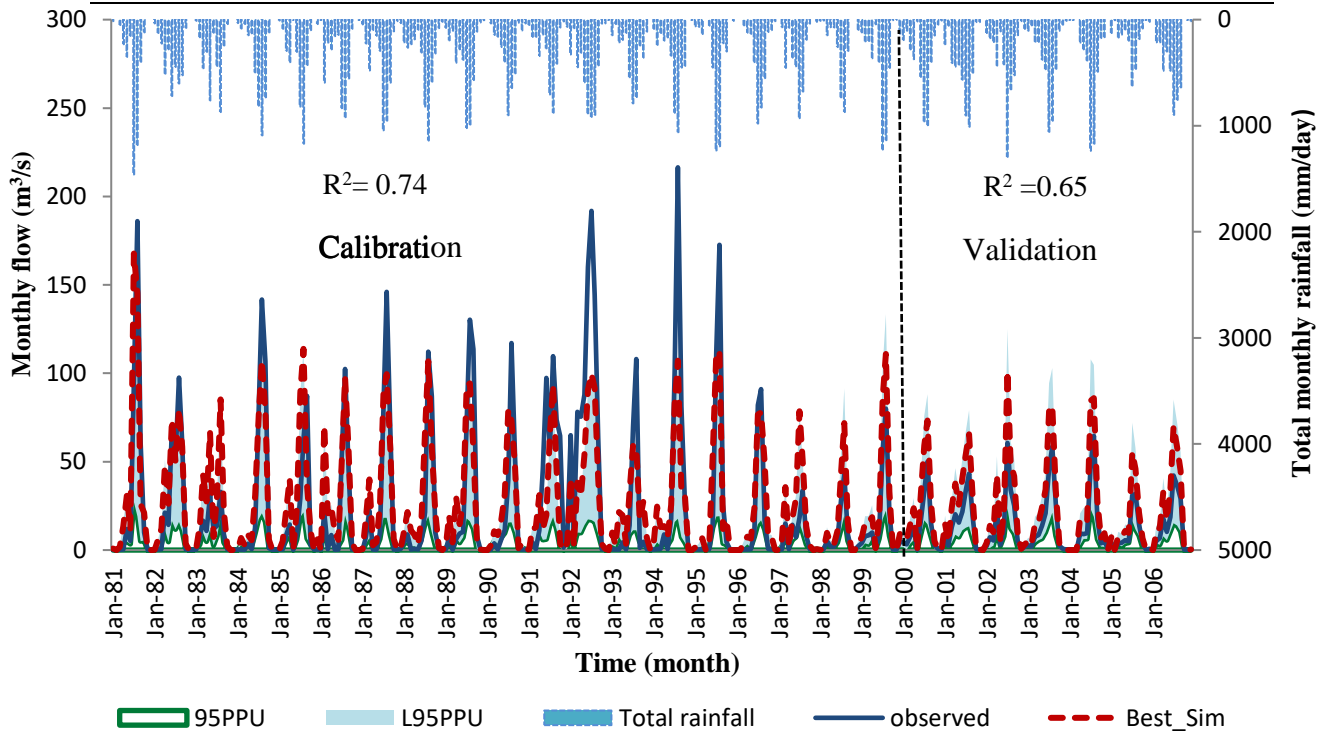


Figure 4.2 Calibration, validation and uncertainty analysis of flow data

Setegn *et al.*, (2011), Santhi *et al.*, (2001), Moriasi *et al.*, (2007), and Benaman *et al.*, (2005) suggested that the prediction efficiency of the calibrated model can be a good agreement if R^2 and NES values are greater than 0.6 and when the value of PBIAS is between $\pm 15 \leq$ and $\leq \pm 30$. since in the present study, the values of R^2 and NSE were 0.74

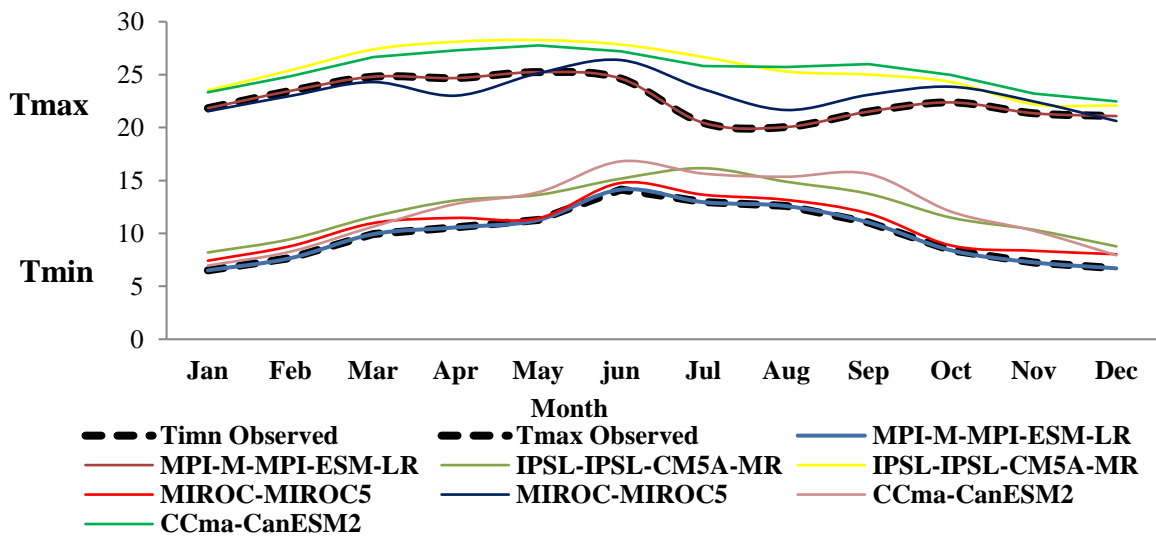
and 0.65, respectively which shows good relation with (Abbaspour *et al.*, 2007), and the PBIAS which is 1.65 and 0.7 for calibration and validation then the result is which is more perform according to Gupta *et al.*,(1999) of the observed and the simulated streamflow of the Mojo catchment showed good relations with reasonable performance (Gonfa and Kumar, 2016).

4.2. Analysis of the Performance climate GCM models

4.2.1. Selection of GCM Model

Analyzing the performances of GCM models with the SWAT model shows a good agreement in Ethiopia basins for instance (Jilo *et al.*, (2019): Dile *et al.*, (2013): Setegn *et al.*, (2011)). The performance checking of PBIAS, R^2 and NES were used to select the model performance. The SWAT Analysis and calibration of the observed data are evaluated in Section 4.2.1 up to 4.2.4. The monthly mean maximum and minimum temperature and precipitation pattern compared to the observation are given in Figure (4.3 (A) and (B)).

A)



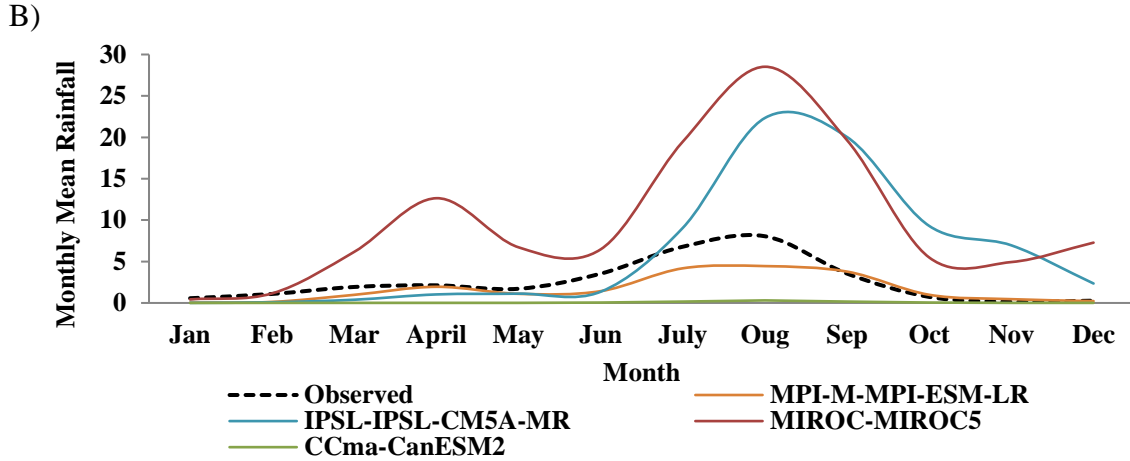
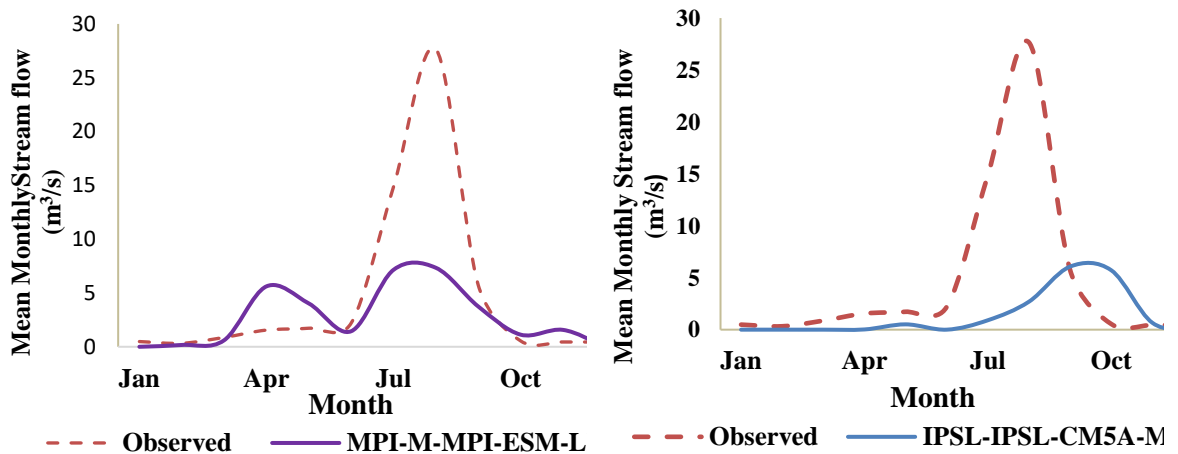


Figure 4.3 Comparison of observed and historical GCMs Models (variability among the four GCMs) time series of 1981-2005 for Temperature max, min and rainfall before bias correction figure (A) and figure (B) respectively.

4.2.2. Validation of GCMs Models

Validation was done based on a 5-year simulation from 2001-2005. Here also four GCM models used to select for the comparison of a better-fitted Model. Applying SWAT model has been frequently used to investigate climate change impacts on agro-hydrological systems (System and Dam, 2018) and simulated result shows that good performance with climate models relation Jilo *et al.*, (2019) so to analysis the performance of the candidate models in the catchment historical data was used for validation. The figure shows that the mean monthly of simulate and observed streamflow and the validation statistics for all the four models are shown in the figure (4.4) and table (4.4).



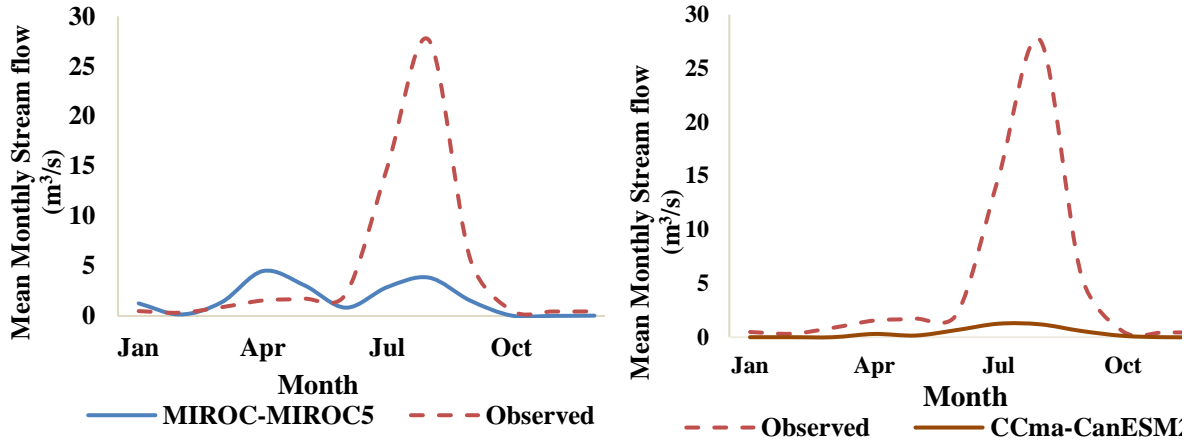


Figure 4.4 Validation of candidate GCM models simulation output and validated streamflow data of Mojo catchment form 2001-2005

Table 4.4. SWAT hydrological model performance under validation and calibration periods of GCM models and observed data.

Parameter	Calibration		Validation		
	Observed	MIROC-MIROC5	IPSL-IPSL-CM5A-MR	MPI-M-MPI-ESM-LR	CCma-CanESM2
(NES)	0.73	0.13	0.02	0.16	0.16
(R ²)	0.74	0.17	0.01	0.21	0.29
(PBIAS)	1.6	65.7	70.8	42.3	93.5

Figure 4.4 and Table 4.4 shows that the atmosphere-only validation was done to evaluate how models perform with observed and climate models based on their performance without bias correction, the daily streamflow, and distribution value of the model. Percent bias measures the average tendency of the simulated data to be larger or smaller than the observations (Gupta et al., 1999). Models that performed with the least Percent of Bias indicated good underlying atmospheric dynamics (Teutschbein and Seibert, 2012). From the validation, two models were highlighted for bias correction as having reasonable skill in the region, Max Planck Institute for Meteorology Earth System Model (MPI-M-MPI-ESM-LR), and Model for Interdisciplinary Research on Climate (MIROC-MIROC5) (Table 4.5).

Table 4.5 Selected GCM Models used for analysis

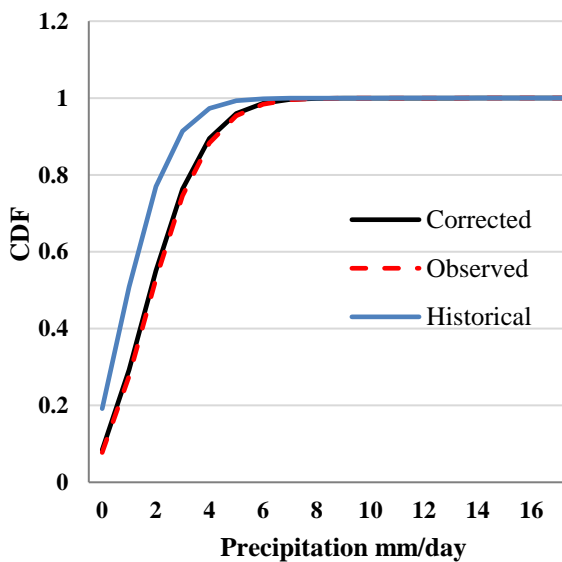
Id No	Model
1	MIROC-MIROC5
2	MPI-M-MPI-ESM-LR

4.2.3. Analysis of Bias corrected climate data and observed data

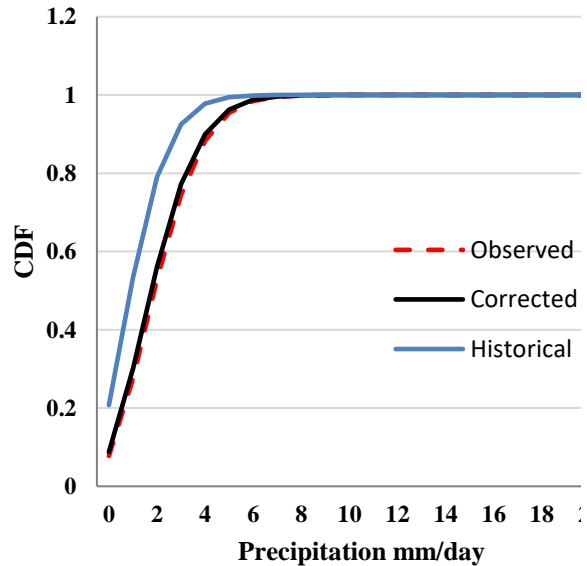
Analysis of the bias correction is more important before proceed to the next level. Models were examined based on a historical period (1981–2005), observed data (1981-2005) and future scenario data (4.5 and 8.5) form 2006-2080 were corrected. The bias correction method used for daily precipitation, temperature maximum and minimum and performs good relations with the observed precipitation and temperature data. Figure 4.5 and Appendix (10 and 11) show that the historical bias correction with respect to observed data of the two GCMs models.

We use these same models to estimate the change in temperature and precipitation. Models which is indicated in (Table 4.5) and shows that the models performed well in the given metrics. For the future climate data, from the Intergovernmental Panel on Climate Change (IPCC, 2014) defined Representative Concentration Pathways (RCPs) we have used RCP 8.5 and RCP 4.5 scenario, which represents the highest greenhouse emission level with rising radiative forcing pathways.

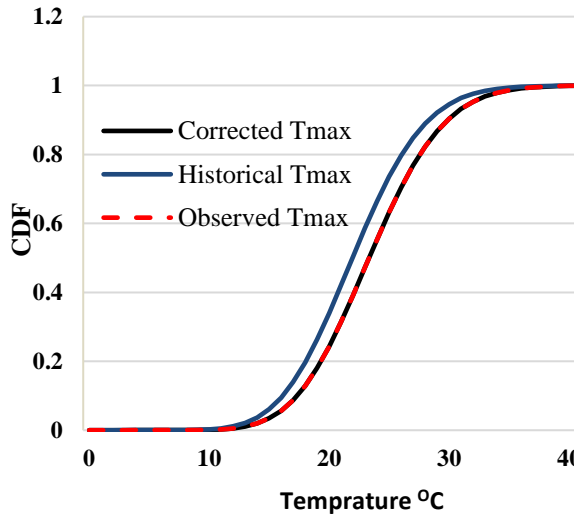
A) MPI-M-MPI-ESM-LR



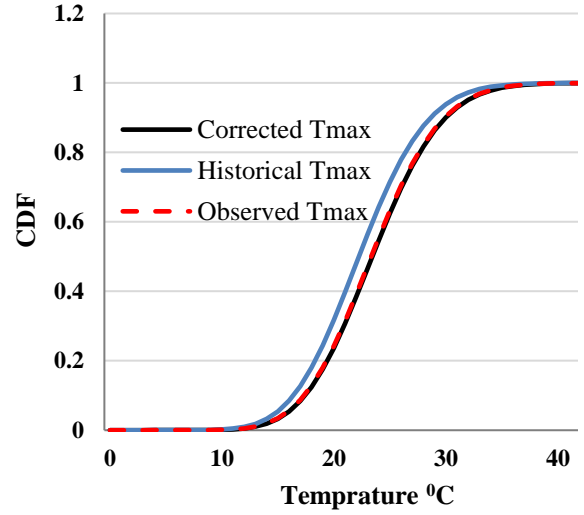
B) MIROC-MIROC5



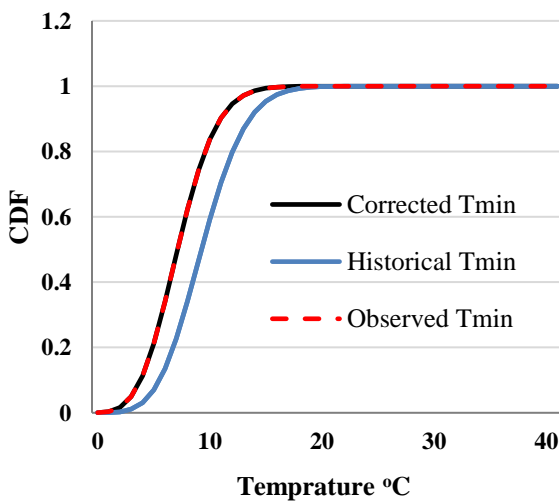
C) MPI-M-MPI-ESM-LR



D) MIROC-MIROC5



E) MPI-M-MPI-ESM-LR



F) MIROC-MIROC5

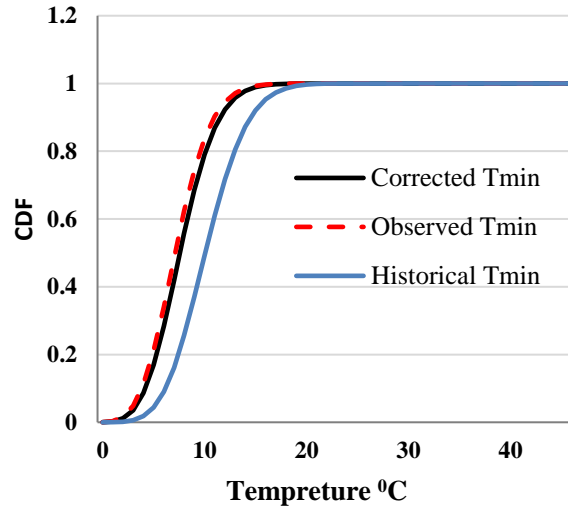


Figure 4.5 shows Cumulative Distribution Function before and after bias correction with respect to observed data and Historical data from (1981-2005), fig (A) and (B) Gamma distribution for precipitation of GCMs model MPI-M-MPI-ESM-LR and MIROC-MIROC5 respectively, normal distribution C, D, for temperature min, E and F for temperature max.

SWAT well simulates the hydrology of Mojo catchment and forced to generate historical streamflow under both bias-corrected historical precipitation and temperature climate data's in order to analyze the performance. Table (4.6) and figure (4.6) show that the relationship with bias-corrected streamflow output and observed streamflow for the selected GCMs models and, the performance of PBIAS was increased for both models.

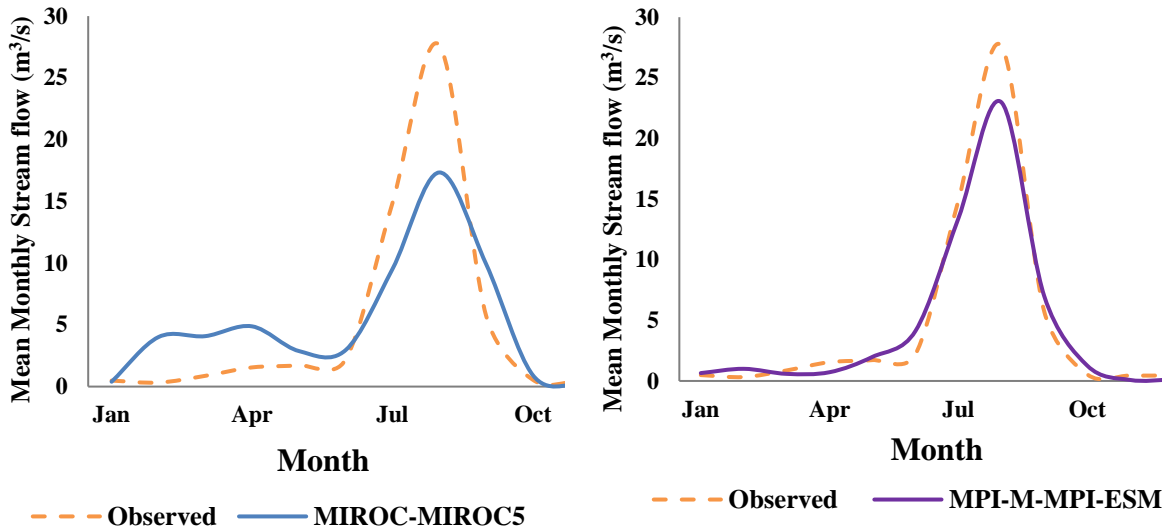


Figure 4.6 Validation output Annual mean streamflow of MIROC-MIROC5 and MPI-M-MPI-ESM-LR from (2002-2005)

Table 4.6. Performance evaluation streamflow validation output of model MIROC-MIROC5 and MPI-M-MPI-ESM-LR

Parameter	Validation		
	Observed	MIROC-MIROC5	MPI-M-MPI-ESM-LR
(NES)	0.73	0.43	0.53
(R ²)	0.74	0.47	0.54
(PBIAS)	1.6	9.6	5.1

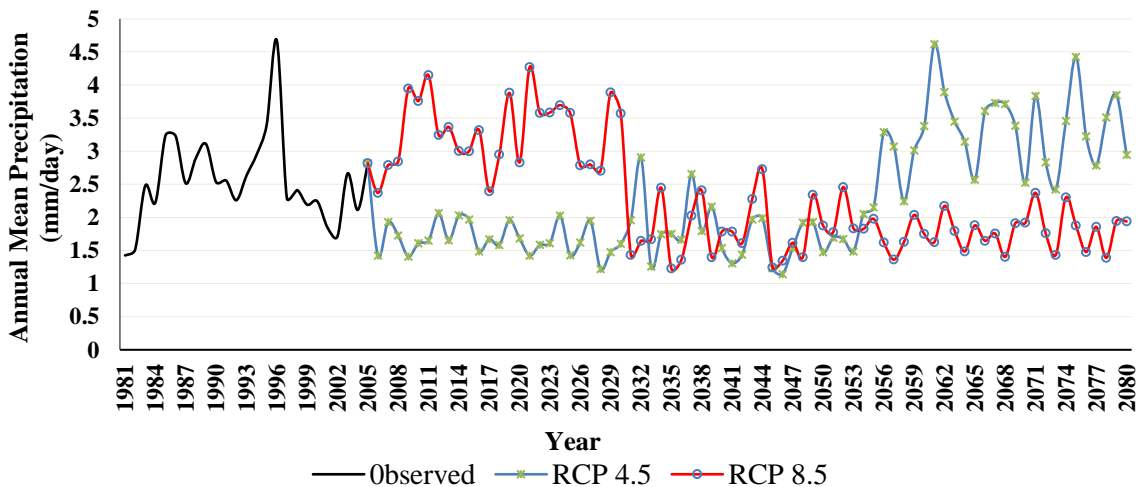
4.3. Analysis of climate change Future scenarios

Analysis of the future scenario was done for two selected GCMs models. The analysis classified into three categories from 2006-2030 Near future, from 2031-2055 Mid future and for 2056-2080 Far future. Calibration and validation were done in section 4.2 after fitted the sensitive parameters.

4.3.1. Change in projected precipitation GCMs scenarios

The result of the study after bias corrections of raw precipitation shows that the mean annual precipitation in the future selected models generally shows fluctuation over Mojo catchment seems the change become occur in Awash basin also Taye, (2018) and Hailemariam, (1999) using old SERES. The change in precipitation for both model scenarios shows slightly different behavior on the model scenarios and periods. The figure (4.7) shows that change in mean annual precipitations varies over MIROC-MIROC5 model scenarios which are increasing from + 24 to + 49% for the entire period RCP4.5 and decreasing in RCP8.5 climate scenarios over all future time periods from 47 to 25%. Also, model MPI-M-MPI-ESM-LR shows a slight decrease in RCP 4.5 ranges from 33.8 to 33.1% and an increase in RCP 8.5 varies from 31.9 to 34.8% for all scenarios. Supporting the present study's findings, Intergovernmental Panel on Climate Change IPCC, (2014) reported an increase of precipitation with heavy precipitation events over the world.

MIROC-MIROC5



MPI-M-MPI-ESM-LR

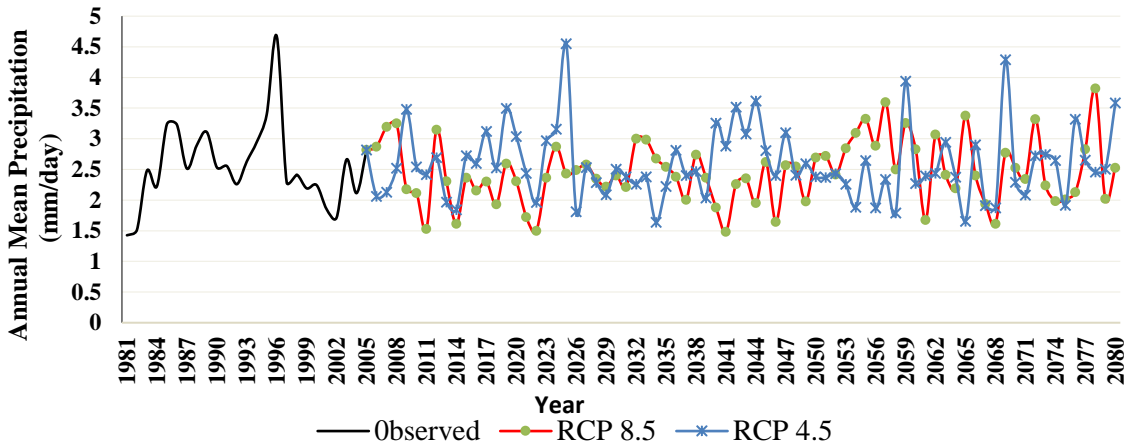
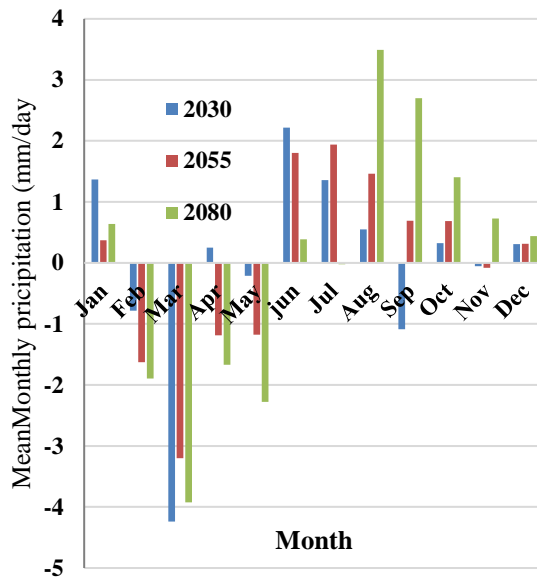


Figure 4.7 Annual precipitation (1981-2080) at Mojo catchment for model MIROC-MIROC5 and MPI-M-MPI-ESM-LR under RCP 4.5 and RCP 8.5 climate scenario

In all future time periods, Model MPI-M-MPI-ESM-LR shows that Kiremt (wet) season (June–September) precipitation change shows a cumulative increasing change over both scenarios but September under RCP 4.5 at Near period (2030), and July RCP 8.5 at MID periods shows a decreasing change. Belg (short rainy) season (February–May) precipitation amount decreased for all periods but for the month of April at Near period under RCP 4.5 shows some increase change in precipitation. The Bega (dry) season (October–January) showed an increase for all RCP 4.5 scenario and mixed trend where precipitation decreased for the Far future (2080) period under RCP 8.5 climate scenarios the study figure (4.8)

MPI-M-MPI-ESM-LR

A) RCP 4.5



B) RCP 8.5

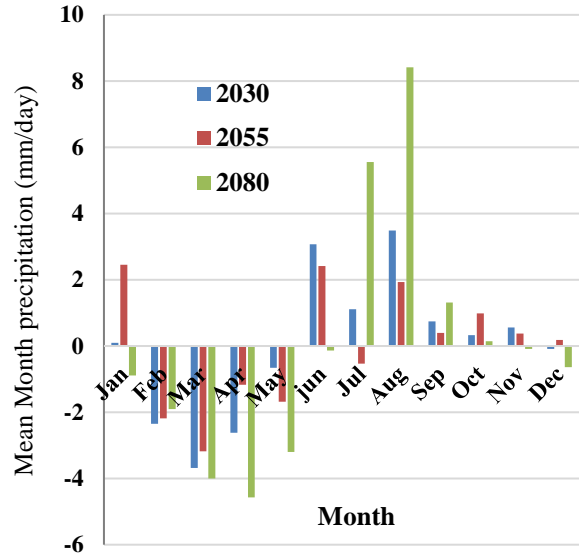
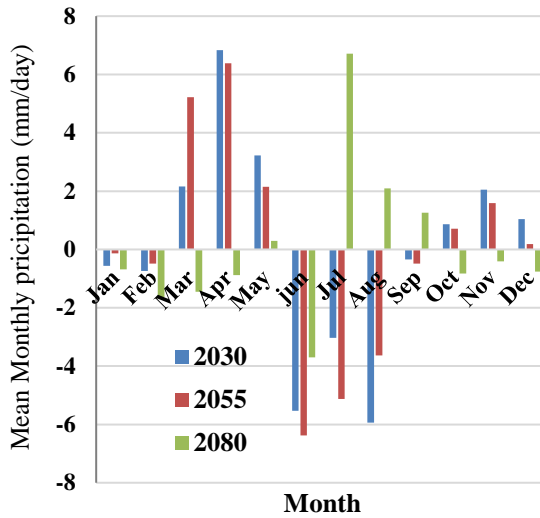


Figure 4.8 Annual Monthly mean of Precipitation (2006-2080) for the Model MPI-M MPI-ESM-LR under RCP 4.5 and 8.5

Change in precipitation over the model MIROC-MIROC5 shows that the rainy season Kiremt (wet) season (June–September) become decrease but in the FAR period July under RCP 4.5 and Near period under RCP 8.5 shows the high increasing change occurs in both scenarios. To the reverse Belg (short rainy) season (February–May) becoming increasing in a change in both scenarios. The Bega (dry) season (October–January) shows that mixed change for both scenarios, In RCP 8.5 scenario except October and November for Far future (2080) and Mid future (2055) respectively shows increase change the rest becoming decrease such, results of increase precipitation were related to other findings reported over the Awash basin (Taye, 2018) and figure(4.9).

MIROC-MIROC5

A) RCP 4.5



B) RCP 8.5

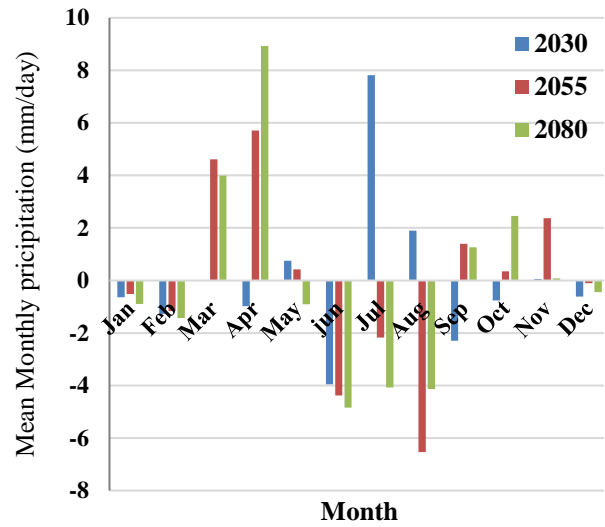


Figure 4.9 Annual Monthly mean of Precipitation (2006-2080) for the Model MIROC-MIROC5 under RCP 4.5 and 8.5

Table 4.7 Annual Monthly mean variation of Precipitation change (2006-2080) for the Model MPI-M-MPI-ESM-LR under RCP 4.5 and 8.5

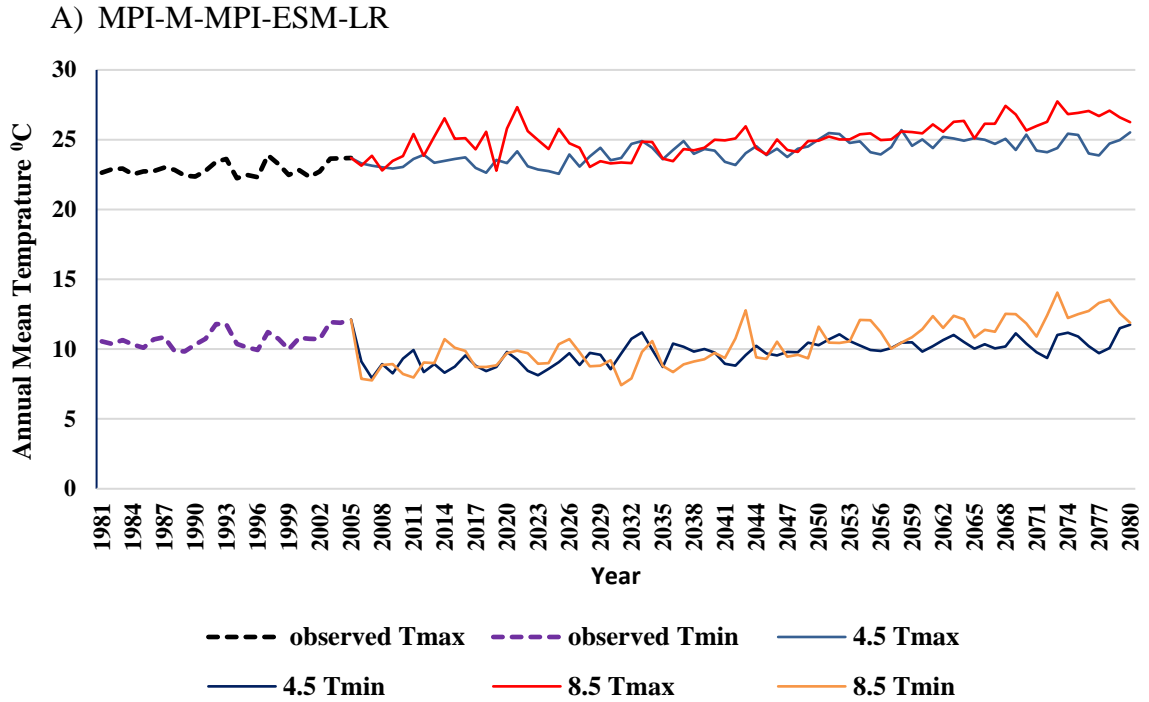
Period	Jan	Feb	Mar	Apr	May	Jun	Jul	Aug	Sep	Oct	Nov	Dec
Mean Monthly precipitation change (%) RCP 4.5												
2030	1.37	-0.78	-4.24	0.25	-0.21	2.21	1.36	0.55	-1.09	0.32	-0.05	0.31
2055	0.37	-1.63	-3.20	-1.18	-1.18	1.80	1.94	1.46	0.69	0.69	-0.08	0.31
2080	0.64	-1.89	-3.93	-1.67	-2.28	0.39	-0.02	3.49	2.70	1.40	0.73	0.44
Mean Monthly precipitation Change (%) RCP 8.5												
2030	0.10	-2.35	-3.69	-2.62	-0.66	3.07	1.11	3.48	0.74	0.32	0.56	-0.09
2055	2.45	-2.19	-3.18	-1.17	-1.68	2.42	-0.53	1.93	0.40	0.99	0.37	0.19
2080	-0.89	-1.90	-4.00	-4.57	-3.20	-0.14	5.56	8.41	1.31	0.14	-0.08	-0.63

Table 4.8 Annual Monthly mean variation of Precipitation change (2006-2080) for the Model MIROC-MIROC5 under RCP 4.5 and 8.5

Period	Jan	Feb	Mar	Apr	May	Jun	Jul	Aug	Sep	Oct	Nov	Dec
Mean Monthly precipitation change (%) RCP 4.5												
2030	-0.57	-0.74	2.15	6.83	3.22	-5.54	-3.03	-5.94	-0.34	0.87	2.05	1.03
2055	-0.14	-0.49	5.23	6.38	2.15	-6.38	-5.12	-3.64	-0.48	0.71	1.59	0.18
2080	-0.69	-1.64	-1.45	-0.88	0.30	-3.70	6.71	2.09	1.26	-0.83	-0.41	-0.76
Mean Monthly precipitation Change (%) RCP 8.5												
2030	1.93	1.30	-0.92	3.19	0.55	3.82	1.78	-4.72	-6.90	-0.12	0.06	0.02
2055	2.90	0.10	-0.73	0.77	-1.44	3.86	-1.14	-1.74	-3.36	0.57	0.23	-0.03
2080	-0.45	-0.32	-0.73	-1.85	-1.61	3.32	4.01	-1.05	-2.51	0.98	0.29	-0.06

4.3.2. Change in projected Temperature GCMs scenarios

After bias correction, Mojo catchment exhibits an increase in projected minimum and maximum temperature under both GCM models and RCP climate scenarios (Figure 4.10). The model MIROC-MIROC5 mean annual minimum temperature varies from + 1.19 to + 3.57 °C under RCP 8.5 and from + 1 to + 1.99 °C under RCP 4.5 climate scenarios for the three-time periods such analysis is related with the result (Fox *et al.*, 2018). Similarly, the mean annual maximum temperature showed an increasing trend and varies from + 1 to + 1.74 °C under RCP8.5 and from + 0.99 to + 1.74 °C under RCP4.5 over the two scenarios at future time periods. It also shows that the model under MPI-M-MPI-ESM-LR the temperature maximum in both scenarios becoming increase varies from + 0.45 to 1.875 °C under RCP 4.5 and +0.47 to 1.97 °C under RCP 8.5, and Also to the revers the temperature minimum shows an a decreasing variation from -1.81 to -0.30 °C under RCP 4.5 for all periods and from -1.55 to -0.83 °C for RCP 8.5 till Mid period but in the Far future period the RCP 8.5 becoming increase by 1.21°C.



B) MIROC-MIROC5

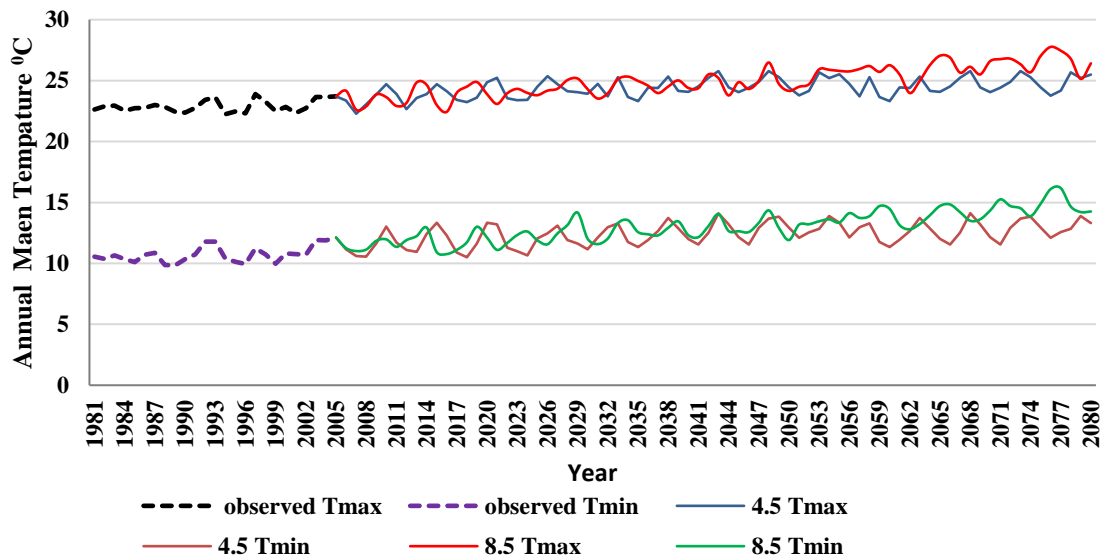
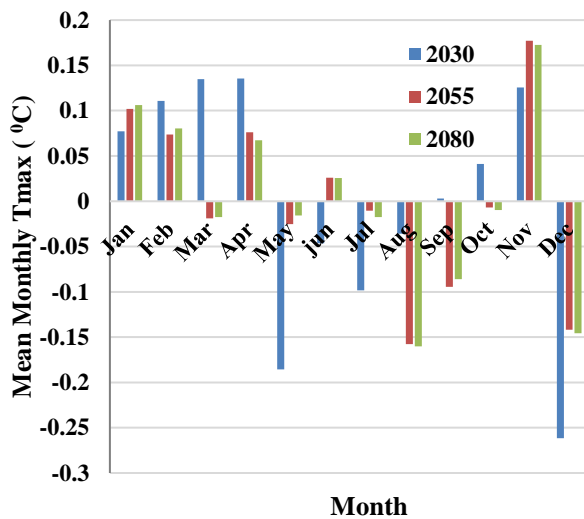


Figure 4.10 Annual monthly mean of temperature maximum and minimum (1981-2080) at Mojo catchment for model MPI-M-MPI-ESM-LR (A) and MIROC-MIROC5 (B) under RCP4.5 and RCP8.5 climate scenario

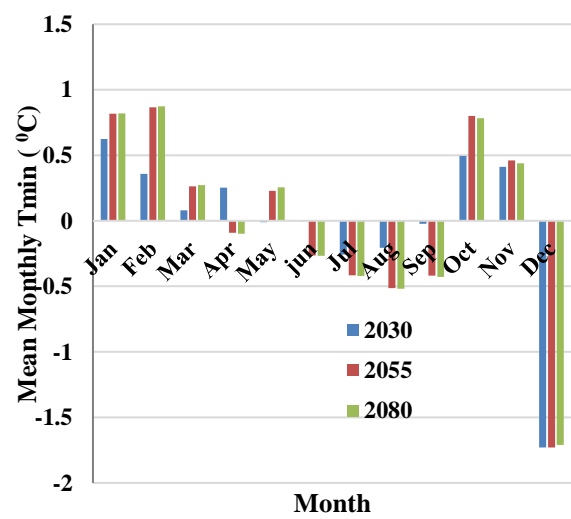
The seasonal variation of change in temperature over Mojo catchment shows that reasonable change in both GCM models. Model MIROC-MIROC5 shows that the minimum temperature on the Kiremt season (June–September) decrease in all periods but the maximum temperature except June at Mid and Far period under RCP 4.5 and RCP 8.5 at Far period and September at Near period under RCP 8.5 shows increase in change the rest shows decreasing under both scenarios. On the other hand, Belg season (February–May) shows an increasing temperature maximum change in both RCP scenarios except March at Mid and Far future under the RCP 4.5 and May at Near and April at Far future period of RCP 8.5 scenarios become decrease. Similarly, the temperature minimum under Belg season shows an increasing change in both scenarios without including April at the Mid and Far future period under RCP 4.5 and April and May at Far and Near period respectively under the RCP 8.5 scenario. The Bega (dry) season (October–January) shows that mixed change in temperature maximum and minimum under both scenarios. In this season the minimum temperature shows increasing change except December at all periods under both scenarios but in the maximum temperature shows mixed characteristics under three periods in the October under RCP 4.5 at Mid and Far period, December for both scenarios show a decreasing change in temperature the rest of period shows an increasing temperature change in both scenarios figure (4.11).

MIROC-MIROC5

Tmax 4.5



Tmin 4.5



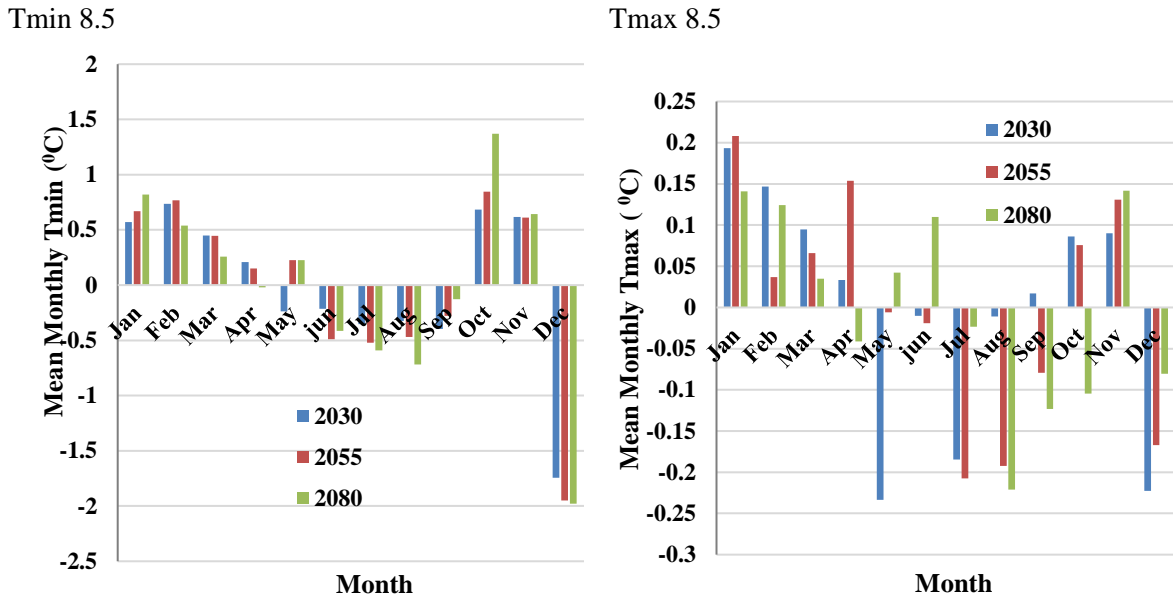


Figure 4.11 Annual Monthly mean of temperature maximum and minimum (2006-2080) for the Model MIROC-MIROC5 under RCP 4.5 and 8.5

Under the model MPI-M-MPI-ESM-LR, the seasonal variation of change shows not that much fluctuation in both scenarios. The temperature variation over Kiremt season over the minimum and maximum temperature shows a decrease in change in both RCP 4.5 and RCP 8.5 respectively scenarios, to the reverse under Belg season, shows an increasing maximum and minimum temperature change in both RCP 8.5 and 4.5 respectively and in Bega season except October and November shows an decreasing in change under both maximum and minimum temperature of RCP 8.5 and 4.5 respectively over entire period. The variation of maximum temperature for Kiremt season under the RCP 4.5 scenario shows that increasing change except for June and September which shows decreasing change for all periods. And also, for RCP 8.5 minimum temperature at month July and august it shows increasing change except for August at the Far future period and the rest months become decreasing in change. At Belg season the maximum and minimum temperature in both RCP 4.5 and RCP 8.5 scenarios respectively the month February and April shows increase in change. Also, for the month May a minimum and maximum temperature become increase under RCP 8.5 and RCP 4.5 for entire period but for RCP 4.5 the maximum temperature at Mid period shows decreasing in change. In the dry season of Bega, the decreasing change occur at October, November under maximum

4.5 scenario for all period and December under minimum temperature RCP 8.5 in Mid period the rest months shows an increasing change. (Taye, 2018) also shows the seasonal variation of the average temperature change factors for the entire Awash basin for both maximum and minimum temperature near-term to the end of the century the increase in temperature becomes high for both maximum and minimum temperature Figure (4.12).

A) MPI-M-MPI-ESM-LR

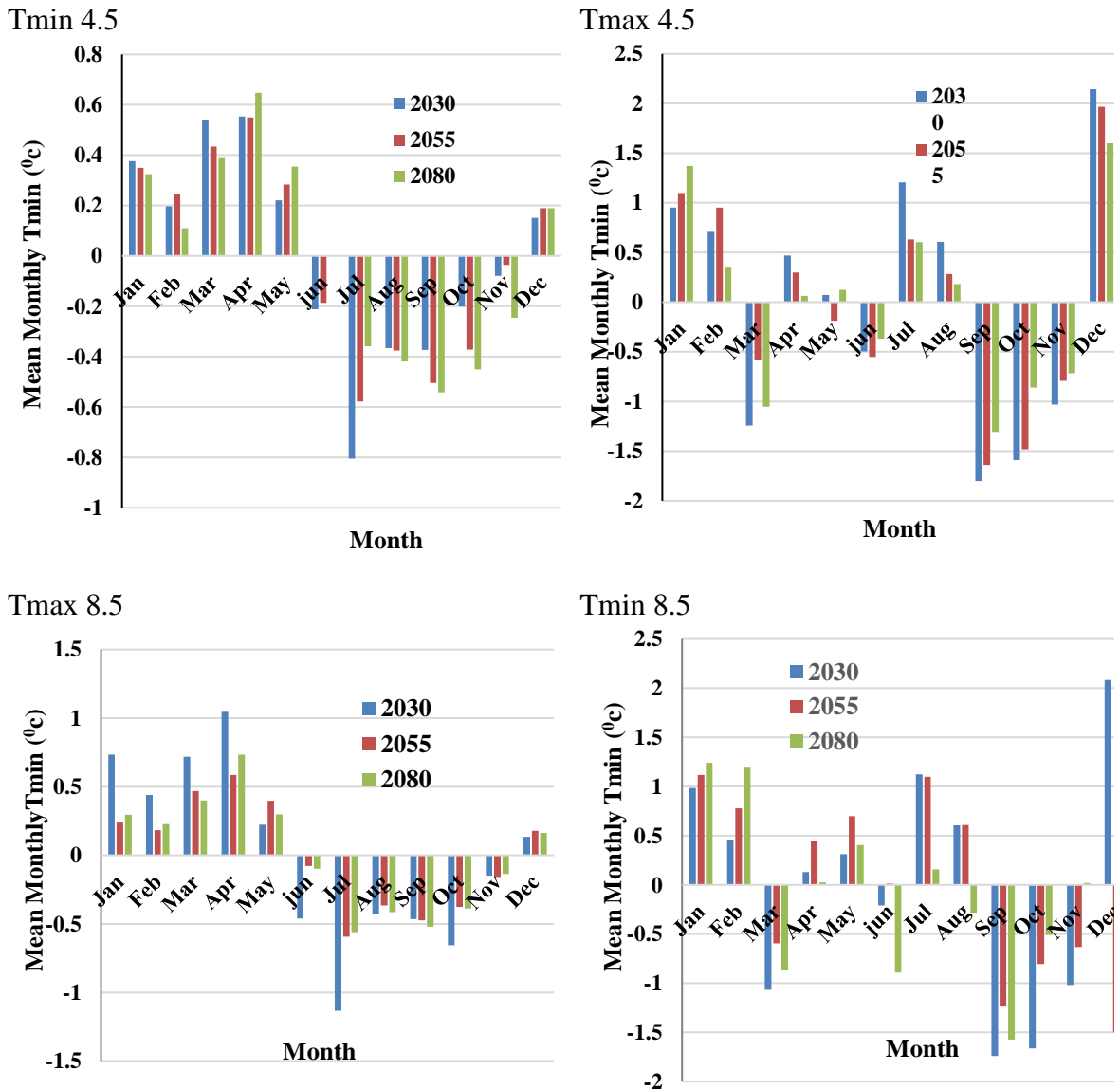


Figure 4.12 Annual Monthly mean of Temperature maximum and minimum change (2006-2080) for the Model MPI-M-MPI-ESM-LR under RCP 4.5 and 8.5

Table 4.9 Mean Monthly variation of temperature maximum and minimum change (2006-2080) for the Model MIROC-MIROC5 (A) and MPI-M-MPI-ESM-LR under RCP 4.5 and 8.5

A)

Period	Jan	Feb	Mar	Apr	May	Jun	Jul	Aug	Sep	Oct	Nov	Dec
Mean Month Tmax (°C) RCP 4.5												
2030	0.08	0.11	0.13	0.14	-0.19	-0.05	-0.10	-0.04	0.00	0.04	0.13	-0.26
2055	0.10	0.07	-0.02	0.08	-0.03	0.03	-0.01	-0.16	-0.09	-0.01	0.18	-0.14
2080	0.11	0.08	-0.02	0.07	-0.02	0.03	-0.02	-0.16	-0.09	-0.01	0.17	-0.15
Mean Month Tmin (°C) RCP 8.5												
2030	0.62	0.36	0.08	0.25	-0.01	0.00	-0.26	-0.20	-0.02	0.50	0.41	-1.73
2055	0.82	0.87	0.26	-0.09	0.23	-0.27	-0.41	-0.51	-0.42	0.80	0.46	-1.73
2080	0.82	0.87	0.27	-0.10	0.26	-0.27	-0.42	-0.52	-0.43	0.78	0.44	-1.71
Mean Month Tmax (°C) RCP 4.5												
2030	0.19	0.15	0.09	0.03	-0.23	-0.01	-0.18	-0.01	0.02	0.09	0.09	-0.22
2055	0.21	0.04	0.07	0.15	-0.01	-0.02	-0.21	-0.19	-0.08	0.08	0.13	-0.17
2080	0.14	0.12	0.04	-0.04	0.04	0.11	-0.02	-0.22	-0.12	-0.10	0.14	-0.08
Mean Month Tmin (°C) RCP 8.5												
2030	0.57	0.74	0.45	0.21	-0.24	-0.22	-0.35	-0.32	-0.40	0.68	0.62	-1.74
2055	0.67	0.77	0.45	0.15	0.23	-0.49	-0.52	-0.47	-0.28	0.85	0.61	-1.95
2080	0.82	0.54	0.26	-0.02	0.23	-0.41	-0.59	-0.72	-0.13	1.37	0.64	-1.98

B)

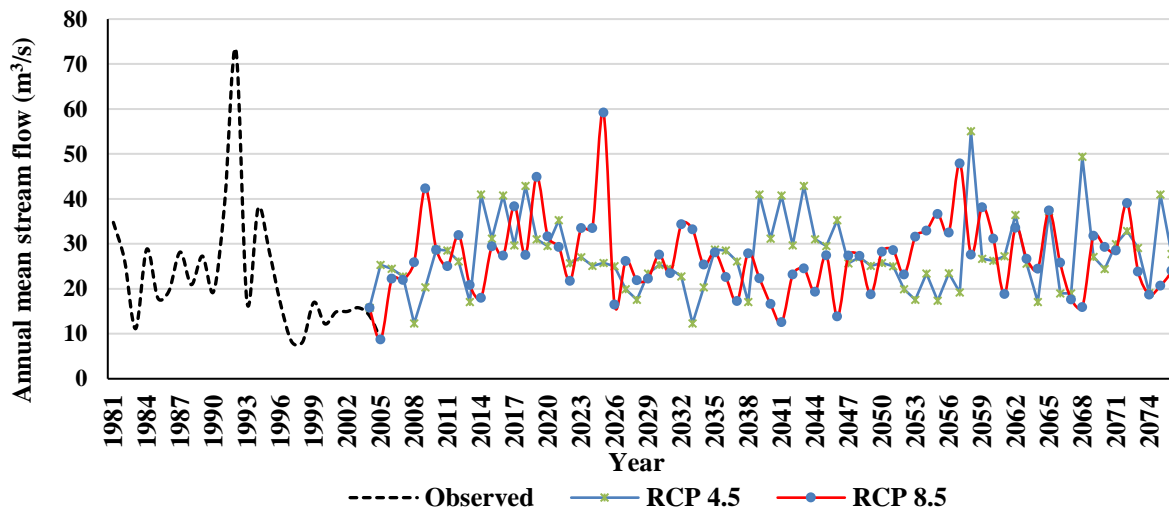
Period	Jan	Feb	Mar	Apr	May	Jun	Jul	Aug	Sep	Oct	Nov	Dec
Mean Month Tmax (°C) RCP 4.5												
2030	0.38	0.20	0.54	0.55	0.22	-0.21	-0.80	-0.37	-0.37	-0.20	-0.08	0.15
2055	0.35	0.25	0.43	0.55	0.28	-0.19	-0.58	-0.38	-0.50	-0.37	-0.04	0.19
2080	0.33	0.11	0.39	0.65	0.35	0.00	-0.36	-0.42	-0.54	-0.45	-0.25	0.19
Mean Month Tmin (°C) RCP 4.5												
2030	0.95	0.70	-1.2	0.47	0.07	-0.49	1.20	0.60	-1.8	-1.58	-1.03	2.14
2055	1.09	0.95	-0.6	0.29	-0.18	-0.55	0.63	0.28	-1.64	-1.48	-0.79	1.96
2080	1.37	0.35	-1.1	0.06	0.12	-0.36	0.60	0.18	-1.31	-0.86	-0.72	1.6
Mean Month Tmax (°C) RCP 8.5												
2030	0.73	0.44	0.72	1.05	0.22	-0.46	-1.13	-0.43	-0.47	-0.66	-0.15	0.13
2055	0.24	0.18	0.47	0.59	0.40	-0.08	-0.59	-0.37	-0.47	-0.38	-0.16	0.18
2080	0.30	0.23	0.40	0.73	0.30	-0.10	-0.56	-0.41	-0.52	-0.39	-0.14	0.16
Mean Month Tmin (°C) RCP 4.5												
2030	0.99	0.46	-1.07	0.13	0.31	-0.21	1.12	0.61	-1.74	-1.66	-1.02	2.08
2055	1.12	0.78	-0.59	0.44	0.70	0.01	1.10	0.61	-1.23	-0.81	-0.63	-1.50
2080	1.24	1.19	-0.87	0.03	0.40	-0.89	0.16	-0.28	-1.57	-0.51	0.02	1.08

4.4. Hydrological Change of Projected Precipitation and Temperature on Streamflow

4.4.1. Change in Projected streamflow

SWAT hydrological model calibrated and validated the streamflow of Mojo catchment at Mojo gauged station and model results of streamflow was considered for comparative analysis for a baseline period of 1981–2005 and projection periods 2030 (2005–2030), 2055s (2031–2055), and 2080s (2056–2080) under both GCMs models and climate scenarios. The figure showed that the annual mean of two models with reference to the baseline (observed). The model MPI-M-MPI-ESM-LR shows that with reference to the baseline the streamflow for both scenarios become increases. Under RCP 4.5 the stream increases by 4.62 m³/s, 4.30 m³/s, and 7.79 m³/s by the year Near (2030), Mid (2055) and Far (2080) respectively. For scenario 8.5 the increase becomes 6.68 m³/s, 2.64 m³/s, 6.31 m³/s by the year Near, Far and Future periods respectively. According to Gizaw *et al.*, (2017) also the streamflow becomes shows an increase in the projected annual streamflow in the Awash basin by the 2050s and 2080s. Change in model MIROC-MIROC5 shows a decreasing stream flow change at Near and Mid period of RCP 4.5 scenario by -6.32 m³/s and -5.08 m³/s respectively some of the results Daba, (2015) and Taye, (2018) which is related with decreasing streamflow happened in 2050 and 2080 over the Awash basin but in Mojo catchment the decreasing happens starting from Near and Mid periods and under RCP 4.5 but at Far future period the streamflow shows increases change by 19 m³/s. Similarly, for the RCP 8.5 Near period increase by 18.33 m³/s and for Mid, Far future period decreases by 4.27 m³/s and 5.76 m³/s respectively which is the same as (Taye, 2018) and (Daba, 2015) Figure (4.13).

A) MPI-M-MPI-ESM-LR



B) MIROC-MIROC5

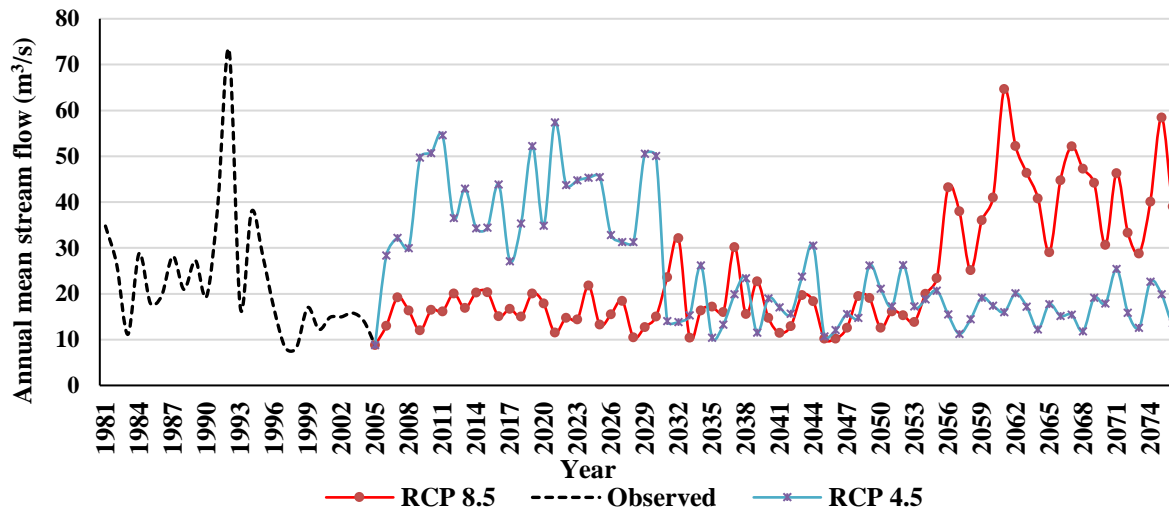


Figure 4.13 The annual mean of simulated streamflow (1981-2080) at Mojo catchment for model MPI-M-MPI-ESM-LR (A) and MIROC-MIROC5 (B) under RCP4.5 and RCP8.5 climate scenarios

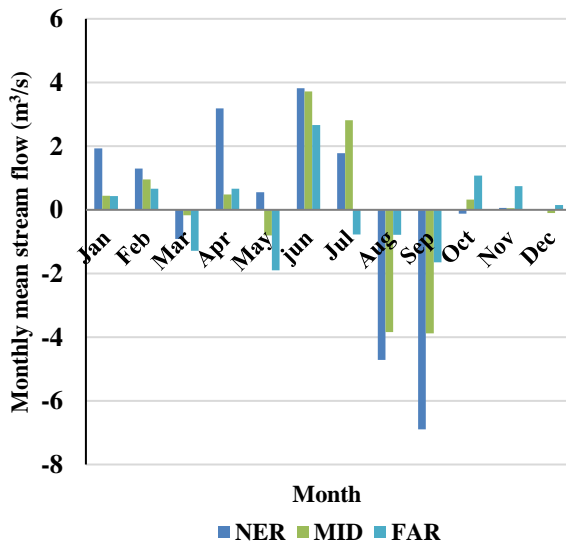
Seasonal projection streamflow showed a mixed increasing and decreasing trend in both Models (Figure 4.14) and (Table 4.10). The seasonal variation of Streamflow under the model MPI-M-MPI-ESM-LR show that in Kiremt (main rainy) season (June–September) the streamflow becoming decrease in July at far and Mid period under RCP 4.5 and 8.5 scenarios respectively, and August September at entire period under both RCPs become decrease and Also, Bega (dry) season (October–January), streamflow shows increase

under both RCP climate scenarios for the all periods except October Near period at both RCPs, December at Mid period under RCP 4.5 and RCP 8.5 at all period and January at far period become decrease. Similarly, In the Belg season (February–May), streamflow shows increased change in all periods February and April under 4.5 scenario, February and April at Near period under RCP 8.5 and May at Near period under both scenarios the rest become shows a decreasing change.

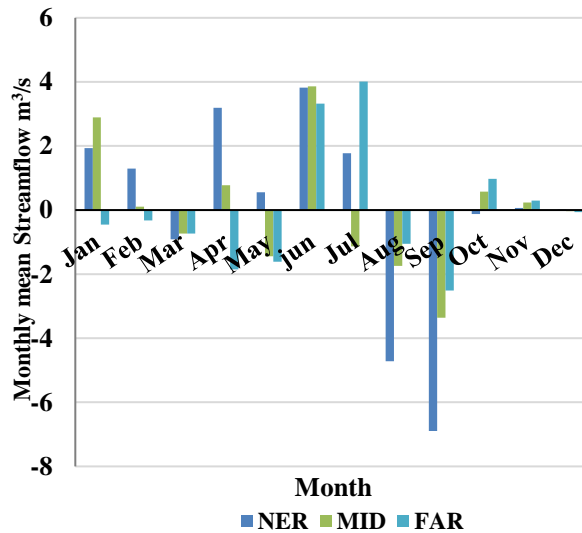
The seasonal variation continues under the model MIROC-MIROC5 shows that at Kiremt season become decreases in both scenarios except July at a far period under 4.5 and Near pod under 8.5 scenarios. For short rainy season, Belg in periods and RCPs shows an increasing change and also for Bega season shows slightly increase at November in all periods under both scenarios, at December in all period under RCP 8.5, October at mid-period in all RCPs and October at Near and far period under RCP 4.5 and 8.5 respectively. The rest shows a decreasing change.

MPI-M-MPI-ESM-LR

RCP 4.5

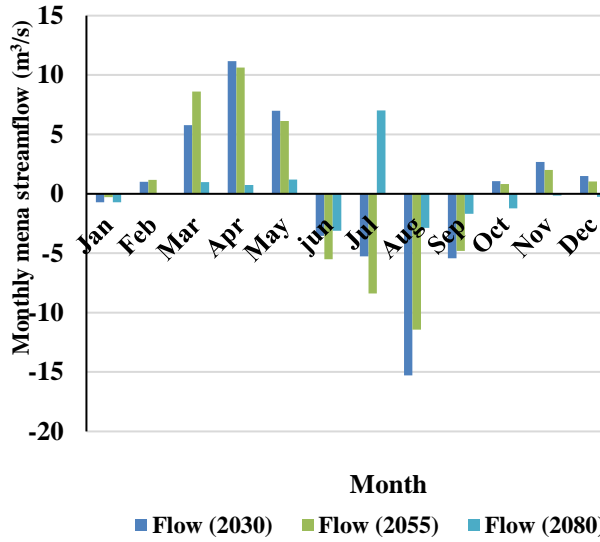


RCP 8.5



MIROC-MIROC5

RCP 8.5



RCP 4.5

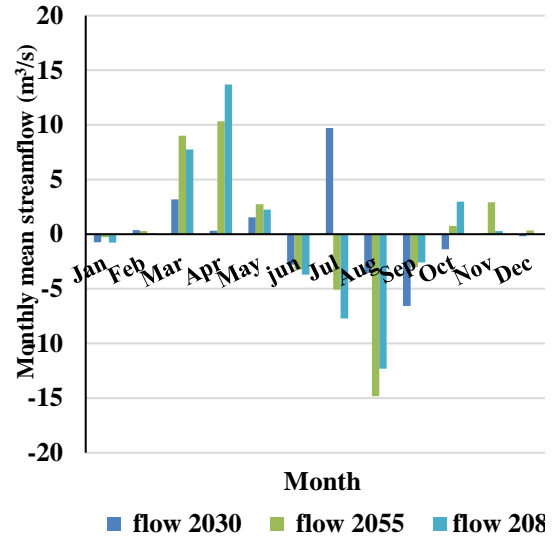


Figure 4.14 The annual mean of simulated streamflow change (%) (1981-2080) at Mojo catchment for model MPI-M-MPI-ESM-LR and MIROC-MIROC5 under RCP4.5 and RCP8.5 climate scenarios

Table 4.10 Mean Monthly variation of Streamflow change (%) (2006-2080) for the Model MIROC-MIROC5 and MPI-M-MPI-ESM-LR under RCP 4.5 and 8.5

MPI-M-MPI-ESM-LR

Period	Jan	Feb	Mar	Apr	May	Jun	Jul	Aug	Sep	Oct	Nov	Dec
Mean Monthly streamflow change (%) RCP 4.5												
2030	1.93	1.30	-0.92	3.19	0.55	3.82	1.78	-4.72	-6.90	-0.12	0.06	0.02
2055	0.45	0.95	-0.17	0.49	-0.80	3.71	2.82	-3.84	-3.88	0.32	0.05	-0.10
2080	0.43	0.67	-1.29	0.66	-1.90	2.66	-0.77	-0.78	-1.65	1.08	0.75	0.16
Mean Monthly streamflow change (%) RCP 8.5												
2030	1.93	1.30	-0.92	3.19	0.55	3.82	1.78	-4.72	-6.90	-0.12	0.06	0.02
2055	2.90	0.10	-0.73	0.77	-1.44	3.86	-1.14	-1.74	-3.36	0.57	0.23	-0.03
2080	-0.45	-0.32	-0.73	-1.85	-1.61	3.32	4.01	-1.05	-2.51	0.98	0.29	-0.06

MIROC-MIROC5

Period	Jan	Feb	Mar	Apr	May	Jun	Jul	Aug	Sep	Oct	Nov	Dec
Mean Monthly streamflow change (%) RCP 4.5												
2030	-0.70	1.01	5.79	11.18	6.99	-3.53	-5.28	-15.29	-5.43	1.07	2.68	1.51
2055	-0.29	1.16	8.62	10.63	6.13	-5.50	-8.38	-11.43	-4.80	0.82	2.01	1.03
2080	-0.70	0.02	0.99	0.74	1.21	-3.11	7.02	-2.87	-1.68	-1.22	-0.15	-0.25
Mean Monthly Streamflow change (%) RCP 8.5												
2030	-0.74	0.38	3.20	0.31	1.54	-2.80	9.72	-3.54	-6.57	-1.38	0.05	-0.18
2055	-0.27	0.29	9.03	10.33	2.73	-3.23	-5.07	-14.83	-3.01	0.75	2.93	0.35
2080	-0.78	0.09	7.76	13.68	2.25	-3.69	-7.70	-12.32	-2.59	2.99	0.28	0.02

4.4.2. Impact of Future Precipitation and Temperature Change on the streamflow

What we have seen from the above analysis is that there is a variation of increasing decreasing of precipitation as well as temperature projection that leads to fluctuation over the streamflow of Ethiopia basins Mengistu and Sorteberg, (2012), Gizaw *et al.*, (2017) and Chaemiso *et al.*, (2016) this fluctuation also shows on the Mojo catchment. The two models used in the analysis show that the variation of streamflow occurs with the different occurrence of temperature and precipitation results. In the model MPI-M-MPI-ESM-LR shows that the annual mean of stream flow under RCP 8.5 indicates that decreasing from 29.7 m³/s to 25.0 m³/s under Near (2006-2030) and Mid (2031-2055) periods respectively and under Far period become increase by 28.7 m³/s and also the precipitation increase by 2.35 mm/day, 2.45 mm/day and 2.57 mm/day under Near, Mid and Far period respectively, So this variation has relation with stream flow of Mojo catchment with an increase precipitation leads to increase streamflow which related with Jilo *et al.*, (2019) over logiya catchment. But the maximum temperature increases from 24.55⁰C to 24.60⁰C at Near, Mid periods respectively and 26.22⁰C under the Far period and the minimum temperature also becomes increase from 9.17⁰C, 9.90⁰C and 11.95⁰C under a period of Near, Mid and Far respectively. Similarly, under the RCP 4.5, the streamflow variation becomes decrease from 29.12 m³/s, to 27.06 m³/s under Near and Mid future periods and also stream flow becomes increase by 29.18 m³/s by the period of

Far future. from the hydrological perspective, and the maximum temperature becomes increase from 23.35⁰C to 25.05⁰C under the Near and Mid period and the decrease temperature occurred under the Far period by 24.77⁰C leads to decreasing of streamflow in the Near and Mid period which related with (Dile *et al.*, 2013). Also, the temperature minimum shows an increasing trend from 8.923⁰C to 10⁰C under the Near and Mid period and 10⁰C under the Far future period.

The variation under the model MIROC-MIROC5 shows that the annual mean streamflow becomes decrease trend shows on the RCP 8.5 from 40.78 m³/s to 18.16 m³/s under Near and Mid period and 16.68 m³/s under Far future period. Increases streamflow under RCP 4.5 from 16.12 m³/s to 17.55 m³/s in the period of Near and Mid Future and 41.74 m³/s in the period of the Far Future. The increase of maximum temperature from 23.90 ⁰C to 24.82 ⁰C under the period of Near and Mid period and 26.18 ⁰C in the period of Far future under RCP 8.5 and decrease of precipitation from 3.29 mm/day to 1.82 mm/day by the period of Near and Mid future and 1.77 mm/day under Far future period. The condition becomes more favorable to high evapotranspiration and causes decrease streamflow by the increase in maximum temperature in both periods of Near and Mid Future as well as Far future of RCP 8.5 which is a related result with Taye, (2018) at awash basin and Molla and Abdisa, (2018) at Baro Akobo basin. change in temperature on water availability was assessed based on climate change scenarios for the catchment (Chaemiso *et al.*, 2016). the minimum temperature in both scenarios shows that an increasing trend under RCP 8.5 from 11.93⁰C to 12.91⁰C under the Near and Mid period and also 14.70 ⁰C under the far period. For the RCP 4.5, the minimum temperature shows that 11.14 ⁰C, 12.71 ⁰C, and 12.70 ⁰C under Near, Mid and far future period respectively.

5. CONCLUSIONS AND RECOMMENDATIONS

5.1. Conclusion

Climate change effect is likely to be alterations in hydrologic cycles and changes in water availability. In this study, we investigated the impact of climate change on the hydrological response of Mojo catchment, was investigating.

This research evaluated the impact of climate change on Mojo catchment hydrology resulting from CORDEX-Africa mid-rand and high-level RCP climate scenarios (RCP 4.5 and RCP 8.5). Calibrated SWAT hydrological model was then used to select the appropriate GCM model and transform these future climate scenarios to projected streamflow used as an input for reservoirs planning and management. Projected precipitation and temperature from ensemble CORDEX-Africa RCP scenarios have systematic errors (bias) that may lead to biased simulated streamflow which is not corrected by calibration of the hydrological model. However, Quantile mapping with Gamma distribution for precipitation and Normal distribution method for temperature used to correct the biases and improves precipitation and streamflow simulations. Analyzing the SWAT model for performance assessment of climate GCMs models over the Mojo catchment shows a good relationship with the observed data so SWAT model is so much more suitable for the catchment of the study area. After selecting the performed GCM models two of them show good relation with the observed data which is MPI-M-MPI-ESM-LR and MIROC-MIROC5 models over the Mojo catchment. For analysis of the future climate impact on the catchment scenarios classified into three periods Near future (2006-2030), Mid future (2031-2055) and Far future (2056-2080) periods. Mid-range RCP 4.5 and high-level RCP 8.5 climate scenarios showed that projected temperature consistently increases across the Mojo catchment and decrease precipitation projection annually under RCP 8.5 and increase under RCP 4.5 in the model of MIROC-MIROC5. Under the model, MPI-M-MPI-ESM-LR shows a slight decrease in the RCP 4.5 scenario and an increase in the RCP 8.5 scenario. The seasonal variation of Kiremt and Bega including Belg season which shows a mixed trend. Projected higher temperature and precipitation increase under RCP4.5 and RCP8.5 climate scenarios expected to decrease projected streamflow of Mojo catchment. This study result showed

that climate change will affect the planning and operational over the Mojo catchment. Therefore, the effect of projected precipitation and streamflow should be included in the feasibility assessment of Mojo catchment planning. Future research on impact assessments should focus on integrated approaches linking climate, hydrology, water resources, and ecosystem models to sustain and improve the development of the river and its basin in a changing environment.

5.2. Recommendation

This study involved over four model's analysis and two of them model outputs used were each possessed a certain level of uncertainty. Hence, the results of this study should be taken with care and be considered indicative of future flow.

This study should be extended by considering combined changes in land use, soil and other climate variables in addition to the changes in climate (i.e. precipitation and temperature).

The outcome of this study is based on two GCMs and two RCPs scenarios. However, it is often recommended to apply further analysis based on the output of different GCMs and RCP scenarios so as to make a comparison between different models as well as to explore a wide range of climate change scenarios that would result in different hydrological impacts. Hence this work should be extended in the future by including different GCMs and RCP scenarios.

The GCMs were downscaled to catchment with 50 km *50 km Grid in the study uses one ensemble for the analysis, in fact, all downscaled data should also use as an additional ensemble value to taste how much the model uncertainty minimize.

Water resources are highly linked with climate, so the prospect of global climate change has serious implications for water resources. As water resources stress become acute in the future as a result of a combination of climate impacts and escalating human demand, there will be intensifying conflicts between human and environmental demands on water resources. Therefore, there is a need to minimize the sensitivity to climate change. One way to minimize this risk is to make the economy more diversified, and agricultural technology should optimize water usage through efficient irrigation and crop development.

Moreover, research activities should be intensified in this area in order to explore the impact of climate change on various sectors including integrated water resource uses. This will contribute partly to the long way towards sustainability if impacts of climate change are considered at all levels from planning to execution and management of water resource development projects.

The physically-based, spatially distributed, and public domain Soil and Water Assessment Tool (SWAT) is found to be a very appropriate tool to simulate both historical as well as impacted hydrological processes in the catchment. Therefore, SWAT can be utilized very well for hydrological simulations in Mojo catchment. Besides, the model should be further tested for its suitability in other catchments of Ethiopia.

The output of any model depends on the quality of the input data. Lack of quality climate and hydrological data was one of the challenges in this study. Hence, responsible bodies should give due attention to the acquisition and recording of reliable data.

REFERENCE

- Abbaspour, K. C. *et al.* (2007) 'Modelling hydrology and water quality in the pre-alpine/alpine Thur watershed using SWAT', *Journal of hydrology*. Elsevier, 333(2–4), pp. 413–430.
- Abbaspour, K. C. (2007) 'SWAT Calibration and Uncertainty Programs'.
- Abbate, E. and Sagri, M. (1980) 'Volcanites of Ethiopian and Somali Plateaus and major tectonic lines', *Atti Convegni Lincei*, 47, pp. 219–227.
- Abebe, T. *et al.* (2005) 'Geological map (scale 1: 200,000) of the northern Main Ethiopian Rift and its implication for the volcano-tectonic evolution of the rift', *Geol. Soc. Am. Map Chart Ser., MCH094*.
- Abraham, L. Z., Roehrig, J. and Chekol, D. A. (2007) 'Climate Change Impact on Lake Ziway Watershed Water Availability ', 3.
- Adeba, D., Kansal, M. L. and Sen, S. (2015) 'Assessment of water scarcity and its impacts on sustainable development in Awash basin, Ethiopia', *Sustainable Water Resources Management*. Springer, 1(1), pp. 71–87.
- Alemseged, T. H. and Tom, R. (2015) 'Evaluation of regional climate model simulations of rainfall over the Upper Blue Nile basin', *Atmospheric Research*. doi: 10.1016/j.atmosres.2015.03.013.
- Arnold, J. G. *et al.* (2012) 'SWAT: Model use, calibration, and validation', *Transactions of the ASABE*. American Society of Agricultural and Biological Engineers, 55(4), pp. 1491–1508.
- Arnold, J. G. and Fohrer, N. (2005) 'SWAT2000: current capabilities and research opportunities in applied watershed modelling', *Hydrological Processes: An International Journal*. Wiley Online Library, 19(3), pp. 563–572.
- Benaman, J., Shoemaker, C. A. and Haith, D. A. (2005) 'Calibration and validation of

soil and water assessment tool on an agricultural watershed in upstate New York’, *Journal of Hydrologic Engineering*. American Society of Civil Engineers, 10(5), pp. 363–374.

Bernstein, L. *et al.* (2008) *Climate change 2007: Synthesis report: An assessment of the intergovernmental panel on climate change*. IPCC.

Borah, D. K. and Bera, M. (2003) ‘Watershed-scale hydrologic and nonpoint-source pollution models: Review of mathematical bases’, *Transactions of the ASAE*. American Society of Agricultural and Biological Engineers, 46(6), p. 1553.

Cannon, A. J., Sobie, S. R. and Murdock, T. Q. (2015) ‘Bias correction of GCM precipitation by quantile mapping: How well do methods preserve changes in quantiles and extremes?’, *Journal of Climate*, 28(17), pp. 6938–6959. doi: 10.1175/JCLI-D-14-00754.1.

Chaemiso, S. E., Abebe, A. and Pingale, S. M. (2016) ‘Assessment of the impact of climate change on surface hydrological processes using SWAT: a case study of Omo-Gibe river basin, Ethiopia’, *Modeling Earth Systems and Environment*. Springer, 2(4), pp. 1–15.

CHANGE–IPCC, I. P. O. N. C. (2000) ‘Land use, land-use change, and forestry: special report of the IPCC’. Cambridge, Cambridge University Press.

Cheung, W. H., Senay, G. B. and Singh, A. (2008) ‘Trends and spatial distribution of annual and seasonal rainfall in Ethiopia’, *International Journal of Climatology: A Journal of the Royal Meteorological Society*. Wiley Online Library, 28(13), pp. 1723–1734.

Choi, J., Socolofsky, S. A. and Olivera, F. (2008) ‘Hourly Disaggregation of Daily Rainfall in Texas Using Measured Hourly Precipitation at Other Locations’, *Journal of Hydrologic Engineering*. doi: 10.1061/(ASCE)1084-0699(2008)13:6(476).

Chokkavarapu, N. and Mandla, V. R. (2019) ‘Comparative study of GCMs, RCMs,

downscaling and hydrological models: a review toward future climate change impact estimation', *SN Applied Sciences*. Springer, 1(12), p. 1698.

Christensen, J. H. *et al.* (2010) 'Weight assignment in regional climate models', *Climate Research*, 44(2–3), pp. 179–194.

Conway, D. (1997) 'A water balance model of the Upper Blue Nile in Ethiopia', 42(October).

Cooper, P. J. M. *et al.* (2008) 'Coping better with current climatic variability in the rain-fed farming systems of sub-Saharan Africa: An essential first step in adapting to future climate change?', *Agriculture, ecosystems & environment*. Elsevier, 126(1–2), pp. 24–35.

Curry, J. A. and Lynch, A. H. (2002) 'Comparing arctic regional climate model', *Eos, Transactions American Geophysical Union*. Wiley Online Library, 83(9), p. 87.

Daba, M. (2015) 'Evaluating Potential Impacts of Climate Change on Surface Water Resource Availability of Upper Awash Sub-basin, Ethiopia rift valley basin.'

Dile, Y. T., Berndtsson, R. and Setegn, S. G. (2013) 'Hydrological response to climate change for gilgel abay river, in the lake tana basin-upper blue Nile basin of Ethiopia', *PloS one*. Public Library of Science, 8(10), p. e79296.

Dodman, D. (2009) 'Blaming cities for climate change? An analysis of urban greenhouse gas emissions inventories', *Environment and urbanization*. SAGE Publications Sage UK: London, England, 21(1), pp. 185–201.

Feser, F. *et al.* (2011) 'Regional climate models add value to global model data: a review and selected examples', *Bulletin of the American Meteorological Society*. American Meteorological Society, 92(9), pp. 1181–1192.

Flato, G. *et al.* (2014) 'Evaluation of climate models', in *Climate change 2013: the physical science basis. Contribution of Working Group I to the Fifth Assessment Report of the Intergovernmental Panel on Climate Change*. Cambridge University Press, pp.

741–866.

Fowler, H. J., Kilsby, C. G. and O’Connell, P. E. (2007) ‘S. Blenkinsop, and C. Tebaldi, 2007: Linking climate change modelling to impacts studies: Recent advances in downscaling techniques for hydrological modelling’, *Int. J. Climatol*, 27, pp. 1547–1578.

Fox, K. M. *et al.* (2018) ‘Climate Change Adaptation in Ethiopia: Developing a Method to Assess Program Options’, in *Resilience*. Elsevier, pp. 253–265.

Fu, C. *et al.* (2005) ‘Regional climate model intercomparison project for Asia’, *Bulletin of the American Meteorological Society*. American Meteorological Society, 86(2), pp. 257–266.

Garcia, F. (2012) ‘Tests to identify outliers in data series’, *Pontifical Catholic University of Rio de Janeiro*, ..., pp. 1–16. Available at: http://habcam.who.edu/HabCamData/HAB/processed/Outlier Methods_external.pdf.

Gassman, P. W. *et al.* (2007) ‘The soil and water assessment tool: historical development, applications, and future research directions’, *Transactions of the ASABE*. American Society of Agricultural and Biological Engineers, 50(4), pp. 1211–1250.

Gassman, P. W. *et al.* (2013) ‘Soil and Water Assessment Tool : Historical Development , Applications , and Future Research Directions , The The Soil and Water Assessment Tool : Historical Development , Applications , and Future Research Directions’, (March 2007). doi: 10.13031/2013.23637.

Gedefaw, M. *et al.* (2018) ‘Trend Analysis of Climatic and Hydrological Variables in the Awash River Basin , Ethiopia’, pp. 1–14. doi: 10.3390/w10111554.

Getahun, Y. S. (2018) ‘Impact of Climate Change on Hydrology of the Upper Awash River Basin (Ethiopia): Inter-comparison of old SRES and new RCP scenarios’, (April 2015).

Giorgi, F. (2005) ‘Climate change prediction’, *Climatic Change*. Springer, 73(3), pp.

239–265.

Giorgi, F. *et al.* (2008) ‘The regional climate change hyper-matrix framework’, *Eos, Transactions American Geophysical Union*. Wiley Online Library, 89(45), pp. 445–446.

Giorgi, F., Jones, C. and Asrar, G. R. (2009) ‘Addressing climate information needs at the regional level: the CORDEX framework’, *World Meteorological Organization (WMO) Bulletin*, 58(3), p. 175.

Girma, W. (2013) ‘Hydrological Impacts of Climate Change in Lake Hawasa Watershed , Ethiopia MSc Thesis Hydrological Impacts of Climate Change in Lake Hawasa Watershed , Ethiopia’.

Gissila, T. *et al.* (2004) ‘Seasonal forecasting of the Ethiopian summer rains’, *International Journal of Climatology: A Journal of the Royal Meteorological Society*. Wiley Online Library, 24(11), pp. 1345–1358.

Gizaw, M. S. *et al.* (2017) ‘Potential impact of climate change on streamflow of major Ethiopian rivers’, *Climatic Change*. Springer, 143(3–4), pp. 371–383.

Gonfa, Z. B. *et al.* (2015) ‘Optimal Land Use Planning in Mojo Watershed with Multi-Objective’, pp. 10–17.

Gonfa, Z. B. and Kumar, D. (2016) ‘Application of Soil and Water Assessment Tool Model to Estimate Runoff and Sediment Yield from Mojo Watershed’, pp. 2081–2091. doi: 10.15680/IJRSET.2016.0502058.

Grey, D. and Sadoff, C. W. (2007) ‘Sink or swim? Water security for growth and development’, *Water policy*. IWA Publishing, 9(6), pp. 545–571.

Grubbs, F. E. and Beck, G. (1972) ‘Extension of sample sizes and percentage points for significance tests of outlying observations’, *Technometrics*. Taylor & Francis, 14(4), pp. 847–854.

Gudeta, K. (2010) 'Faculty of Science GIS-Based Conservation Priority Area Identification in Mojo River Watershed On the Basis of Erosion Risk By : School of Graduate Studies Faculty of Science GIS-Based Conservation Priority Area Identification in Mojo River Watershed On t', (June).

Gupta, A. (2009) 'An Ecologically-Sustainable Surface Water Withdrawal Framework For Cropland Irrigation-A case study in Alabama'.

Gupta, H. V., Sorooshian, S. and Yapo, P. O. (1999) 'Status of automatic calibration for hydrologic models: Comparison with multilevel expert calibration', *Journal of Hydrologic Engineering*. American Society of Civil Engineers, 4(2), pp. 135–143.

Haerter, J. O. *et al.* (2010) 'Climate model bias correction and the role of timescales', pp. 7863–7898. doi: 10.5194/hessd-7-7863-2010.

Haile, G. G. and Kasa, A. K. (2015) 'Irrigation in Ethiopia: A review', *Acad. J. Agric. Res*, 3(10), pp. 264–269.

Hailemariam, K. (1999) 'Impact of climate change on the water resources of Awash River Basin, Ethiopia', *Climate Research*, 12(2–3), pp. 91–96.

Haktanir, T. and Citakoglu, H. (2014) 'Trend, independence, stationarity, and homogeneity tests on maximum rainfall series of standard durations recorded in Turkey', *Journal of Hydrologic Engineering*. American Society of Civil Engineers, 19(9), p. 5014009.

Hawkins, E. and Sutton, R. (2009) 'The potential to narrow uncertainty in regional climate predictions', *Bulletin of the American Meteorological Society*. American Meteorological Society, 90(8), pp. 1095–1108.

Hawkins, E. and Sutton, R. (2011) 'The potential to narrow uncertainty in projections of regional precipitation change', *Climate Dynamics*. Springer, 37(1–2), pp. 407–418.

Heo, J. H. *et al.* (2019) 'Probability distributions for a quantile mapping technique for a

bias correction of precipitation data: A case study to precipitation data under climate change', *Water (Switzerland)*, 11(7). doi: 10.3390/w11071475.

Her, Y. *et al.* (2016) 'Comparison of uncertainty in multi-parameter and multi-model ensemble hydrologic analysis of climate change', *Hydrol. Earth Syst. Sci. Discuss*, pp. 1–44.

Her, Y. *et al.* (2019) 'Uncertainty in hydrological analysis of climate change: multi-parameter vs . multi-GCM ensemble predictions', *Scientific Reports*. Springer US, (March), pp. 1–22. doi: 10.1038/s41598-019-41334-7.

IPCC (2014) 'Mitigation of climate change', *Contribution of Working Group III to the Fifth Assessment Report of the Intergovernmental Panel on Climate Change*, 1454.

IPCC III, W. G. (2001) 'Third assessment report', *Summary for policymakers.-2001*.

Ismail, W. N., Zin, W. Z. and Ibrahim, W. (2017) 'Estimation of rainfall and stream flow missing data for Terengganu, Malaysia by using interpolation technique methods', *Malaysian Journal of Fundamental and applied Sciences*, 13(3).

Jaramillo, J. *et al.* (2011) 'Some like it hot: the influence and implications of climate change on coffee berry borer (*Hypothenemus hampei*) and coffee production in East Africa', *PloS one*. Public Library of Science, 6(9), p. e24528.

Jilo, N. B. *et al.* (2019) 'Evaluation of the Impacts of Climate Change on Sediment Yield from the Logiya Watershed, Lower Awash Basin, Ethiopia', *Hydrology*, 6(3), p. 81. doi: 10.3390/hydrology6030081.

Jones, C., Giorgi, F. and Asrar, G. (2011) 'The Coordinated Regional Downscaling Experiment: CORDEX—an international downscaling link to CMIP5', *CLIVAR exchanges*. International CLIVAR Project Office Southampton, United Kingdom, 16(2), pp. 34–40.

Kalin, L. and Hantush, M. M. (2003) 'Evaluation of Sediment Transport Models and

Comparative Application of Two Watershed Models’, (September).

Kattsov, V. *et al.* (2013) ‘Evaluation of Climate Models 9’.

Klimont, Z., Smith, S. J. and Cofala, J. (2013) ‘The last decade of global anthropogenic sulfur dioxide: 2000–2011 emissions’, *Environmental Research Letters*. IOP Publishing, 8(1), p. 14003.

Knutti, R. (2008) ‘Should we believe model predictions of future climate change?’, *Philosophical Transactions of the Royal Society A: Mathematical, Physical and Engineering Sciences*. The Royal Society London, 366(1885), pp. 4647–4664.

Larsson, R. (2019) ‘An Integrated Simulation-Based Methodology for Considering Weather Effects on Formwork Removal Times’, in *Advances in Informatics and Computing in Civil and Construction Engineering*. Springer, pp. 415–422.

Leggett, J. *et al.* (1992) ‘Emissions scenarios for the IPCC: an update’, *Climate change*, pp. 69–95.

Leonard, R. A. and Knisel, W. G. (1995) ‘Modelling pesticide fate with GLEAMS’, *European Journal of Agronomy*. Gauthier-Villars, 4(4), pp. 485–490. doi: 10.1016/S1161-0301(14)80100-7.

Loucks, D. P. and Van Beek, E. (2017) *Water resource systems planning and management: An introduction to methods, models, and applications*. Springer.

Luo, M., Liu, T. and Meng, F. (2018) ‘Comparing Bias Correction Methods Used in Downscaling Precipitation and Temperature from Regional Climate Models: A Case Study from the Kaidu River Basin in Western China’. doi: 10.3390/w10081046.

McSweeney, C. F. *et al.* (2015) ‘Selecting CMIP5 GCMs for downscaling over multiple regions’, *Climate Dynamics*. Springer, 44(11–12), pp. 3237–3260.

Mearns, L. O. *et al.* (2003) ‘Guidelines for use of climate scenarios developed from

regional climate model experiments’. Data Distribution Center of IPCC. TGCI.A.

Mearns, L. O. *et al.* (2013) ‘Climate change projections of the North American regional climate change assessment program (NARCCAP)’, *Climatic Change*. Springer, 120(4), pp. 965–975.

Mengistu, D. T. and Sorteberg, A. (2012) ‘Sensitivity of SWAT simulated streamflow to climatic changes within the Eastern Nile River basin’, *Hydrology and Earth System Sciences*. Copernicus GmbH, 16(2), pp. 391–407.

Ming, Y. *et al.* (2005) ‘Geophysical Fluid Dynamics Laboratory general circulation model investigation of the indirect radiative effects of anthropogenic sulfate aerosol’, *Journal of Geophysical Research: Atmospheres*. Wiley Online Library, 110(D22).

Molla, S. and Abdisa, T. (2018) ‘INVESTIGATING CLIMATE CHANGE IMPACT ON STREAM FLOW OF BARO-AKOBO RIVER BASIN CASE STUDY OF BARO CATCHMENT .’, 6(5).

Moriasi, D. *et al.* (2015) ‘Hydrologic and Water Quality Models: Performance Measures and Evaluation Criteria’, (January 2016). doi: 10.13031/trans.58.10715.

Moriasi, D. N. *et al.* (2007) ‘Model evaluation guidelines for systematic quantification of accuracy in watershed simulations’, *Transactions of the ASABE*. American society of agricultural and biological engineers, 50(3), pp. 885–900.

Moss, R. H. *et al.* (2010) ‘The next generation of scenarios for climate change research and assessment’, *Nature*. Nature Publishing Group, 463(7282), pp. 747–756. doi: 10.1038/nature08823.

Nash, J. E. and Sutcliffe, J. V (1970) ‘River flow forecasting through conceptual models part I—A discussion of principles’, *Journal of hydrology*. Elsevier, 10(3), pp. 282–290.

Pachauri, R. K. *et al.* (2014) ‘Climate change 2014: synthesis report. Contribution of Working Groups I’, *II and III to the fifth assessment report of the Intergovernmental*

Panel on Climate Change. Geneva, Switzerland: IPCC, 151.

Paeth, H. *et al.* (2011) 'Progress in regional downscaling of West African precipitation', *Atmospheric science letters*. Wiley Online Library, 12(1), pp. 75–82.

Papadimitriou, V. (2004) 'Prospective primary teachers' understanding of climate change, greenhouse effect, and ozone layer depletion', *Journal of Science Education and Technology*. Springer, 13(2), pp. 299–307.

Pasten-Zapata, E. *et al.* (2019) 'Climate model evaluation and ensemble selection progress'. AQUACLEW Consortium.

Pirozynski, K. A. and Malloch, D. W. (1975) 'The origin of land plants: a matter of mycotrophism', *Biosystems*. Elsevier, 6(3), pp. 153–164.

Rahman, T. (2019) 'Addressing Climate Change and grassroots level adaptation measures to food security in Northwestern Bangladesh'.

Rahmato, D. (1999) 'Water resource development in Ethiopia: Issues of sustainability and participation', in. Forum for Social Studies.

Renard, B. *et al.* (2008) 'Regional methods for trend detection: Assessing field significance and regional consistency', *Water Resources Research*. Wiley Online Library, 44(8).

Res, C. and Hailemariam, K. (1999) 'Impact of climate change on the water resources of Awash River Basin , Ethiopia', 12, pp. 91–96.

Riahi, K. *et al.* (2011) 'RCP 8.5—A scenario of comparatively high greenhouse gas emissions', *Climatic Change*. Springer, 109(1–2), p. 33.

Richter, B. D. *et al.* (2010) 'Lost in development's shadow: the downstream human consequences of dams.', *Water Alternatives*, 3(2).

Rummukainen, M. (1997) *Methods for statistical downscaling of GCM simulations*.

SMHI.

Sagri, M. *et al.* (2008) 'Latest Pleistocene and Holocene river network evolution in the Ethiopian Lakes Region', *Geomorphology*. Elsevier, 94(1–2), pp. 79–97.

Santhi, C. *et al.* (2001) 'Validation of the swat model on a large river basin with point and nonpoint sources 1', *JAWRA Journal of the American Water Resources Association*. Wiley Online Library, 37(5), pp. 1169–1188.

Seo, S. B. and Kim, Y. O. (2018) 'Impact of spatial aggregation level of climate indicators on a national-level selection for representative climate change scenarios', *Sustainability (Switzerland)*, 10(7). doi: 10.3390/su10072409.

Setegn, S. G. *et al.* (2011) 'Impact of climate change on the hydroclimatology of Lake Tana Basin, Ethiopia', *Water Resources Research*. doi: 10.1029/2010WR009248.

De Silva, R. P., Dayawansa, N. D. K. and Ratnasiri, M. D. (2007) 'A comparison of methods used in estimating missing rainfall data', *Journal of agricultural sciences*. The Faculty of Agricultural Sciences of the Sabaragamuwa University of Sri Lanka, 3(2).

Socolofsky, S., Adams, E. E. and Entekhabi, D. (2001) 'Disaggregation of Daily Rainfall for Continuous Watershed Modeling', *Journal of Hydrologic Engineering*. doi: 10.1061/(ASCE)1084-0699(2001)6:4(300).

Solomon, S. *et al.* (2007) 'Climate Change 2007: The Physical Science Basis; Contribution of Working Group I to the Fourth Assessment Report of the Intergovernmental Panel on Climate Change-Summary for Policymakers', *IPCC Working Groups Reports*. Cambridge university press.

Solomon, S. (2007) 'IPCC (2007): Climate change the physical science basis', in *AGU Fall Meeting Abstracts*.

Sonder, K. (2015) 'The Water of the Awash River Basin: a Future Challenge to Ethiopia', (January).

System, M. and Dam, B. (2018) ‘Sustainability Assessment of the Water’, pp. 1–21. doi: 10.3390/w10121723.

Takle, E. S. *et al.* (2007) ‘Transferability intercomparison: an opportunity for new insight on the global water cycle and energy budget’, *Bulletin of the American Meteorological Society*. American Meteorological Society, 88(3), pp. 375–384.

Taye, M. T. *et al.* (2011) ‘Assessment of climate change impact on hydrological extremes in two source regions of the Nile River Basin’, *Hydrology and Earth System Sciences*. doi: 10.5194/hess-15-209-2011.

Taye, M. T. (2018) ‘Climate Change Impact on Water Resources in the Awash Basin, Ethiopia’, pp. 1–16. doi: 10.3390/w10111560.

Teutschbein, C. and Seibert, J. (2012) ‘Bias correction of regional climate model simulations for hydrological climate-change impact studies: Review and evaluation of different methods’, *Journal of Hydrology*. Elsevier, 456, pp. 12–29.

Thomson, A. M. *et al.* (2011) ‘RCP4 . 5 : a pathway for stabilization of radiative forcing by 2100’, pp. 77–94. doi: 10.1007/s10584-011-0151-4.

Van Vuuren, D. P. *et al.* (2011) ‘The representative concentration pathways: an overview’, *Climatic change*. Springer, 109(1–2), p. 5.

Van Vuuren, D. P. *et al.* (2014) ‘A new scenario framework for climate change research: scenario matrix architecture’, *Climatic Change*. Springer, 122(3), pp. 373–386.

Wale, A. and Texas, W. (2015) ‘Climate Change Impact on Stream Flow in the Upper Gilgel Abay Catchment , Blue Nile basin ’, (July). doi: 10.1007/978-3-319-18787-7.

Wayne, G. P. (2013) ‘Representative Concentration Pathways’.

Wehner, E. (2001) ‘Testing the modelling system T AL S IM for the Upper and Middle Awash Basin in Ethiopia Table of Contents’, (June).

Wilby, R. L. *et al.* (2004) 'Guidelines for use of climate scenarios developed from statistical downscaling methods', *Supporting material of the Intergovernmental Panel on Climate Change, available from the DDC of IPCC TGCIA*, 27.

Winchell, M. *et al.* (2010) 'Arc SWAT interface for SWAT 2009. Users' guide. Grassland', *Soil and Water Research Laboratory, Agricultural Research Service, and Blackland Research Center, Texas Agricultural Experiment Station: Temple, Texas, 76502*, p. 495.

Wood, A. W. *et al.* (2004) 'Hydrologic implications of dynamical and statistical approaches to downscaling climate model outputs', *Climatic change*. Springer, 62(1–3), pp. 189–216.

Woodward, A. and Scheraga, J. D. (2014) 'Looking to the future: challenges for scientists studying climate change and health', pp. 61–78.

Worku, G. *et al.* (2018) 'Evaluation of regional climate models performance in simulating rainfall climatology of Jemma sub-basin, Upper Blue Nile Basin, Ethiopia', *Dynamics of Atmospheres and Oceans*. doi: 10.1016/j.dynatmoce.2018.06.002.

Yozgatligil, C. and Yazici, C. (2016) 'Comparison of homogeneity tests for temperature using', 81(April 2015), pp. 62–81. doi: 10.1002/joc.4329.

APPENDIX

Appendix 1 Test of Homogeneity of rainfall

Chefedonsa (1980-2010)		Ejere (1980-2010)	
K	91.000	K	56.000
T	1991	T	1994
p-value (Two-tailed)	0.535	p-value (Two-tailed)	0.806
Alpha	0.05	Alpha	0.05
Debrezeyit (1980-2010)		Mojo (1980-2010)	
K	90.000	K	122.000
T	1995	T	1991
p-value (Two-tailed)	0.280	p-value (Two-tailed)	0.061
Alpha	0.05	Alpha	0.05

Appendix 1 Test of outlier of rainfall of four stations

Chefedonsa (1975-2010)				Chefedonsa	
year	Annual Max	year	Annual Max		
1975	32	1993	40	Number of data	36
1976	32.1	1994	23.275	S	0.278
1977	35.3	1995	27.651	K _N	2.639
1978	42.15	1996	53.017	k _{NS}	0.733
1979	34	1997	31	Var	0.08
1980	37.4	1998	45.3	X _L	19.9
1981	44.5	1999	43.6	X _H	86
1982	45.6	2000	31.1	x-bar	3.72
1983	70	2001	26.7	Max	70
1984	50.9	2002	27.5	Min	23.275
1985	62.5	2003	55.6		
1986	56.2	2004	30.2		
1987	47.2	2005	68.8		
1988	38.9	2006	48.2		
1989	41.8	2007	57.3		
1990	56	2008	40.2		
1991	51	2009	36.5		
1992	35.5	2010	50.2		

Debrezeyit (1980-2010)

year	Annual Max	year	Annual Max
1980	75	1996	62
1981	38.4	1997	57
1982	39.2	1998	70
1983	46.4	1999	53.6
1984	42.8	2000	47
1985	54.9	2001	39.8
1986	42.645	2002	44.7
1987	45.8	2003	45.6
1988	32.5	2004	46.2
1989	37.8	2005	37
1990	42.3	2006	74.4
1991	44.98	2007	38.1
1992	39.996	2008	45.9
1993	29.662	2009	31.5
1994	34.6	2010	44.6
1995	32.4		

Debrezeyit	
Number of data	31
S	0.24
k _N	2.58
k _{NS}	0.61
Var	0.06
X-bar	3.79
X _L	24.05
X _H	82.02
Max	75
Min	29.662

Ejere (1980-2010)

year	Annual Max	year	Annual Max
1980	33	1996	66
1981	56	1997	34
1982	46	1998	64
1983	61	1999	65
1984	48	2000	45
1985	63	2001	39
1986	43	2002	70
1987	59	2003	57
1988	28	2004	59
1989	68	2005	56
1990	52	2006	64
1991	48	2007	48
1992	31	2008	56
1993	56	2009	52
1994	41	2010	42
1995	55		

Ejere	
Number of data	31
S	0.24
k _N	2.6
k _{NS}	0.62
X _L	27.0
X _H	94
X-bar	3.9
Max	70
Min	28

Mojo (1980-2010)

year	Annual max	year	Annual max	Mojo	
1980	52	1996	45	Number of data	31
1981	50	1997	54	S	0.2
1982	71	1998	79	k _N	2.6
1983	57	1999	49	k _{NS}	0.6
1984	48	2000	45	X _L	27.3
1985	65	2001	43	X _H	94.4
1986	34	2002	47	x-bar	3.9
1987	48	2003	78	Max	79
1988	45	2004	47	Min	34
1989	61	2005	56		
1990	62	2006	35		
1991	69	2007	39		
1992	35	2008	78		
1993	48	2009	48		
1994	39	2010	56		
1995	36				

Appendix 2 Test of outlier of Streamflow at Mojo gauge stations (1980-2010)

year	Annual Max	year	Annual Max	Mojo gauge station	
1980	186.01	1996	33.70	Number of data	31
1981	97.46	1997	14.08	S	0.906
1982	32.93	1998	48.87	K _n	2.578
1983	141.72	1999	26.70	k _{NS}	2.335
1984	87.25	2000	20.95	Var	0.82
1985	102.33	2001	20.08	X _L	5.4
1986	146.05	2002	35.33	X _H	578
1987	112.14	2003	43.29	X-bar	3.72
1988	130.32	2004	17.78		
1989	117.06	2005	15.00		
1990	132.44	2006	24.59		
1991	215.57	2007	26.66		
1992	107.94	2008	26.35		
1993	216.45	2009	30.36		
1994	172.71	2010	13.96		
1995	91.07				

Appendix 4 Table 4.2 trend analysis of streamflow (1981-2011)

1981-1996		1997-2011	
Kendall's tau	0.2167	Kendall's tau	-0.1619
S	26.0000	S	-17.0000
Var(S)	0.0000	Var(S)	0.0000
p-value (Two-tailed)	0.2650	p-value (Two-tailed)	0.4351
alpha	0.05	alpha	0.05

Appendix 5 Trend analysis of rainfall of four stations

Chefedonsa (1975-2010)		Ejere (1980-2010)	
Kendall's tau	0.035	Kendall's tau	0.063
S	22.000	S	29.000
Var(S)	0.000	Var(S)	3446.333
p-value (Two-tailed)	0.777	p-value (Two-tailed)	0.633
Alpha	0.05	Alpha	0.05
Debrezeyit (1980-2010)		Mojo (1980-2010)	
Kendall's tau	-0.006	Kendall's tau	-0.063
S	-3.000	S	-29.000
Var(S)	0.000	Var(S)	3444.333
p-value (Two-tailed)	0.973	p-value (Two-tailed)	0.633
Alpha	0.05	Alpha	0.05

Appendix 6 GCM model and their institutions (source: https://is-enes.data.github.io/CORDEX_RCMs_info.html)

Model Name	Institute	Institution Name
CLMcom-CCLM4-8-17	CLMcom	Climate Limited-area Modelling Community (CLM-Community)
CLMcom-CCLM4-8-17- CLM3-5	CLMcom	Climate Limited-area Modelling Community (CLM-Community)
CLMcom-CCLM5-0-0	CLMcom	Climate Limited-area Modelling Community (CLM-Community)
CLMcom-CCLM5-0-2	CLMcom	Climate Limited-area Modelling Community (CLM-Community)
CLMcom-CCLM5-0-6	CLMcom	Climate Limited-area Modelling Community (CLM-Community)
DMI-HIRHAM5	DMI	Danish Meteorological Institute
GERICS-REMO2009	GERICS	Helmholtz-Zentrum Geesthacht, Climate Service Center Germany
GERICS-REMO2015	GERICS	Climate Service Center Germany
ICTP-RegCM4-3	ICTP	Abdus Salam International Centre for Theoretical Physics
ICTP-RegCM4-6	ICTP	Abdus Salam International Centre for Theoretical Physics
ICTP-RegCM4-7	ICTP	Abdus Salam International Centre for Theoretical Physics
MPI-CSC-REMO2009	MPI-CSC	Helmholtz-Zentrum Geesthacht, Climate Service Center, Max Planck Institute for Meteorology
SMHI-RCA4	SMHI	Swedish Meteorological and Hydrological Institute, Rossby Centre
SMHI-RCA4-SN	SMHI	Swedish Meteorological and Hydrological Institute, Rossby Centre
SMHI-RCAO	SMHI	Swedish Meteorological and Hydrological Institute, Rossby Centre
SMHI-RCAO-SN	SMHI	Swedish Meteorological and Hydrological Institute, Rossby Centre
UQAM-CRCM5	UQAM	Universite du Quebec a Montreal
UQAM-CRCM5-SN	UQAM	Universite du Quebec a Montreal

Appendix 7 Selected sensitivity parameters and their ranges fitted maximum and minimum value

Parameters	Parameter Descriptions	Max Value	Min Value
r__CN2.mgt	SCS runoff curve number	104.84	122.35
v__ALPHA_BF.gw	Baseflow alpha factor (days)	-0.07	-0.07
v__GW_DELAY.gw	Groundwater delay (days)	-24.37	-16.62
	Threshold depth of water in the shallow aquifer		
v__GWQMN.gw	required for return flow to occur (mm)	1.20	1.20
r__SURLAG.bsn	Surface runoff lag time	9.79	9.87
r__SOL_K ().sol	Saturated hydraulic conductivity	103.85	106.48
r__SOL_ALB ().sol	Moist soil albedo	0.07	0.08
	Effective hydraulic conductivity in main channel		
r__CH_K2.rte	alluvium	-148.33	-125.77
r__CH_N2.rte	Manning's "n" value for the main channel	-0.10	-0.10
r__SLSOIL.hru	Slope length for lateral subsurface flow	322.31	324.54
r__ESCO.hru	Soil evaporation compensation factor	0.83	0.83
r__CANMX.hru	Maximum canopy storage	72.35	72.78
r__EPCO.hru	Plant uptake compensation factor	0.02	0.03
r__SLSUBBSN.hru	Average slope length	66.15	66.82
r__SOL_AWC ().sol	Available water capacity of the soil layer	0.36	0.37
r__BIOMIX.mgt	Biological mixing efficient	0.07	120.00
r__CH_COV1.rte	Channel erodibility factor	0.05	0.34
r__GW_REVAP.gw	Groundwater "revap" coefficient	0.02	0.20
	Concentration of nitrate in groundwater		
r__SHALLST.gw	contribution to streamflow from subbasin (mg N/l)	105.00	534.00
r__RCHRG_DP.gw	Deep aquifer percolation fraction	0.08	0.50
r__SOL_Z ().sol	Depth from soil surface to bottom of layer	167.00	805.00
r__USLE_P.mgt	USLE equation support pra	0.06	0.70
r__REVAPMN.gw	Groundwater "revap" coefficient	53.73	105.88

Appendix 8 Sensitive parameters fitted value descriptions

Parameter Name	Fitted Value
R_CN2.mgt	80.36
V_ALPHA_BF.gw	0.04
V_GW_DELAY.gw	107.96
V_GWQMN.gw	1.33
R_SURLAG.bsn	10.97
R_SOL_K(.).sol	224.04
R_SOL_ALB(.).sol	0.01
R_CH_K2.rte	98.98
R_CH_N2.rte	-0.05
R_SLSOIL.hru	231.84
R_ESCO.hru	0.66
R_CANMX.hru	44.67
R_EPCO.hru	0.11
R_SLSUBBSN.hru	100.07
R_SOL_AWC(.).sol	0.30
R_USLE_P.mgt	0.81
R_USLE_K(.).sol	0.36

Appendix 9 Global sensitive parameters of SWAT-CUP



Appendix 10 The change of Bias correction of Historical data with respect to observed rainfall from (1981-2005) for the two GCM models

	Observed	Historical	Corrected
MIROC-MIROC5			
Mean	2.557	1.572	2.434
Beta	2.614	2.349	2.614
STDEV	6.299	3.693	6.362
Alpha	1.038	0.669	0.931
MPI-M-MPI-ESM-LR			
Mean	2.557	1.652	2.474
Beta	2.535	2.401	2.535
STDEV	6.299	3.966	6.271
Alpha	1.038	0.688	0.976

Appendix 11 The change of Bias correction of Historical data with respect to observed maximum and minimum temperature from (1981-2005) for the two GCM models

	Observed Tmin	Observed Tmax	Historical Tmin	Historical Tmax	Corrected Tmax	Corrected Tmin
MIROC-MIROC5						
Mean	7.78	24.00	10.74	22.90	24.10	8.25
Beta	4.67	4.52	3.24	2.38	3.95	3.79
STDEV	1.67	5.31	3.31	9.61	6.09	2.18
Alpha	12.96	127.49	35.58	220.13	146.84	17.95
MPI-M-MPI-ESM-LR						
Mean	7.78	24.00	9.93	22.61	24.00	7.78
Beta	4.67	4.52	3.31	2.64	4.52	4.67
STDEV	1.67	5.31	3.00	8.55	5.31	1.67
Alpha	12.96	127.49	29.76	193.30	127.48	12.96

Appendix 12 CORDEX-Africa (AFR-44) regional and global circulation models (Source: http://is-enes-data.github.io/CORDEX_status.html)

Domain	Regional Model	GCM Models
AFR-44	CCLMA-8-17	CNRM-CERFACS-CNRM-CM5
AFR-44	CCLMA-8-17	ECMWF-ERAINT
AFR-44	CCLMA-8-17	ICHEC-EC-EARTH
AFR-44	CCLMA-8-17	MOHC-HadGEM2-ES
AFR-44	HIRHAM5	ECMWF-ERAINT
AFR-44	HIRHAM5	ICHEC-EC-EARTH
AFR-44	HadRM3P	ECMWF-ERAINT
AFR-44	RACMO22T	ECMWF-ERAINT
AFR-44	RACMO22T	ICHEC-EC-EARTH
AFR-44	RCA4	Ccma-CanESM2
AFR-44	RCA4	CNRM-CERFACS-CNRM-CM5
AFR-44	RCA4	ECMWF-ERAINT
AFR-44	RCA4	ICHEC-EC-EARTH
AFR-44	RCA4	MIROC-MIROC5
AFR-44	RCA4	MOHC-HadGEM2-ES
AFR-44	RCA4	MPI-M-MPI-ESM-LR
AFR-44	RCA4	NCC-NorESM1-M
AFR-44	RCA4	NOAA-GFDL-GFDL-ESM2M